Ilker Tas

The Flexible Multi-Mode Power Plant Solution

Addressing Energy Transition Challenges and Improving Frequency Stability in Low-Inertia Systems

School of Technology and Innovations
Master's Thesis in Smart Energy

Vaasa 2025

UNIVERSITY OF VAASA
School of Innovation and Technology
Author: Ilker Tas
Title of the Thesis: The Flexible Multi-Mode Power Plant Solution: Addressing Energy Transition Challenges and Improving Frequency Stability in Low-Inertia Systems
Degree: Master of Science in Technology
Discipline: Smart Energy
Supervisors: Hannu Laaksonen & Mustafizur Rahman & Ville Telatie
Year: 2025 **Pages:** 122

ABSTRACT:
The primary goal behind the global energy transition is to reduce greenhouse gas emissions by shifting the source of energy generation from fossil fuels to renewables such as wind and solar. This transition brings many changes to power systems; however, this thesis focuses on three key aspects: renewable energy integration, structural changes in modern power systems, and changes on the demand side.

Due to the intermittent, variable, and low-inertia nature of renewable energy sources, the global energy transition also creates challenges in power systems, such as the increasing need for flexibility, stability, controllability of the generation-load balance, and reliability. To address these challenges, solutions are being explored worldwide. This thesis proposes a solution concept, "The Flexible Multi-Mode Power Plant Solution," which is particularly beneficial for microgrids (both islanded and grid-connected) and power networks with high renewable penetration. The solution concept is in the form of a hybrid power plant and consists of internal combustion engine generating sets, synchronous condensers, and battery energy storage systems. As the name implies, the solution concept relies on operating the power plant in different modes, created by the inclusion or exclusion of its components.

Moreover, to validate the power plant solution concept, frequency stability simulation studies are conducted employing DIgSILENT PowerFactory, one of the leading power system analysis software programs. To create simulation models, the IEEE 14-Bus system is used as a template, representing an islanded microgrid. There are four voltage levels in the simulation models: 0.63 kV (battery energy storage system bus voltage), 0.69 kV (wind and solar plant bus voltage), 11 kV (internal combustion engine generating set bus voltage), and 33 kV (grid voltage). The frequency of the system is 50 Hz, and the total active power of loads is chosen as 100 MW. In the simulation models, the Wärtsilä internal combustion engine generating set model is used to represent synchronous generation. The synchronous condenser model is created based on the Wärtsilä internal combustion engine generating set model. For the battery energy storage system, a model from one of the leading inverter manufacturers is used. Lastly, for renewable generation, WECC models of wind and solar power plants from the DIgSILENT PowerFactory library are used. Different study cases are created to assess how the solution concept improves frequency stability under different modes. According to the results of the simulation studies, it is observed that the power plant solution concept significantly improves frequency stability, particularly in low-inertia power systems. Specifically, in one case, the maximum frequency deviation and RoCoF are reduced by 79.2% and 74.6%, respectively.

Overall, "The Flexible Multi-Mode Power Plant Solution" concept offers a promising approach to achieving cleaner, more flexible, and more stable power systems.

KEYWORDS: Flexibility, Energy transition, Inertia, Frequency stability, IEEE 14-Bus System

Contents

Figures

Tables

Abbreviations

BESS	Battery Energy Storage System
CCGT	Combined-Cycle Gas Turbine
CIGRE	Conseil International des Grands Reseaux Electriques
DER	Distributed Energy Resources
DG	Distributed Generation
DR	Demand Response
EMS	Energy Management System
ES	Energy Storage
EV	Electric Vehicle
ICE	Internal Combustion Engine
IEEE	Institute of Electrical and Electronics Engineers
IoT	Internet of Things
IRENA	International Renewable Energy Agency
OCGT	Open-Cycle Gas Turbine
PCC	Point of Common Coupling
PEC	Power Electronic Converter
PLL	Phase-Locked Loop
PMS	Power Management System
PV	Photovoltaic
REEC	Renewable Energy Electrical Control
REGC	Renewable Energy Generator/Converter
RES	Renewable Energy Source
RoCoF	Rate of change of frequency
SC	Synchronous Condenser
SCR	Short-Circuit Ratio
VRE	Variable Renewable Energy
WECC	Western Electricity Coordinating Council

1 Introduction

The global energy landscape is undergoing a profound transition. The shift from traditional fossil fuel-based power generation to generation from renewable energy sources (RESs) such as wind and solar is reshaping power systems. While this transition supports environmental sustainability, it also introduces significant challenges in power systems in many aspects such as the increasing need for flexibility, stability, controllability of the generation-load balance, and reliability.

With the increasing penetration of RESs in power systems, the need for flexibility and reliability also rises, as power generation from RESs depends on weather conditions, time of day, and seasonal variations. As a result, flexible resources are essential in modern power systems to meet these requirements.

Power system stability is also significantly challenged by the growing penetration of RESs into the grid. While traditional power generation systems use large rotating machines that naturally stabilize grid frequency by resisting sudden changes, most RES-based generation units, especially wind and solar, connect to the grid through inverters, which do not inherently provide inertia and therefore cause frequency stability problems. In addition, power generation fluctuations caused by RESs create frequency deviations that may lead to frequency instability. Moreover, due to the limited capability of RESs to provide reactive power and the inability of inverters to regulate voltage as effectively as traditional generators, voltage stability issues arise with the expanding share of RES-based generation in power systems.

The controllability of the generation-load balance is also challenged by the increasing share of RES-based generation in power systems. Forecasting challenges associated with RESs, the complexity of coordinating generation and load balance, and the lack of dispatchability in RES-based generation make real-time generation-load balancing difficult to manage, requiring additional systems to improve control capabilities.

Further details about the global energy transition and its associated challenges are provided in Chapters 2 and 3.

1.1 Thesis Motivation

To address and mitigate the energy transition challenges in power systems caused by the increasing penetration of RESs mentioned above, various solutions are being explored. This thesis also proposes a promising solution concept, “The Flexible Multi-Mode Power Plant Solution,” which consists of internal combustion engine (ICE) generating sets, synchronous condensers (SCs), and battery energy storage systems (BESSs), detailed in Chapter 4.

Additionally, to validate the effectiveness of this power plant solution concept, frequency stability simulation and analysis are included in Chapters 5 and 6. This thesis was conducted for Wärtsilä Finland.

1.2 Research Methods

Throughout this thesis, the descriptive research method was primarily used in Chapters 2, 3, 4, and 5. In these chapters, the analytical research method was also employed for deriving formulas. For the frequency stability simulation studies presented in Chapters 5 and 6, analytical, computational, and case study research methods were utilized.

Frequency stability simulation studies consisted of:

- Development of simulation models.
- Creation of study cases.
- Analysis of simulation results.

Simulation models were developed as follows:

- DIgSILENT PowerFactory software was used to conduct frequency simulation studies.
- The Institute of Electrical and Electronics Engineers (IEEE) 14-Bus system model was used as a template, which was taken from DIgSILENT PowerFactory library.
- Grid voltage and total active power of the loads were chosen as 33 kV and 100 MW, respectively.
- The Wärtsilä ICE generating set model was used for synchronous generation units.
- Western Electricity Coordinating Council (WECC) models, which were taken from DIgSILENT PowerFactory library, of wind and solar power plants were used for the renewable generation units.
- The SC model was created based on Wärtsilä ICE generating set model.
- The BESS model was provided by one of the leading inverter manufacturers.

After developing the simulation models, 28 study cases were created to analyze and validate the effectiveness of the power plant solution concept in terms of frequency stability. The study cases were created based on:

- Three different shares of synchronous and renewable generation.
- Three different disturbances.
- Six different operation modes of power plant.

A summary of the created study cases is shown in **Table 1.**

Renewable Generation Share	Disturbance	Number of Study Cases
40 %	Synchronous generation unit trip	4
40 %	The largest load trip	4
40 %	The largest generation unit trip	4
70 %	Synchronous generation unit trip	4
70 %	The largest load trip	4
70 %	The largest generation unit trip	4
100 %	The largest load trip	2
100 %	The largest generation unit trip	2

Table 1. Study Cases.

1.3 Thesis Outline and Structure

This thesis is structured as follows: Chapter 2 provides an overview of the global energy transition, discussing renewable energy integration, structural changes in modern power systems, and changes on the demand side. Chapter 3 explores the challenges of global energy transition, focusing on the increasing need for flexibility, stability, controllability of the generation-load balance, and reliability. Chapter 4 introduces the concept of the Flexible Multi-Mode Power Plant Solution by detailing its components, operating modes and their applications in addressing energy transition challenges, as well as its operational philosophy. Chapter 5 describes the development of simulation models for frequency stability, and the creation of study cases. Chapter 6 presents and analyzes simulation results to evaluate the effectiveness of the power plant solution concept in terms of frequency stability. Chapter 7 concludes the thesis by summarizing the key findings from the frequency stability simulations and suggesting possible future studies.

2 Global Energy Transition

2.1 Introduction

Energy transitions have historically occurred for two main reasons: the development of new technologies and the emergence of energy sources with superior features (Blázquez et al., 2019). Because of these reasons, sources of energy have changed from biomass to coal, coal to oil, and oil to natural gas. The current global energy transition follows a similar trajectory: shifting the source of energy from all types of fossil fuels (coal, oil, and natural gas) to renewables such as wind and solar (S&P Global, 2020).

Although most of the past energy transitions were achieved over a long time, the current energy transition needs to happen very fast because of excessive carbon emissions (Blázquez et al., 2019). In **Figure 1,** the penetration speed of different fuels can be seen. The x-axis represents the years, while the y-axis indicates the percentage share of each fuel over time. The 1% penetration level is chosen as the starting point for each fuel. The dashed line labeled "Renewables in ET" represents the penetration speed of wind and solar energy, where ET refers to Energy Transition.

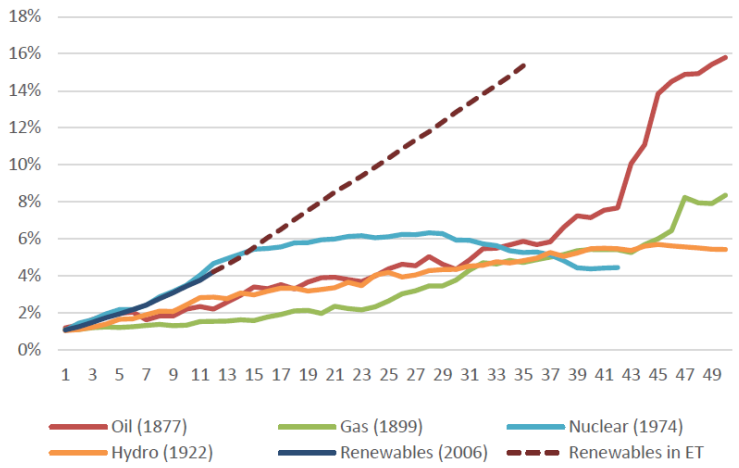

Figure 1. Penetration speed of different fuels in the global energy system (Blázquez et al., 2019).

Based on different scenarios, the share of wind and solar energy generation in total energy generation will be between 12% and 17% in 2040 (Blázquez et al., 2019).

Although many aspects of power systems are evolving with the global energy transition mentioned above, this thesis focuses on three main changes: renewable energy integration, structural changes in modern power systems, and changes on the demand side.

2.2 Renewable Energy Integration

As the population of the world increases, the demand for energy also increases. According to estimations, total energy consumption is expected to increase by nearly 40% by 2035, with an average of 1.4% increase each year. Similarly, the demand for oil is predicted to increase by an average of 0.8% each year during the same period. Since global oil reserves are estimated to last for only about 40 years, the importance of energy production from RESs becomes crucial for the future (Badal et al., 2019).

Figure 2 shows the global renewable energy capacity growth between 2017 and 2030. The green color represents actual growth in renewable energy capacity from 2017 to 2023 (in GW), while the red color indicates projected growth from 2024 to 2030 (in GW). MENA stands for the Middle East and North Africa, and ASEAN refers to the Association of Southeast Asian Nations.

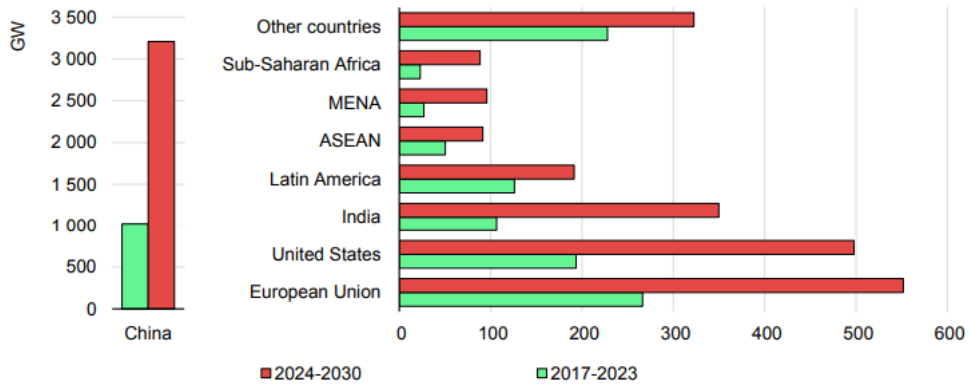

Figure 2. Global renewable energy capacity growth for 2017-2030 (International Energy Agency, 2024).

Figure 3 shows the global renewable energy capacity growth by technology segment between 2010 and 2030. As shown in the figure, photovoltaic (PV) and wind are expected to dominate renewable energy capacity growth in the coming years.

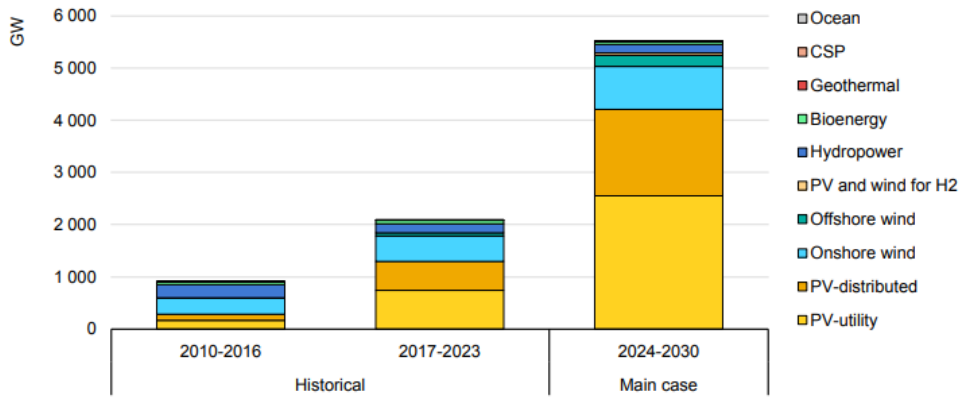

Figure 3. Global renewable electricity capacity growth by technology segment for 2010-2030 (International Energy Agency, 2024).

Figure 4 shows the projected share of global energy generation from renewables between 2030 and 2050. As shown in the figure, the share of renewable energy is expected to increase from around 40% in 2030 to around 80% by 2050.

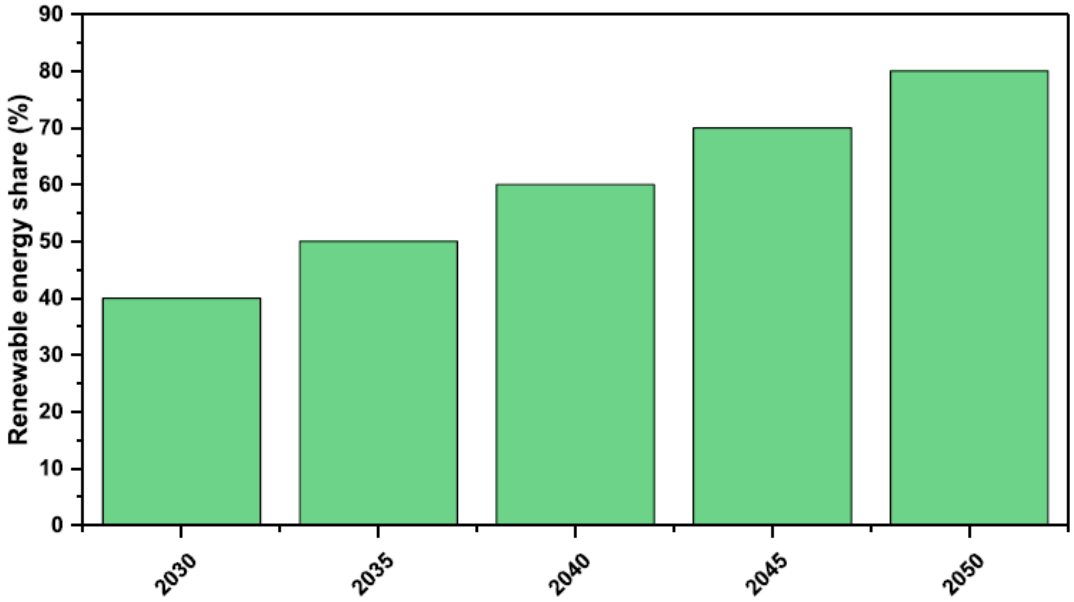

Figure 4. Projection of global energy generation from renewables (Hassan et al., 2024).

2.3 Structural Changes in Modern Power Systems

While numerous changes are ongoing, this thesis focuses on three key structural changes occurring in modern power systems due to the energy transition: the integration of power electronic devices into the grid, the connection of distributed energy resources (DERs) to distribution networks, and the emergence of microgrids.

2.3.1 The Integration of Power Electronic Devices into the Grid

Over the past few decades, power electronic devices have gained importance in areas such as automation and control, energy efficiency, and energy conversion. By playing a significant role in renewable energy systems, they also help reduce carbon emissions (Chakraborty, 2011).

With the help of power electronic devices, the effective integration of RESs into the grid is made possible. For example, in PV and wind systems, converters are used for DC/AC,

AC/DC, and DC/DC conversions. Moreover, power electronic devices help mitigate power system issues such as voltage and frequency fluctuations and reactive power compensation, which are caused by the intermittent and variable nature of RESs such as wind and solar (Tang et al., 2021).

Furthermore, with the increasing large-scale penetration of RESs into the grids, the need for advanced power electronic technologies becomes essential. Grid-forming inverters and multiport converters are examples of such technologies (Tang et al., 2021). With these technologies, renewable energy systems can operate independently without relying on traditional synchronous generators. Moreover, they provide grid stability by regulating frequency and voltage as well as improving energy conversion efficiency. Grid-forming inverters are also employed in BESSs, which is discussed in Chapter 4.1.2.

In conclusion, as the penetration of RESs increases, power electronic devices will play a key role in ensuring the reliable and efficient operation of the grid. Applications of power electronic devices are shown in **Figure 5.**

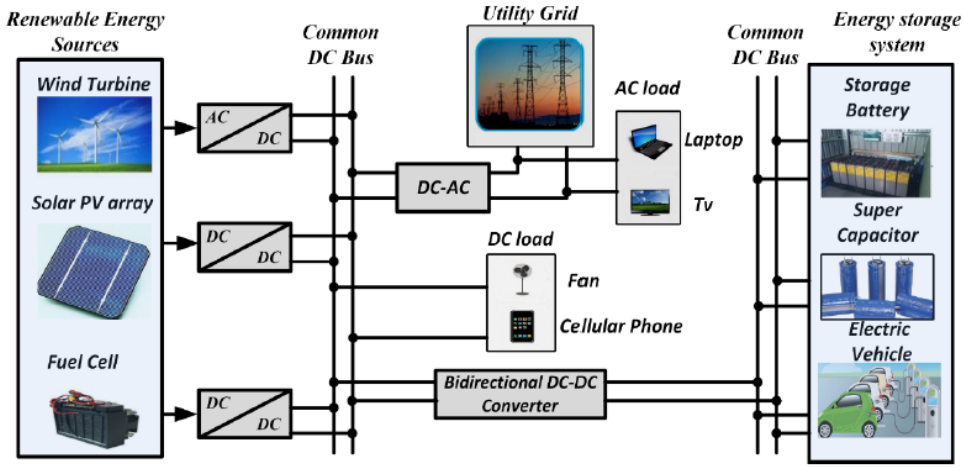

Figure 5. Applications of power electronic devices (Alatai et al., 2021).

2.3.2 The Connection of DERs to Distribution Networks

DERs are small-scale power generation or storage technologies that improve or replace traditional electrical systems, according to the US Federal Energy Regulatory Commission (Wang & Mori, 2024). Although they are primarily integrated into low-voltage distribution networks, they can also be connected to medium-voltage distribution networks (Caballero-Peña et al., 2022).

DERs include distributed generation (PV systems), storage systems (e.g., batteries), and electric vehicles (EVs). They have become popular in recent years due to their ease of integration into the distribution network at high volumes (Caballero-Peña et al., 2022).

DERs offer numerous benefits to consumers. By employing DERs, consumers can generate and consume electricity according to their needs, thereby reducing their reliance on the main distribution networks. Moreover, energy storage systems improve resilience by protecting consumers against electricity outages. EVs support energy transition by encouraging people to replace their fossil-fueled cars with electric ones (International Energy Agency, 2022).

In summary, integrating DERs into distribution networks is fundamental to the global energy transition. Through DER integration, grid resilience is improved, greenhouse gas emissions are reduced, energy generation is decentralized, and the number of prosumers is increased (Caballero-Peña et al., 2022).

2.3.3 The Emergence of Microgrids

Microgrids are localized and autonomous electrical systems in which electricity is generated, distributed, and stored according to the needs of communities (Shahzad et al., 2023). Typically, microgrids include DERs such as solar panels, wind-powered generators, and energy storage systems. Advanced power system control strategies are

used in microgrids, which make them beneficial where the electricity supply is unstable, unreliable, or expensive. The following are the characteristics of a microgrid (Hossain et al., 2019):

- Includes electricity generation units, ESSs, loads, and control strategies.
- Consists of distributed generation (DG) units, whose ratings are less than 100 MW.
- Consists of AC and/or DC distribution networks.
- Connects and disconnects from the utility grid at a point of common coupling (PCC).
- Generates reference voltage and frequency during islanded operation.
- Controls the supplied power for both islanded and grid-connected operations.
- Adapts to unexpected situations such as unintentional islanding or faults.

Three types of microgrids exist based on the type of power injection into the distribution network: AC, DC, and hybrid microgrids (Hossain et al., 2019).

AC microgrids: As the name implies, AC microgrids supply AC power into the distribution network. The primary advantage of AC microgrids is the easy connection to the existing utility grid without using converters and their controls (Hossain et al., 2019). There are three types of AC distribution systems: single-phase, three-phase with neutral point lines, and three-phase without neutral point lines.

DC microgrids: DC microgrids have become popular due to the availability of DC sources such as solar and fuel cells and improvement of modern power electronic devices (Hossain et al., 2019). Shipboard power systems, telecommunication systems, and EVs are examples of DC power system applications. The differences between AC and DC microgrids are presented **in Table 2.**

Factors	AC Microgrids	DC Microgrids
Conversion efficiency	Multiple energy conversions reduce efficiency	Less conversion processes increase efficiency
Transmission efficiency	Continuous reactive current loss reduces efficiency	Absence of reactive components increases efficiency
Stability	Affected by external disturbances	Free from external effects
Synchronization	Synchronization required	No synchronization issues
Power supply reliability	Supply can be affected during seamless transfer	Power supply generally reliable
Microgrid controls	Control process complex due to frequency	Simple control approach
Protection system	Simple, cheap and mature protection schemes	Complex, costly and immature protection components
Suitability	AC loads	DC loads
Calculation methods	Complex numbers involved	Only real numbers used

Table 2. AC and DC microgrid comparison (Hossain et al., 2019).

Hybrid microgrids: These microgrids include AC and DC distribution networks, with a microgrid central controller. The benefit of hybrid microgrids is to enhance the efficiency of the network by minimizing power conversion stages, decreasing the number of interfacing devices, improving reliability, and reducing energy costs (Hossain et al., 2019). With hybrid microgrids, consumers can use AC or DC power depending on their specific needs. A hybrid microgrid structure is shown in **Figure 6.**

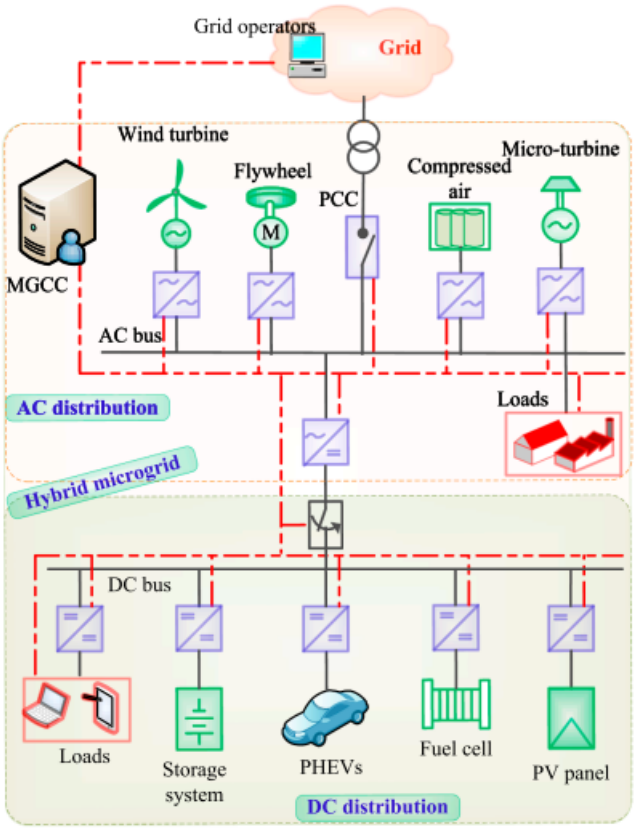

Figure 6. A hybrid microgrid structure (Hossain et al., 2019).

Moreover, microgrids can be grouped according to their locations as islanded or grid-connected (Hossain et al., 2019).

Islanded microgrids: Islanded microgrids are also known as remote, standalone or autonomous microgrids (Hossain et al., 2019). These microgrids are not connected to the utility grids because of geographical reasons or grid limitations. They operate in remote areas such as military zones and islands.

Grid-connected microgrids: Grid-connected microgrids are also known as urban microgrids (Hossain et al., 2019). They are usually connected to the utility grid via PCC, where they can exchange power. A grid-connected microgrid can operate as an islanded microgrid in case of unusual situations such as faults or maintenance on the utility grid.

The concept of microgrids is particularly important in this thesis because, in Chapters 5 and 6, the frequency stability performance of the power plant solution concept is assessed using an islanded AC microgrid model based on the IEEE 14-Bus system.

2.4 Changes on the Demand Side

Energy transition changes the behavior of demand side i.e. consumers. Nowadays, consumers want to be independent from utility companies. They aim to become prosumers, i.e., produce and sell their own electricity, as discussed in Subchapter 2.3.2. Moreover, consumers prefer to use energy which is produced by renewables. According to some research and analysis, generally people want to pay for cleaner electricity (Blázquez et al., 2019).

In addition, the management of energy consumption is also changing as the integration of RESs into the grids increases (Kuzemko et al., 2017). This shift is driven by the demand-side management technologies such as demand response (DR), smart meters, and energy storage.

DR refers to the adjustment of electricity consumption according to the signals given by utility companies or grid operators. The aim of DR is to shift or reduce electricity consumption during peak demand periods. DR not only improves grid efficiency and stability by balancing supply and demand but also decreases the cost of electricity for customers. DR is feasible, especially in Nordic countries, where electricity is used for space and water heating (Kirkerud et al., 2021). For example, in Finland, with the help of DR programs, consumers reduce their electricity consumption during winter when heating demand peaks. Similarly, in Sweden, demand-side management is improved by using smart meters, with which electricity consumption can be adjusted in real-time.

Furthermore, due to the increasing complexity of the electrical grid and the interaction between prosumers and utility operators in the future, the use of advanced communication and monitoring systems, such as Internet of Things (IoT), machine-to-machine (M2M) communication, and Supervisory Control and Data Acquisition (SCADA) is also expected to increase (Lopes et al., 2019).

In summary, with the demand-side changes discussed above, consumers will increasingly take active roles in the future, rather than passively receiving energy services.

3 Challenges of the Global Energy Transition

The global energy transition brings a wide range of developments in modern power systems, including increasing penetration of RESs and DERs into electrical networks, a growing number of power electronic devices, and more widespread bidirectional power flows (Meegahapola et al., 2021).

Since technologies that come with the global energy transition have an interdependent nature, their integration with traditional power systems will create complex challenges. These challenges will affect and change the operation of power grids. In fact, in countries where renewable energy generation has a high share, such as Australia, the UK, and Ireland, challenges related to the energy transition have already been observed (Meegahapola et al., 2021).

While the global energy transition introduces many challenges, the following subchapters discuss four key areas: the increasing need for flexibility, stability, controllability of the generation-load balance, and reliability.

3.1 The Increasing Need for Flexibility

According to Conseil International des Grands Reseaux Electriques (CIGRE), flexibility is "the capability to consume or produce electrical energy in response to changing power system conditions" (Hillberg et al., 2022, p. 3). With the energy transition, the share of renewable energy generation in power systems increases steadily, creating greater flexibility demands on existing traditional generation units (Agora Energiewende, 2017).

The main reason for the increasing need for flexibility is the nature of RESs (Agora Energiewende, 2017). Unlike traditional generation, RESs cannot easily follow demand because their output depends on weather conditions as well as daily and seasonal changes.

Moreover, the marginal cost of RESs is nearly zero, i.e., as long as the primary resource such as wind or sun is available, they generate energy with negligible operating costs. These factors contribute to the increasing need for flexibility to respond to variations in renewable generation.

To meet the increasing need for flexibility that arises from the integration of RESs, several options are currently available (Agora Energiewende, 2017). One option is to increase the flexibility of existing power plants, which is discussed in Chapter 4.1.1. Another option is to use traditional energy storage technologies, such as pumped hydro storage, or newer energy storage technologies, such as batteries.

3.2 Stability

Kundur (1994) defined power system stability as follows:

> Power system stability may be broadly defined as that property of a power system that enables it to remain in a state of operating equilibrium under normal operating conditions and to regain an acceptable state of equilibrium after being subjected to a disturbance. (p. 17)

In stability evaluation, the primary focus is on the behavior of the power system when subjected to a disturbance (Kundur, 1994). The disturbance can be small or large. Continuous load changes are an example of small disturbances (Kundur, 1994). In such cases, the system must operate satisfactorily and adjust itself accordingly to meet the load changes.

On the other hand, short circuits, loss of a generator, loss of a load, or a tie loss between two subsystems are examples of large disturbances (Kundur, 1994). More aspects of the system are affected by large disturbances. For example, a short circuit causes variations in the power transfer, the rotor speed of synchronous machines, and bus voltages.

With the energy transition, generation from power electronic converter (PEC)-interfaced RESs started to emerge and change the power system domain (Meegahapola et al., 2020). The operational differences between PEC-interfaced generation and conventional synchronous generation affect power system stability.

As an example, one of the differences is that, while conventional synchronous generation dynamics are analyzed in the time range between 10^{-2} to 10^{3} s, PEC-interfaced RES power system dynamics analysis is moved to between 10^{-6} to 10^{-4} s due to the inverter switching dynamics (Meegahapola et al., 2020). **Figure 7** shows the timescales of the dynamics of PEC-interfaced generation (electromagnetic) and conventional synchronous generation (electromechanical).

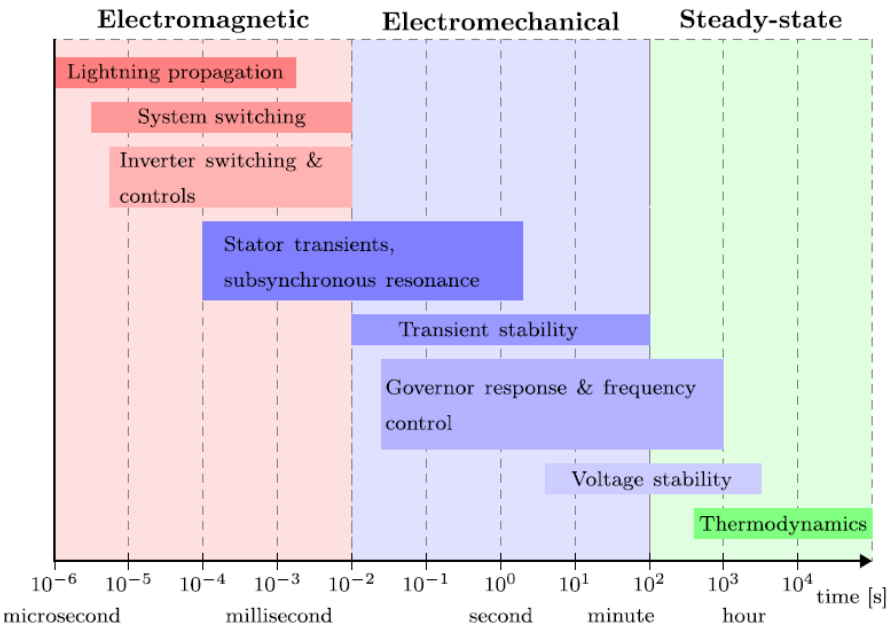

Figure 7. Electromagnetic and electromechanical power system dynamics (Meegahapola et al., 2020).

The replacement of conventional synchronous generation with PEC-interfaced RES results in reduced inertia (stored energy capacity), lower short-circuit strength, and decreased ability to respond to frequency and voltage changes, all of which affect power system stability in the following areas (Meegahapola et al., 2020):

- Frequency stability
- Voltage stability
- Rotor angle stability
- Sub-synchronous resonance and oscillatory stability

3.2.1 Frequency Stability

According to the IEEE/CIGRE Task Force, frequency stability is “the ability of the power system to maintain steady-state frequency, following a severe system upset, resulting in a significant imbalance between generation and load" (as cited in Abdulraheem & Gan, 2016, p. 5688).

The frequency of the power system should remain within an acceptable range (Shrestha & Gonzalez-Longatt, 2021). The nominal frequency and acceptable frequency ranges for some countries are shown in **Table 3.**

Countries	Nominal Frequency (Hz)	Frequency Limits (Hz)	Frequency Limits (p.u.)
Germany	50	$47.5 < f_{grid} < 51.5$	$0.95 < f_{grid} < 1.03$
Denmark	50	$48.5 < f_{grid} < 51$	$0.97 < f_{grid} < 1.02$
Spain	50	$47.5 < f_{grid} < 51.5$	$0.95 < f_{grid} < 1.03$
Canada	60	$59.4 < f_{grid} < 60.6$	$0.99 < f_{grid} < 1.01$
China	50	$49.5 < f_{grid} < 50.2$	$0.99 < f_{grid} < 1.004$
Puerto Rico (PREPA)	60	$57.5 < f_{grid} < 61.5$	$0.96 < f_{grid} < 1.025$
USA (NERC)	60	$58.5 < f_{grid} < 61$	$0.98 < f_{grid} < 1.02$
Japan (east)	50	$47.5 < f_{grid} < 51.5$	$0.95 < f_{grid} < 1.03$
Japan (west)	60	$58 < f_{grid} < 61.8$	$0.97 < f_{grid} < 1.03$
Australia	50	$47.5 < f_{grid} < 52$	$0.95 < f_{grid} < 1.04$
South Africa	50	$49 < f_{grid} < 51$	$0.98 < f_{grid} < 1.04$
Malaysia	50	$47 < f_{grid} < 52$	$0.94 < f_{grid} < 1.04$
Ireland	50	$49.5 < f_{grid} < 50.5$	$0.99 < f_{grid} < 1.01$
Romania	50	$47.5 < f_{grid} < 52$	$0.95 < f_{grid} < 1.04$
South Africa	50	$47.5 < f_{grid} < 52$	$0.95 < f_{grid} < 1.04$
Brazil	60	$56 < f_{grid} < 63$	$0.93 < f_{grid} < 1.05$

Table 3. Frequency limits for some countries (Landera et al., 2023).

For the frequency to remain within an acceptable range, total generation and total demand should be as close as possible (Shrestha & Gonzalez-Longatt, 2021). However, imbalances between generation and demand continuously occur due to their dynamic

nature, resulting in frequency deviations. If these deviations remain within acceptable limits, no significant impact will be observed on the power system. On the other hand, if frequency deviations exceed a certain threshold, the operation, reliability, efficiency, and security of the power system will be affected.

Because of the nonlinear nature of power systems, classification is necessary to understand power system stability (Abdulraheem & Gan, 2016). In the case of frequency stability, classification is based on the time frame. Therefore, frequency stability is classified as short-term and long-term according to the IEEE/CIGRE Task Force.

The duration of a short-term frequency stability is typically within the time frame of a few seconds (Abdulraheem & Gan, 2016). Islanding caused by a lack of generation or inadequate load shedding can be given as an example.

On the other hand, the duration of a long-term frequency stability ranges from ten seconds to several minutes. (Abdulraheem & Gan, 2016). Speed control of a steam turbine and control of a boiler or reactor are examples of long-term frequency stability.

With the energy transition, modern power systems will face short-term frequency stability issues mainly for two reasons (Shrestha & Gonzalez-Longatt, 2021):

a) The increasing penetration of PEC-interfaced RESs reduces system inertia, which is the resistance of a physical object to changes in its state of motion, including its speed and direction (Tielens & Van Hertem, 2016).
b) The unpredictable nature of RESs creates challenges in maintaining the generation-demand balance.

The justification for (a) is as follows:

The swing equation, which relates the imbalance between generation and demand to the frequency deviation, explains that when generation is not equal to demand, frequency deviations occur in power systems (Shrestha & Gonzalez-Longatt, 2021). The equation is expressed as:

$$M \frac{d^2\delta(t)}{dt^2} = P_m - P_e - D \frac{d\delta(t)}{d(t)} \quad (1)$$

where, M is the inertia coefficient in MVAs²/rad, δ(t) is the rotor angle in rad, P_m is the mechanical power input in MW, P_e is the electrical power output in MW, and D is the damping coefficient in Nms.

In this equation, if the damping coefficient (D) is ignored and $M = 2H/\omega_s$ is substituted, the swing equation becomes (per-unit):

$$\frac{2H}{\omega_s} \frac{d^2\delta(t)}{dt^2} = P_m - P_e \quad (2)$$

where H is the inertia constant, and ω_s is the angular velocity of the power system, which is directly related to the frequency of the power system.

In equation (2) inertia constant, H can be expressed as

$$H = \frac{(1/2)j(\omega_0)^2}{S} = \frac{E_{kin}}{S} = \frac{H_i S_i}{S_{sys}} \quad (3)$$

$$H_{sys} = \frac{E_{kin,sys}}{S_{sys}} = \frac{\sum_{i=1}^{n} H_i S_i}{S_{sys}} \quad \text{where;} \quad (4)$$

j is moment of inertia of the machine, ω_0 is nominal rotational speed of machine, S is the rated power of the machine, E_{kin} is the kinetic energy of the machine, H_i is the inertia of the i-th machine, S_i is the rated power of the i-th machine, S_{sys} is the system base, H_{sys} is the equivalent inertia of the whole power system, and $E_{kin,sys}$ is the kinetic energy of the whole power system (Shrestha & Gonzalez-Longatt, 2021).

Equations (2) and (3) explain that, for a synchronous machine with constant rated power, the system inertia is directly proportional to the kinetic energy of the machine. In other words, the larger the machine's kinetic energy, the greater its inertia.

Traditional power systems, which contain synchronous generators, have high kinetic energy and, consequently, high inertia due to the rotating mass of these machines. Higher inertia reduces the rate of change of frequency and enables faster frequency recovery following disturbances (Shrestha & Gonzalez-Longatt, 2021). This happens because through inertia, kinetic energy is released instantaneously and naturally in synchronous generators during imbalances (Billimoria et al., 2020).

In contrast, modern power systems with high penetration of RESs, such as wind and solar, have significantly less kinetic energy and inertia compared to traditional power systems due to the absence of rotating mass in RES technologies (Shrestha & Gonzalez-Longatt, 2021). As a result, the reduction in inertia in modern power systems increases the risk of frequency instability during disturbances, potentially leading to blackouts. Additionally, the rate of change of frequency (RoCoF) and the magnitude of frequency deviations increase significantly in these systems.

3.2.2 Voltage Stability

Hatziargyriou et al., (2021) define voltage stability as “the ability of a power system to maintain steady voltages close to nominal value at all buses in the system after being subjected to a disturbance” (p. 3275). Voltage instability may result from load losses, cascading outages caused by the loss of synchronism in generators, and the tripping of transmission lines or other network components by protection systems (Hatziargyriou et al., 2021).

While most voltage instability cases are undervoltage instability, overvoltage instability also occurs (Hatziargyriou et al., 2021). Overvoltage instability may be experienced due to the capacitive behavior of the electrical network elements, such as capacitors and filter banks, and the operation of under-excitation limiters, whose duty is to prevent generators and synchronous condensers from absorbing excess reactive power.

To achieve voltage stability, generation and transmission systems must be capable of providing the power demanded by loads (Hatziargyriou et al., 2021). This capability is related to the voltage drop that occurs as active and reactive power flow through the inductive reactance of the transmission network. Moreover, it is limited by the maximum power that can be transferred to a specific set of buses.

Voltage stability is commonly classified into two categories: short-term and long-term. Typically, the duration of short-term voltage stability studies is several seconds. Induction motors, electronically controlled loads, high voltage direct current (HVDC) links, and inverter-based generators are influenced by short-term voltage stability (Hatziargyriou et al., 2021).

On the other hand, the duration of long-term voltage stability studies can be up to several minutes. Slower-acting equipment, such as tap-changing transformers and thermostatically controlled loads, is influenced by long-term voltage stability (Hatziargyriou et al., 2021).

Voltage stability is being challenged as inverter-interfaced RESs replace traditional synchronous generators, due to their limited voltage control capability compared to conventional generation systems. As a result, the following voltage stability challenges are expected in power systems (Kanojia & Suthar, 2024):

- Uncertainty in power flow and voltage profiles across the power system.
- Complications with the operation of voltage and reactive power control devices across different regions of interconnected power systems.
- Increased unnecessary operation of discrete reactive and voltage control devices.
- Difficulties in the reactive power market.

3.2.3 Rotor Angle Stability

According to Kundur (1994), rotor angle stability is “the ability of interconnected synchronous machines of a power system to remain in synchronism” (p. 18). Rotor angle stability is concerned with how the output power of synchronous machines changes in response to rotor oscillations. Rotor angle stability is usually categorized into two types, namely small-signal stability and transient stability.

“Small-signal (or small-disturbance) stability is the ability of the power system to maintain synchronism under small disturbances” (Kundur, 1994, p. 23). Small changes in load and generation create these continuous instabilities.

On the other hand, “transient stability is the ability of the power system to maintain synchronism when subjected to a severe transient disturbance” (Kundur, 1994, p. 25). Severe disturbances in power systems, such as faults, create these instabilities, where the generator rotor angle deviates significantly (Kundur, 1994).

Figure 8 shows the rotor angle response of a synchronous machine in three different transient disturbance cases. In Case 1, the rotor angle initially increases to a maximum. After reaching the maximum, it decreases and continues to oscillate with decreasing amplitude until it reaches a steady state. In Case 2, the rotor angle continues to increase until synchronism is lost. In Case 3, during the first swing, the system is stable, but then it becomes unstable due to growing oscillations. This form of instability is not necessarily caused by the transient disturbance but occurs when the post-fault steady-state condition itself is small-signal unstable (Kundur, 1994).

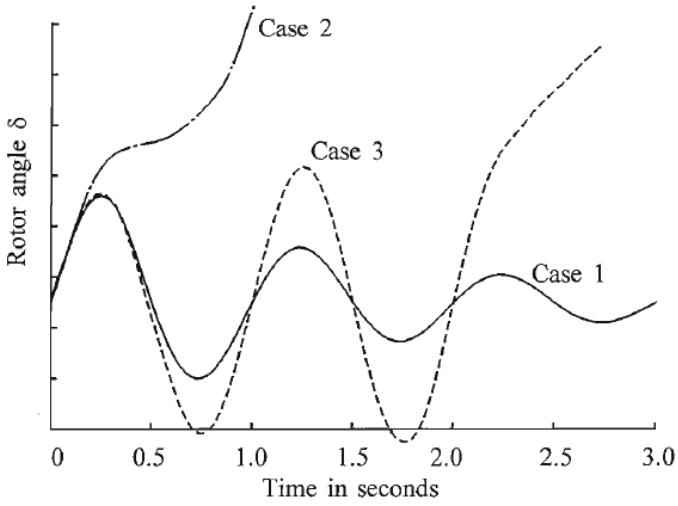

Figure 8. Rotor angle response of three transient disturbances (Kundur, 1994).

In case of a transient disturbance, the rotor angle of a synchronous generator changes according to the swing equation:

$$M\frac{d^2\delta(t)}{dt^2} = P_m - P_e - D\frac{d\delta(t)}{d(t)} \quad (5)$$

where, M is the inertia coefficient in MVAs²/rad, δ(t) is the rotor angle in rad, P_m is the mechanical power input in MW, P_e is the electrical power output in MW, and D is the damping coefficient in Nms. In this equation, M and D are constants for a synchronous generator. Moreover, Pm is typically considered to be constant during the first few seconds of the disturbance. So, the rotor angle stability is determined mainly by P_e.

P_e of the generator is given by the equation:

$$P_e = \frac{EV}{X}\sin(\delta), \text{ where;} \quad (6)$$

E is the internal electromotive force (EMF) of the generator in kV or per-unit, V is the terminal voltage of the generator in kV or per-unit, X is the synchronous reactance of the generator in ohms or per-unit and δ is the rotor angle between E and V.

From equation (6), it can be seen that P_e is affected by the terminal voltage of the generator (Meegahapola et al., 2020). Hence, when the power system is dominated by PEC-interfaced RESs, the rotor angle behavior is determined by their terminal voltage.

Moreover, the reduction in inertia in power grids due to the integration of PEC-interfaced RESs causes an increasing deviation of the terminal voltage angle, which leads to rotor angle instability since the rotor angle is measured with respect to the terminal voltage angle (Meegahapola et al., 2020).

3.2.4 Sub-Synchronous Resonance and Oscillatory Stability

Wind farms are typically installed far from consumption centers, where wind speeds are higher. Generally, capacitors are added in series to the transmission lines that carry wind power to increase transmission capacity and decrease voltage drop (Samanes et al., 2020). However, when the net impedance becomes negative at low frequencies (below the fundamental frequency), the interaction between wind turbine generators and the series capacitors can cause oscillations that may lead to instability. This instability is influenced by the controllers of power converters and the rotational speed of wind turbine generators. This event, in which the electrical grid, wind turbine generators, and the controllers of power converters are involved, is called sub-synchronous resonance and it can limit the integration of wind power plants into the grid.

With the increasing penetration of RESs, sub-synchronous resonance and oscillatory instability become more critical and more complex (Xu et al., 2018). For example, since 2011, in China, the interaction between wind turbine generators and nearby series capacitors has often caused sub-synchronous oscillations with frequencies between 3 and 10 Hz, which have led to wind generator tripping and abnormal transformer vibrations (Xu et al., 2018).

3.3 Controllability of the Generation-Load Balance

Power systems are generally divided into two sides in terms of power flow: the generation side and the load side. In traditional power systems, the generation side is fully controllable, while the load side is fully uncontrollable (Li et al., 2022).

The controllability of the generation-demand balance power systems has changed dramatically over the past few decades. With the increasing penetration of variable renewable energy (VRE) sources in power grids, the generation side has also become partly uncontrollable. To reduce the effects of uncontrollability on both sides, efforts such as demand response programs and the implementation of energy storage systems have started from the load side. In this way, the controllability of loads is being increased (Li et al., 2022).

There are several reasons why controllability of the generation-load balance is a challenge in power systems with high penetration of RESs. In this thesis, three key reasons are discussed: forecasting challenges, coordination complexity, and lack of dispatchability.

1. Forecasting Challenges:

As the integration of RESs into existing power networks has increased over the past few decades, the importance of forecasting their output power has become significant for both economic and reliability reasons.

Forecasting the power output of RESs, especially wind and solar, is challenging due to their variable nature, limited predictability, and instantaneous response to weather phenomena (Sweeney et al., 2020).

2. Coordination Complexity:

In traditional power systems, the balance between generation and load is maintained by power system operators within geographic boundaries known as balancing areas

(Katz et al., 2015). Generally, multiple balancing areas are connected to each other through one interconnection. Balance is usually achieved through unit commitment, which involves starting generators in advance. When power is needed, operators dispatch power from available generators while minimizing operating costs and maintaining reliability.

As mentioned, VRE sources add complexity to the balance of generation and load. The output power of VRE sources cannot be accurately predicted by system operators, as forecasting them with 100% accuracy is not possible. Essentially, there are two types of inaccurate predictions: underprediction and overprediction.

In the case of underprediction, operators underpredict the availability of VRE sources and schedule more generation than needed (Katz et al., 2015). This causes too many generators to run at partial output, which reduces efficiency and increases costs. On the other hand, in an overprediction situation, operators overpredict the availability of VRE sources and schedule less generation than needed. To address the balancing problem, generators with fast-start capability can be used, although they are expensive. Also, in extreme cases, load shedding can be utilized to reduce demand to match generation, however this decreases system reliability.

As a result, traditional balancing methods and balancing areas are expected to change due to the integration of VRE sources, leading to increased coordination complexity between generation and load (Katz et al., 2015).

3. Lack of Dispatchability:

One of the key factors in matching generation and load is being readily dispatchable. The output power cannot be adjusted according to the demand in non-dispatchable generation, except through curtailment, which is the deliberate reduction of output power.

While some RESs, such as hydropower, geothermal, and bioenergy have this property, wind and solar generation do not, and hence they are considered non-dispatchable sources. In any case, generation is not possible when there is no resource (e.g., at night for solar energy or when there is no wind for wind energy) (Hafner & Luciani, 2022).

3.4 Reliability

The main task of a power system is to supply power to consumers as reliably as possible at all times, even during faults. The probability of a device or system performing its tasks over time under its operational conditions is called reliability. Generally, two aspects are considered in power system reliability: adequacy and security (Aruna et al., 2021).

Adequacy is concerned with the current condition of the power system and checks whether proper infrastructure exists to fulfill consumer demand. Scheduled and unscheduled outages of system components can also be considered in the case of adequacy (Aruna et al., 2021).

On the other hand, system security is concerned with the endurance of the power system in the event of sudden disturbances. Short circuits, failure of components, generation system problems, transmission system problems, sudden loss of equipment, and climatic conditions are some examples such disturbances (Aruna et al., 2021).

With energy transition, RESs will become the primary energy source. DGs and microgrids, which are enabled by RESs, will introduce integration and operational challenges. As a result, extensive research and analysis should be conducted on the integration of DGs and microgrids with respect to reliability. Below are some research findings that have already been identified (Aruna et al., 2021):

- The integration of DGs, microgrids, and energy storage systems with decentralized control strategies should be analyzed from a reliability point of

view, considering active and reactive power sharing, power and energy management, and protection management.

- The complexity and interdependency challenges created by integrating new RESs and EVs into the existing grid require more advanced reliability analysis.
- The uncertainties associated with RES-based generation must be studied in terms of both reliability and security.

4 The Flexible Multi-Mode Power Plant Solution

In this chapter, the flexible multi-mode power plant solution concept is proposed to address the energy transition challenges previously discussed in Chapter 3. This solution concept (**Figure 9**), which consists of ICE generating sets, BESSs, and SCs, presents a promising approach to mitigating challenges especially encountered by power grids with high renewable penetration and by microgrids, both islanded and grid-connected.

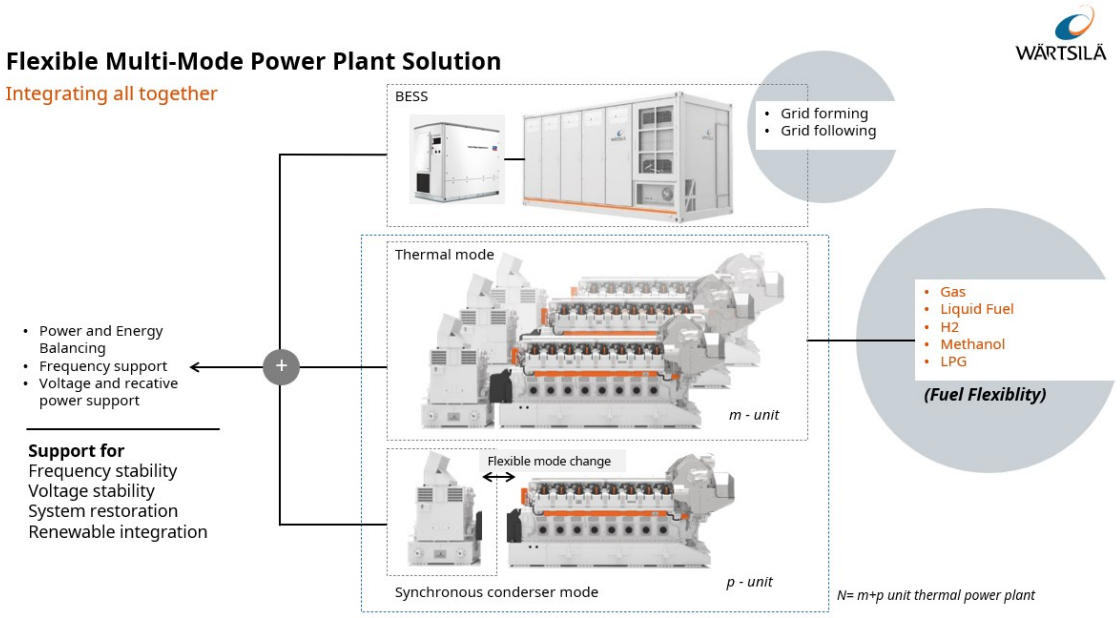

Figure 9. The Flexible Multi-Mode Power Plant Solution.

As the name implies, the solution concept can operate in different modes according to the needs of power systems. By employing eleven different modes (which will be discussed in Subchapter 4.2), the solution concept offers significant advantages in terms of flexibility, stability, controllability of the generation-load balance, reliability, and renewable integration, making it a promising approach for transitioning to a cleaner, more flexible, and stable power system.

4.1 Components of the Flexible Multi-Mode Power Plant Solution

4.1.1 Internal Combustion Engine Generating Sets

Although different types of thermal power generation exist, ICE generating sets are selected for the flexible multi-mode power plant solution concept, as justified below.

To evaluate the flexibility of thermal power generation units, objectives shown in **Figure 10** are used.

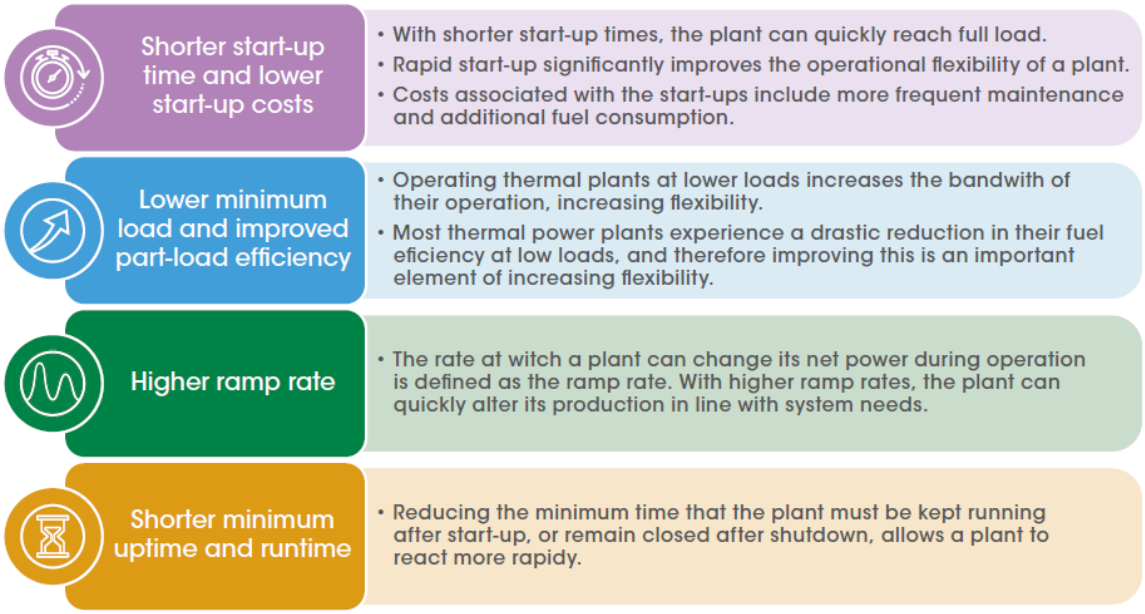

Figure 10. Flexibility parameters (International Renewable Energy Agency (IRENA), 2019).

In general, while baseload power plants are designed with low flexibility, peaking power plants offer comparatively high levels of flexibility (IRENA, 2019). For instance, nuclear power plants, which are baseload power plants, are inflexible. On the other hand, coal and gas power plants (coal power plants are less flexible than gas power plants) that can be used between baseload and peak load offer more flexibility.

In the case of gas power plants, combined-cycle gas turbine (CCGT) power plants are less flexible than open-cycle gas turbine (OCGT) power plants (IRENA, 2019). Gas-fired ICE power plants offer the most flexibility, and they are generally used for applications where high levels of flexibility are needed.

The flexibility of thermal power plants can be increased by retrofitting certain physical components, as well as making operational modifications to achieve the objectives shown in **Figure 10.**

Table 4 shows flexibility parameter values for different thermal power plant technologies. While the first set ("Average plant") corresponds to the values before refurbishment, the second set ("Post flexibilization/advanced plant") corresponds to the values after the refurbishment.

Type of point		Start-up time*	Start-up cost (USD/MW instant start)	Minimum load [% P_{nom}]	Efficiency (at 100% load)	Efficiency (at 50% load)	Avg. ramp rate [% P_{nom}/min]	Minimum uptime	Minimum downtime
Hard coal	Average plant	2–10 h[a]	> 100	25–40%[a]	43%	40%	1.5–4%[a]	48 h	48 h
	Post flexibilisation	80 min–6 h[a]	> 100	10–20%[b]	43%	40%	3–6%[a]	8 h	8 h
Lignite	Average plant	4–10 h[a]	> 100	50–60%[a]	40%	35%	1–2%[a]	48 h	48 h
	Post flexibilisation	75 min–8 h[c]	> 100	10–40%[b]	40%	35%	2–6%[c]	8 h	8 h
CCGT	Average plant	1–4 h[a]	55	40–50%[a]	52–57%	47–51%	2–4%[a]	4 h	2 h
	Post flexibilisation initiatives	30 min–3 h[a]	55	20–40%[c]	52–57%	47–51%	8–11%[c]	4 h	2 h
OCGT	Average plant	5–11 min	< 1–70	40–50%	35–39%	27–32%	8–12%	10–30 min	30–60 min
	Post flexibilisation/ advanced plant	5–10 min	< 1–70	20–50%	35–39%	27–32%	8–15%	10–30 min	30–60 min
ICE[c]	Average plant	5 min	< 1	20% (per unit)	45–47%	45–47%	> 100%	< 1 min	5 min
	Post flexibilisation/ advanced plant	2 min	< 1	10% (per unit)	45–47%	45–47%	> 100%	< 1 min	5 min

* Start-up times are longer for cold start-up (plant shut for more than 48 hours) than for hot start-up (plant shut for less than 8 hours).

Table 4. Flexibility parameters of different thermal power plants (IRENA, 2019).

However, increasing the flexibility of thermal power plants with refurbishments brings disadvantages in terms of cost, efficiency, and operational point of view (IRENA, 2019). For instance, for coal power plants, investments in retrofitting instruments are needed (IRENA, 2019). Moreover, the operational costs are increased since flexibilization in coal power plants brings increased maintenance needs and reduced efficiency.

In the case of CCGT power plants, flexibility is restricted by the heat recovery steam generator, the steam turbine and the balance of plant (IRENA, 2019). Design and operational changes are necessary in these power plants to make them more flexible.

A CCGT power plant can be converted into an OCGT power plant, which offers more flexibility. However, such a conversion is costly since the power plant needs to be out of service during the conversion process (IRENA, 2019). Moreover, with the conversion, the operating efficiency of the power plant can be reduced, which in turn increases the carbon dioxide intensity, CO_2(kg)/kWh.

On the other hand, to increase flexibility, there have been developments in gas turbine power plant technology, which is another type of thermal power plant technology. For example, GE designed a new gas turbine with which the ramp rate improves from 10-20 MW/min to 50 MW/min, and the start-up time improves from 1-4 hours to under 30 minutes (IRENA, 2019).

Lastly, advanced ICEs developed by Wärtsilä offer even higher operational flexibility (as shown in **Table 4**) thanks to their multi-unit design, fast start-up time (2 minutes), fast ramp rate, and the capability to operate at loads as low as 10% (IRENA, 2019). With multi-unit design Wärtsilä ICEs can supply a wide range of electrical power output at high efficiency, which provides reliability and resiliency to the power system compared to large centralized single units, which create significant threats to the grid and have inadequate load efficiency (Wärtsilä, 2020).

In addition to the operational flexibility mentioned above, ICEs can also offer structural flexibility in terms of operating with different fuel options such as liquid fossil fuels (diesel, heavy fuel oil, light fuel oil), gaseous fossil fuels (natural gas), as well as sustainable fuels, such as traditional biofuels and synthetic fuels (Wärtsilä Energy Solutions, n.d.). Moreover, ICEs can switch fuels instantaneously when they operate. For example, a Wärtsilä engine starts operating with a liquid fuel, such as diesel, and then it can switch to a gaseous fuel, such as natural gas, without having performance problems (Wärtsilä Energy Solutions, n.d.).

Furthermore, research on using sustainable fuels in ICEs, especially hydrogen, is continuing. For example, currently, Wärtsilä's gas engines can work with up to 25% hydrogen blended with natural gas. In the future, the operation of 100% hydrogen-fueled ICEs will be made possible (Wärtsilä Energy Solutions, n.d.).

As a result, in terms of operational flexibility, i.e., response to variability in renewable energy generation, financially, and environmentally, ICEs are seen as the best choice for thermal power generation units, and hence they are chosen as thermal power generation units for the flexible multi-mode power plant solution concept.

4.1.2 Battery Energy Storage Systems

Although various types of energy storage technologies exist for power system applications, which will be explained below, BESSs are selected as the energy storage option for the flexible multi-mode power plant solution concept due to their extensive power and energy applications.

There are five different energy storage technologies as shown in **Figure 11.**

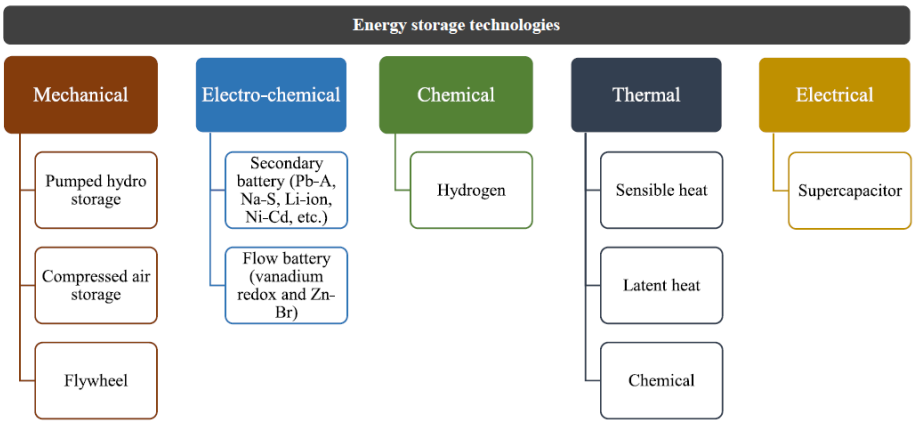

Figure 11. Energy storage technologies (Rahman et al., 2020).

In mechanical energy storage systems, electrical energy is converted into stored mechanical energy. There are three types of mechanical energy storage systems, namely pumped hydro energy storage, compressed air energy storage, and flywheel energy storage (Khan et al., 2024). Pumped hydro energy storage systems store energy by pumping water to a higher elevation, compressed air energy storage systems store energy by compressing air into reservoirs, and flywheel energy storage systems store energy in a rotating flywheel.

Pumped hydro energy storage systems are suitable for bulk energy applications, since their rated capacity is between 100 to 2000 MW. They have high efficiency, long discharge durations, and long lifecycles (Rahman et al., 2020). Flywheel energy storage systems can be used for applications such as grid stability, renewable energy integration, and uninterruptible power supply, thanks to their high efficiency (80-90%), short response time, and long lifetime.

In hydrogen energy storage systems, water is electrolyzed to produce hydrogen and oxygen. While hydrogen is stored, oxygen is released. For electrical grid energy applications, hydrogen is re-electrified by using fuel cells and combined with oxygen to generate electricity. Water and heat are also released in this process (European Association for Storage of Energy, 2016). Low conversion efficiency and high capital cost

are the two main challenges to integrate hydrogen energy storage systems into the utility grids (Rahman et al., 2020).

Thermal energy storage systems store energy by cooling, heating, melting, condensing, or vaporizing materials (Khan et al., 2024). There are three types of thermal energy storage systems: sensible heat energy storage systems, latent heat energy storage systems, and thermochemical energy storage systems. Moreover, based on the operating temperature of the energy storage material, there are two types of thermal energy storage systems: low-temperature energy storage systems and high-temperature energy storage systems. Low-temperature energy storage systems can be used for high-power density applications such as load shaving, industrial cooling, and grid power management.

Electrical energy storage systems consist of capacitors and supercapacitors. Capacitors are created by placing a dielectric layer between the two conducting plates. The size and spacing of the conducting plates determine the energy storage capacity of these systems. The implementation of electrical energy storage systems is limited because of their low energy density (Khan et al., 2024).

There are two types of electro-chemical energy storage systems: secondary batteries and flow batteries. While secondary batteries can be recharged repeatedly, flow batteries store and release electrical energy by using two liquid electrolytes that create reversible electrochemical reactions (Rahman et al., 2020).

Currently, lithium-ion batteries (a secondary battery type) are the most employed electro-chemical batteries. They have applications in electronics, transportation, and power grids due to their higher efficiency, longer life cycle, and higher power and energy density compared to other secondary batteries (Khan et al., 2024).

BESSs, which consist of secondary batteries, are selected as the energy storage option for the flexible multi-mode power plant solution concept. Some of the power and energy applications of BESSs are summarized in **Table 5.**

Applications of BESSs	
Power Applications	**Energy Applications**
Primary Frequency Control	Microgrid Operation
Voltage Control	Islanded Operation
Frequency Stability	Black Start
Voltage Stability	Secondary Frequency Control
Small-Signal Stability	Load Leveling
Fast Frequency Response	Peak Shaving
Spinning Reserve	Renewable Energy Integration
	Renewable Capacity Firming

Table 5. Applications of BESSs.

As previously mentioned, inverters are employed in BESSs. BESSs equipped with grid-forming inverters offer applications such as primary frequency control, voltage control, microgrid operation, islanded operation, and black start. Other applications are offered by both BESSs with grid-forming and grid-following inverters.

Power Applications of BESSs: Power applications of BESSs involve the injection of active and reactive power over short durations (typically seconds to minutes) to maintain the stability of the power systems (Byrne et al., 2018). These applications are discussed in the following content.

- Primary Frequency and Voltage Control:

By using grid-forming BESSs, the voltage magnitude, the voltage angle, and frequency at the PCC are controlled. Some of the control methods for grid-forming inverters include the virtual synchronous generator, virtual synchronous machine, synchronverter, droop-based control, and virtual oscillator (Zuo et al., 2021). Among these methods, while virtual synchronous generator and virtual synchronous machine use a Phase-

Locked Loop (PLL) to decouple power control from frequency control, droop-based controls do not incorporate a PLL. Controllers without a PLL are beneficial because a PLL may cause stability issues, and potential interactions between the PLL and the power controller could lead to problems.

In **Figure 12,** the operation of grid-forming control (PLL-free, droop-based) is shown.

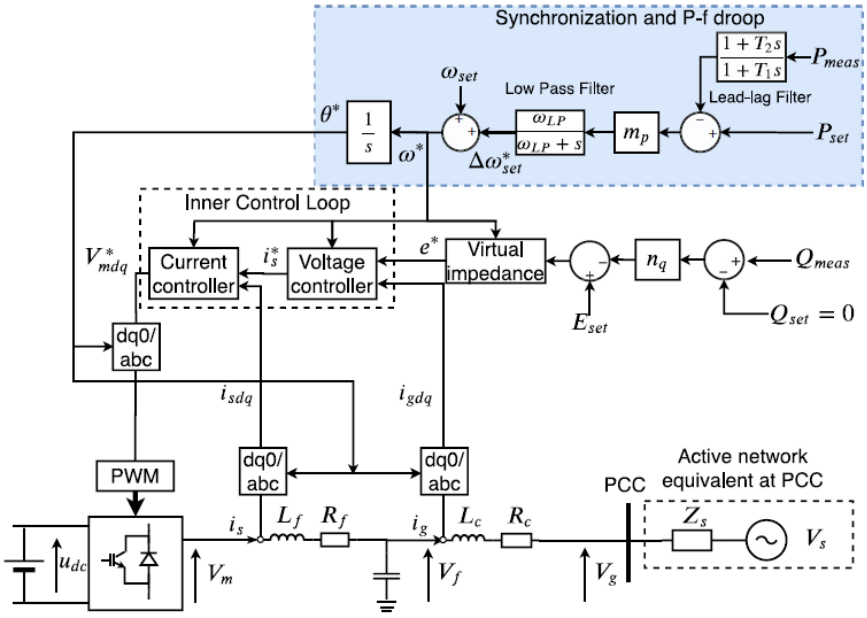

Figure 12. Grid-forming control (Zuo et al., 2021).

Basically, the blue highlighted part is responsible for the inverter synchronization with the grid and primary frequency control (Zuo et al., 2021). There, m_p is the active power-frequency (p-f) droop coefficient. To avoid fast frequency changes dictated by the control of the inverter's terminal and to filter out the noise from active power measurements, a first-order low-pass filter with cut-off frequency ω_{LP}, is added. Moreover, to improve inverter dynamics, a lead-lag filter with time constants T1 and T2 is also added. In the case of voltage control, the reference voltage magnitude is set by the reactive power compensation with droop n_q according to the difference between Q_{meas} and Q_{set}.

- Frequency and Voltage Stability:

By using grid-following BESSs, as shown in **Figure 13,** active and reactive power are controlled by controlling the amplitude and phase of the injected current with respect to the grid voltage at the PCC (Zuo et al., 2021).

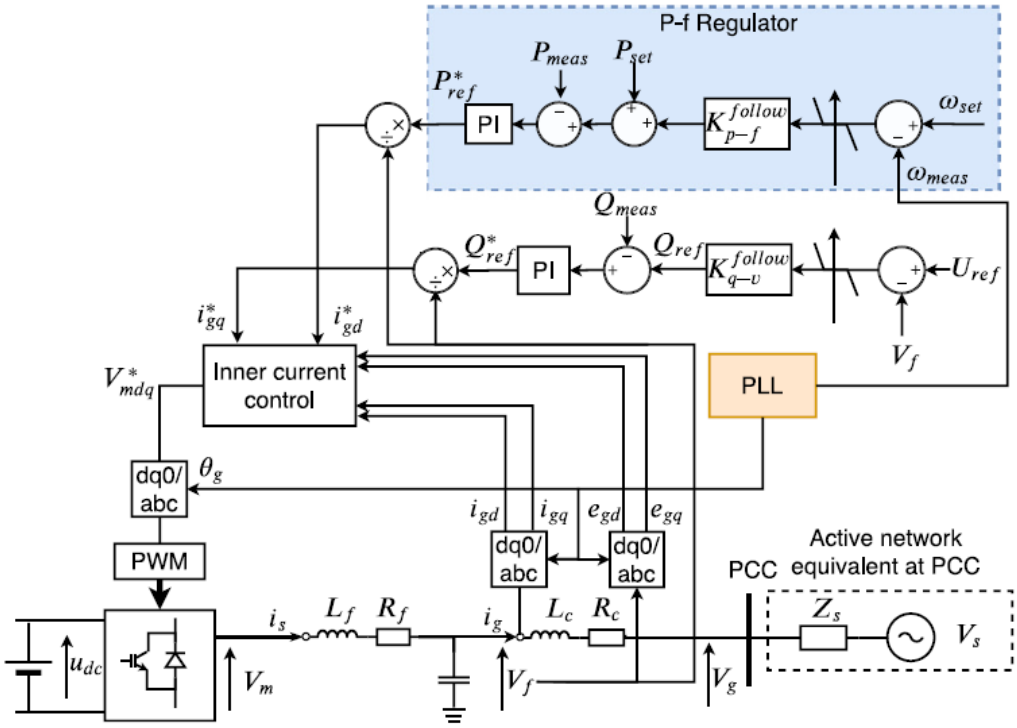

Figure 13. Grid-following control (Zuo et al., 2021).

In grid-following mode, to have the instantaneous value of current reference and voltage reference, a three-phase PLL is required which helps to estimate the fundamental frequency phasor of the grid voltage (Zuo et al., 2021). It should be noted that the active and reactive power are controlled independently.

In grid-following mode, the active power is controlled by f-p control gain, Kf-pfollowing, when measured frequency diverges from the reference frequency (Zuo et al., 2021).
The reactive power is controlled by v-q control gain, Kv-qfollowing, when the difference between measured voltage and reference voltage exceeds the dead-band of ΔVtr (Zuo et al., 2021).

As a result, grid-following BESSs offer frequency and voltage stability by controlling active and reactive power.

- Small-Signal Stability:

Small-signal stability is the stability of power systems in response to small disturbances which create oscillations between 0.1 and 1 Hz (Byrne et al., 2018). To mitigate the small signal instability, the injection of real power into the grid at different locations can be applied according to frequency feedback. BESSs are appropriate for this application.

- Fast Frequency Response:

Fast frequency response involves fast (two seconds or less) detection and correction of frequency deviations created by imbalances between electricity generation and demand (Australian Energy Market Commission, 2021). By charging or discharging batteries almost instantaneously, BESSs can be utilized for fast frequency response and for preventing potential power system outages.

- Spinning Reserve:

Spinning reserve is the generation that is unloaded, synchronized, and ready to serve in case of need for additional load demand or to support contingencies such as a generator or transmission line outage (Hidalgo-León et al., 2017). Spinning reserve is deployed from seconds up to 10 minutes to keep the balance between generation and demand. Thanks to their fast response capability, BESSs offer spinning reserve in power systems.

Energy Applications of BESSs: Energy applications of BESSs generally involve long charge/discharge cycles, which often last more than several hours (Byrne et al., 2018). These applications are discussed in the following content.

- Microgrid Operation:

As explained before, grid-forming BESSs regulate the voltage and frequency of power systems. This capability is especially helpful to mitigate problems that microgrids with high renewable energy penetration suffer such as voltage instability, frequency instability, and low system strength issues (Zhou et al., 2023). Grid-forming BESSs offer

benefits to microgrids with the renewable energy integration, autonomous operation, reliability and robustness improvement.

- Islanded Operation:

Islanded operation is the autonomous operation of an electricity grid separated from the main grid. An islanding operation can happen intentionally or due to a fault. In both cases, despite disconnecting from the main grid, an islanded grid should supply electricity to the area. Transitions from grid-tied to islanded mode, as well as from islanded to grid-tied mode, can be achieved by grid-forming BESSs successfully and stably in grid operation (Rummeny et al., 2020).

- Black Start:

Large generators need an external electricity source to start to generate electricity. This external electricity can be provided from the grid during normal operating conditions. However, after a blackout, generators need to be started with an on-site source of electricity, such as a diesel generator, since the grid can no longer provide external electricity. This process is called a black start. Instead of traditional black start generators, on-site BESSs with grid-forming inverters can be used to provide this process, with which fuel costs and emissions are avoided (National Renewable Energy Laboratory, 2019).

- Secondary Frequency Control:

Secondary frequency control, which typically consists of automatic generation control (AGC), is responsible for bringing the frequency back to its nominal value (Byrne et al., 2018). Operation of a typical secondary frequency control is shown in **Figure 14**.

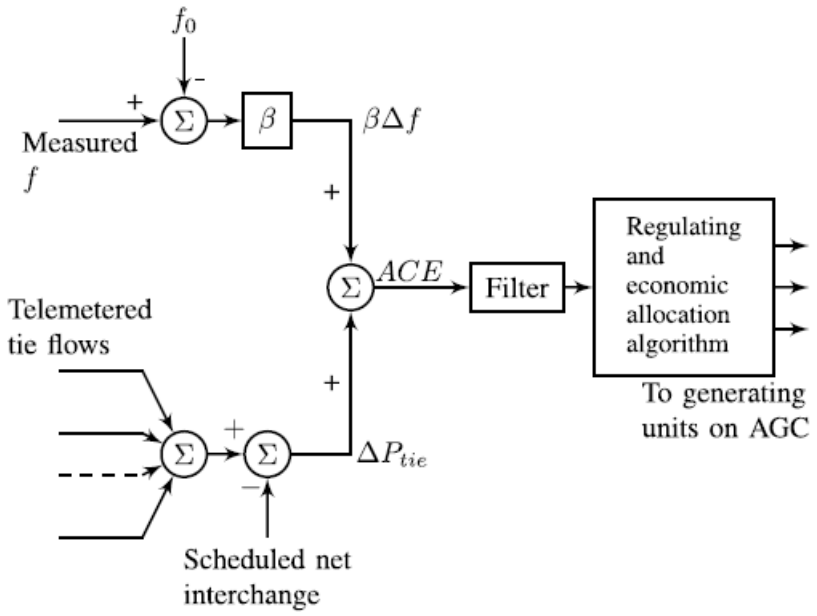

Figure 14. Typical secondary frequency control logic (Byrne et al., 2018).

As shown from **Figure 14,** secondary frequency control uses the area control error (ACE) to adjust generation levels and bring the system frequency back to its nominal value.

ACE is equal to:

$$ACE = \Delta P_{tie} + \beta\Delta f \quad (7)$$

where ΔP_{tie} is the difference between the total telemetered tie flows and the scheduled net interchange, β is the bias factor and unique to each balancing area and is a function of the equivalent frequency droop gain and the equivalent damping, and Δf is the difference between the measured frequency (f), and the reference frequency (f_0). With multiple BESS units, secondary frequency control in power systems can be achieved while maintaining state of charge balance between them (Zhang et al., 2024).

- Load Leveling:

Load leveling is used for balancing electricity generation and demand. It is achieved by storing electricity during low demand periods and releasing it during high demand periods. BESSs can be employed for this application, by charging during off-peak demand hours, and discharging during peak hours (Kim et al., 2019). With this process, stability and reliability of the grid are improved.

- Peak Shaving:

The aim of peak shaving is to decrease the maximum demand of the grid. BESSs can be employed for peak shaving applications by storing energy during low demand periods and releasing it during high demand periods. In this way the load curve is flattened, the need for additional power generation capacity is reduced, grid efficiency is improved, and energy costs are reduced (Gan et al., 2025).

- Renewable Energy Integration:

BESSs are beneficial for renewable energy integration. For example, with a simple charging/discharging scheme, BESSs can store energy in case of a surplus of wind power or release it in case of a shortfall of wind power (Datta et al., 2021). In this way, BESSs can improve the dispatchability of wind power, increase flexibility, and reduce forecast error. Likewise, by using BESSs in PV systems, output power is smoothed out, and dispatchability and flexibility of the system are increased.

- Renewable Capacity Firming:

Renewable capacity firming involves storing renewable energy during periods of high renewable generation and using it during periods of low renewable generation or high demand to ensure a reliable supply (Jaffal et al., 2024). To address the intermittency of RESs such as wind and solar, BESSs play an important role in renewable capacity firming.

4.1.3 Synchronous Condensers

For the flexible multi-mode power plant solution concept, SCs are selected for their applications in addressing energy transition challenges. These applications include reactive power support, voltage support, improved voltage stability, inertia support, short-circuit current support during faults, and an increased short-circuit ratio (SCR) in power systems, which helps mitigate sub-synchronous oscillations.

SCs, also known as synchronous compensators, are synchronous machines that connect to high voltage networks and operate with no mechanical load (freely-spinning). They

are designed for supplying or absorbing reactive power, depending on the value of excitation (field) current (Bompard et al., 2021).

The behavior of SCs is shown in **Figure 15.** As shown from the figure, depending on the value of the excitation current (Ie), SCs can act as capacitors (supplying reactive power, Q is positive) or inductors (absorbing reactive power, Q is negative) (Bompard et al., 2021).

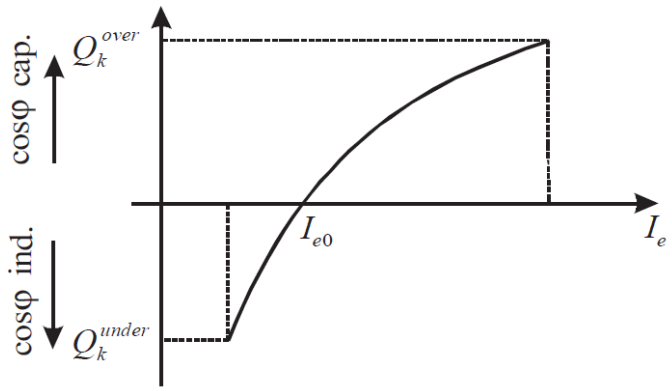

Figure 15. Behavior of SC with respect to excitation current (Bompard et al., 2021).

When needed, SCs support the grid voltage level by supplying or absorbing reactive power during disturbances (Ratnam et al., 2020). Moreover, by continuously providing reactive power and inertia, SCs improve voltage stability during normal operation, mitigating issues related to RES integration and thus enhancing the reliability of the power systems. For example, it has been seen that by employing SCs in rural areas with fragile networks, voltage stability problems, which are generally difficult to address only with power electronic systems, are mitigated (Soleimani et al., 2024).

Since SCs are rotating machines, they provide inertia, which is lacking in modern power systems dominated by RESs. Inertia is especially important during disturbances to prevent frequency instability. Increased inertia from SCs contributes to the reduction of the RoCoF and the frequency nadir (the lowest point of frequency) (Ratnam et al., 2020), as derived in equations (13) and (18) below, respectively.

In case of RoCoF ($\frac{df}{dt}$) :

$$\frac{2H}{\omega_s}\frac{d^2\delta(t)}{dt^2} = P_m - P_e \quad (8)$$

$$\omega_s = 2\pi f \quad (9)$$

$$\frac{d\omega_s}{dt} = 2\pi\frac{df}{dt} \quad (10)$$

$$\frac{d^2\delta(t)}{dt^2} = \frac{d\omega_s}{dt} \quad (11)$$

$$\frac{d^2\delta(t)}{dt^2} = 2\pi\frac{df}{dt} \quad (12)$$

$$\frac{df}{dt} = \frac{Pm - Pe}{2\pi}\ \frac{\omega_s}{2H} \quad (13)$$

Equation (13) shows that an increase in inertia (H) results in a decrease in RoCoF.

In case of frequency nadir:

$$f(t) = f_0 + \int_0^t \frac{df}{dt}\ dt \quad (14)$$

$$\frac{df}{dt} = \frac{Pm - Pe}{2\pi}\ \frac{\omega_s}{2H} \quad (15)$$

$$f(t) = f_0 + \int_0^t \frac{Pm - Pe}{2\pi}\frac{\omega_s}{2H}\ dt \quad (16)$$

$$f(t) = f_0 + \frac{Pm - Pe}{2\pi}\frac{\omega_s}{2H}\ t \quad (17)$$

$$f_{min} = f_0 + \frac{Pm - Pe}{2\pi}\frac{\omega_s}{2H}\ T \quad (18)$$

According to equation (18), higher inertia (H) reduces the frequency drop, resulting in a higher frequency nadir. Note that in equation (18), it is assumed that the frequency reaches its nadir at time T.

As integration of RESs into power systems increases, the available short-circuit current, which is necessary to clear faults and for system protection, decreases (Soleimani et al., 2024). One of the most effective solutions that offers short-circuit current is found to be SCs. By injecting currents rapidly during faults, up to six times their rated capacity, SCs improve the available short-circuit current of power systems, which is important for grid reliability.

As mentioned in Subchapter 3.2.4, the existence of long transmission lines between RESs and load centers decreases the SCR and may cause sub-synchronous oscillations in power systems (Soleimani et al., 2024). According to some study results, it has been observed that by utilizing SCs, the SCR of the power system can be improved, and sub-synchronous oscillations can be mitigated.

Lastly, it is important to note that ICE generating sets can be converted into SCs with certain modifications. For the Flexible Multi-Mode Power Plant Solution concept, either traditional SCs or converted SCs can be utilized. The use of converted units adds additional flexibility to the solution concept, as a single ICE generating set can operate either as a thermal generation unit or as an SC, depending on the power system's needs.

4.2 Modes and Applications of the Flexible Multi-Mode Power Plant Solution for Addressing Energy Transition Challenges

In the previous subchapter, the components of the flexible multi-mode power plant solution concept were introduced. In this solution concept, a total of eleven different operational modes are possible, as shown in **Table 6.**

- Mode 1-3: ICE Generating Sets with or without BESSs
- Mode 4-6: SCs with or without BESSs
- Mode 7-9: ICE Generating Sets and SCs, with and without BESSs
- Mode 10-11: Power and energy BESS

Modes	ICE Generating Sets	SCs	Energy BESSs	Power BESSs
Mode 1	X			
Mode 2	X		X	
Mode 3	X			X
Mode 4		X		
Mode 5		X	X	
Mode 6		X		X
Mode 7	X	X		
Mode 8	X	X	X	
Mode 9	X	X		X
Mode 10				X
Mode 11			X	

Table 6. Operational modes of flexible multi-mode power plant solution concept.

The following content presents the modes and applications of the solution concept for addressing energy transition challenges, based on the information from the previous subchapter. Applications are offered in terms of steady-state operation and transient performance.

Mode 1: ICE Generating Sets

ICE generating sets can be utilized for steady-state operation and during transients.

In steady-state operation, this mode offers:

- Maximum flexibility among thermal generation technologies.
- Effective controllability of the generation-load balance.
- Reliable and efficient baseload or peaking power, with an annual reliability of 99.1% (Wärtsilä, n.d.).
- Renewable energy integration by stabilizing renewable power output during transitional periods or seasonal changes.

- Microgrid and islanded operation.

During transients, this mode offers:

- Faster frequency and voltage response compared to other thermal generation technologies.

Mode 2: ICE Generating Sets with Energy BESSs

This mode is suitable for steady-state operation, and it offers:

- Improved flexibility.
- Improved controllability of the generation-load balance.
- Improved reliability.
- Improved renewable energy integration, load leveling, peak shaving, and renewable capacity firming.
- Improved microgrid and islanded operation with grid-forming BESSs.
- Black start capability: grid-forming BESSs as initial energizer, maintaining load pickup by ICE generating sets.

Mode 3: ICE Generating Sets with Power BESSs

This mode operates during transients. It offers:

- Improved frequency and voltage response with grid-forming BESSs.
- Improved grid resilience.
- Ideal spinning reserve.

Mode 4: SCs

SCs can be utilized for steady-state operation and during transients.

In steady-state operation, this mode offers:

- Reactive power support (supply or absorption).
- Improved voltage profiles across the grid.
- During transients, this mode offers:
- Voltage response improvement.
- Frequency response improvement thanks to its inertial response.
- Increased SCR, which helps mitigate sub-synchronous oscillations.
- Short-circuit current support during faults, which improves reliability.

Mode 5: SCs with Energy BESSs

This mode is suitable for steady-state operation, and it offers:

- Active power support and improved reactive power support.
- Greater voltage profile improvement.
- Microgrid and islanded operation: grid-forming BESSs control frequency and voltage, SCs support voltage stability.
- Black start capability: Enabled by grid-forming BESSs; SCs assist with reactive power support.

Mode 6: SCs with Power BESSs

This mode operates during transients. It offers:

- Greater voltage response improvement through fast injection of reactive power from SCs and BESSs.
- Greater frequency response improvement through fast injection of active power from BESSs and inertia support from the SCs.
- Improved short-circuit current support during faults.

Mode 7: ICE Generating Sets with SCs

This mode can be utilized for steady-state operation and during transients.

In steady-state operation, this mode offers:

- Improved reactive power delivery.
- Greater voltage profiles across the grid.
- Improved microgrid and islanded operation: ICE generating sets control frequency and voltage, and SCs support voltage stability.

During transients, this mode offers:

- Greater frequency response through the fast-ramping capability of ICE generating sets and inertial response of SCs.
- Greater voltage response.

Mode 8: ICE Generating Sets with SCs and Energy BESSs

This is the most comprehensive mode for steady-state operation. This mode offers:

- Superior flexibility.
- Superior controllability of the generation-load balance.

- Superior reliability.
- Advanced renewable integration through variability mitigation, load leveling, peak shaving, and renewable capacity firming.
- Advanced black start capability: grid-forming BESSs as the initial energizer, maintaining load pickup by ICE generating sets, SCs assist with voltage support.
- Advanced microgrid and islanded operations: ICE generating sets as the primary source of power, BESSs for active and reactive power support, SCs for reactive power support.

Mode 9: ICE Generating Sets with SCs and Power BESSs

This is the most comprehensive mode for transients. This mode offers:

- Superior frequency response: inertial response of SCs, almost instantaneous response from BESSs, and fast ramping capability of ICE generating sets.
- Superior voltage response.
- Superior spinning reserve: instantly available BESSs, and standby ICE generating sets.
- Greater grid resilience by fast active and reactive power injection, which prevents cascading failures.
- Greater short-circuit current support during faults.

Mode 10: Power BESSs

Power BESSs operate during transients. The applications of power BESSs were discussed in detail in Subchapter 4.1.2.

Mode 11: Energy BESSs

Energy BESSs is suitable for steady-state operation. The applications of energy BESSs were discussed in detail in Subchapter 4.1.2.

4.3 Operation Philosophy of the Flexible Multi-Mode Power Plant Solution

The Flexible Multi-Mode Power Plant solution concept requires intelligent decision-making to determine and manage transitions between operational modes, especially in microgrids. Optimal functionality is achieved through the coordinated operation of an Energy Management System (EMS) and a Power Management System (PMS).

The EMS optimizes short-term and long-term operational strategies by making decisions to minimize operating costs and maximize system efficiency. On the other hand, the PMS is responsible for real-time stability. It maintains parameters such as frequency, voltage, and power, ensuring they remain within operational thresholds. Moreover, it controls the operation (startup, synchronization, and shutdown) of system components. In summary, while EMS is responsible for energy economic objectives, PMS deals with technical objectives of power systems (Mahdi et al., 2021).

The operation mode selection is determined by real-time forecasts and performance indicators. The EMS processes data such as renewable energy generation forecast, electricity market prices, demand trends, engine fuel availability, battery state of charge, and carbon emissions. Based on the processed data, the EMS chooses the most cost-effective mode, which aligns with the broader energy dispatch schedule.

As a basic example, during periods of high renewable energy generation and low demand, Mode 11 (Energy BESS) can be selected by the EMS from a previous mode to absorb excess energy. Likewise, during periods of need for active and reactive power, Mode 7 (ICE generating set and SC) can be selected by the EMS from a previous mode to provide dispatchable active and reactive power.

As an illustration, a basic mode transition diagram of the solution concept is shown in **Figure 16**. Although many transitions are possible, only some of them are depicted in the diagram, as illustrating all possible transitions is beyond the scope of this thesis.

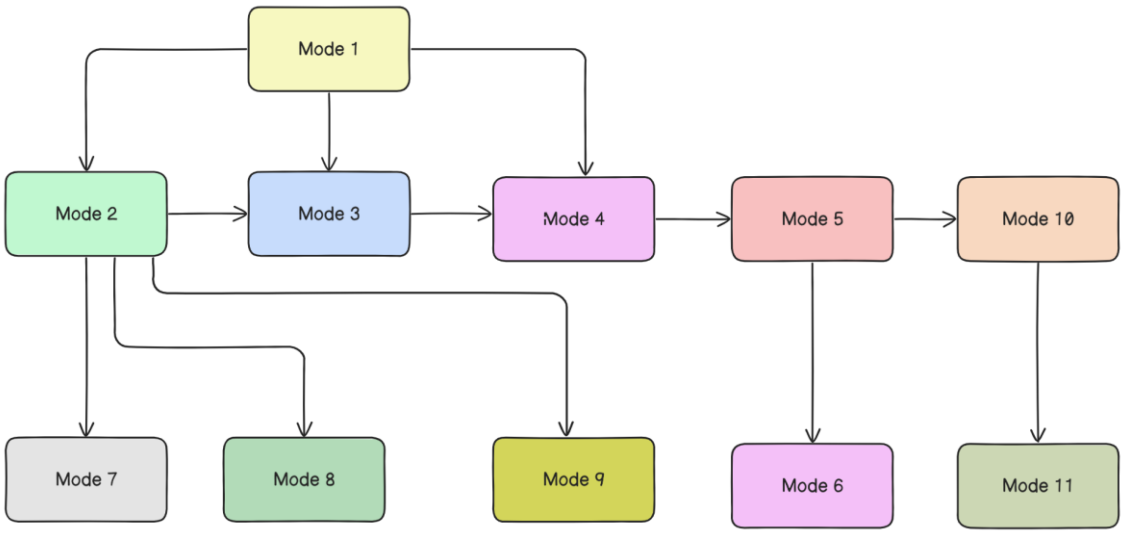

Figure 16. A basic mode transition diagram.

While the EMS decides on optimal operation modes, the PMS initiates and controls actual transitions. Before changing modes, the PMS verifies the new configuration and checks for any violations of system limits regarding voltage stability, frequency stability, active and reactive power margins, and inertia adequacy. For example, it evaluates whether the BESS units can handle the expected transients without reaching their operating limits or the maintenance of voltage stability during the ramp-up of internal combustion engine generating sets. In case of parameter violations or trends that may lead to instability, the PMS can reject the mode decision of EMS and initiate actions such as predefined grid stabilization procedures.

In conclusion, with the integration of EMS and PMS, a dual-layer control structure is constructed, as shown in **Figure 17**. In this structure, the first layer (EMS) ensures economically viable and efficient operation of the power plant, while the second layer (PMS) validates these decisions with a focus on system stability and real-time control.

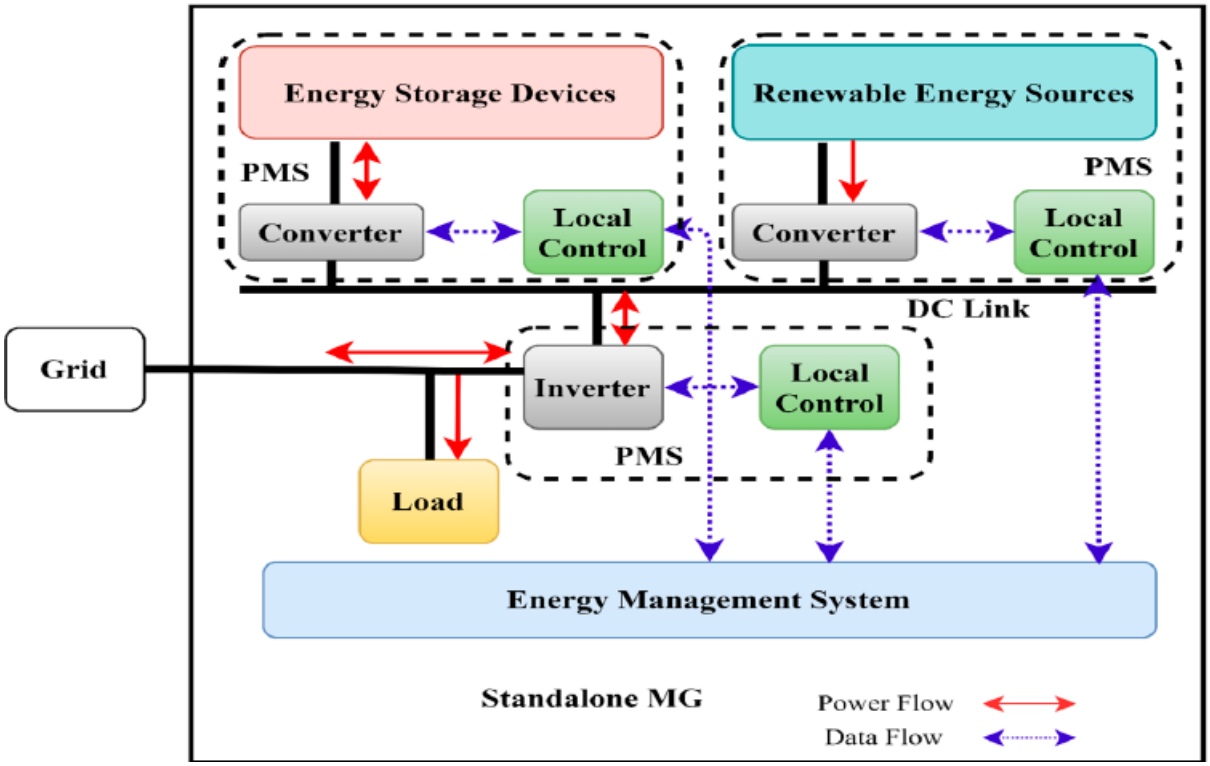

Figure 17. Operation of PMS/EMS system in microgrids (Mahdi et al., 2021).

5 Modeling and Simulation of the Flexible Multi-Mode Power Plant Solution for Frequency Stability

5.1 Development of Simulation Models

PowerFactory software is used for the development of simulation models. Since the primary goal of the frequency stability simulations is to demonstrate the frequency response of the multi-mode power plant solution in grids with high renewable penetration and in microgrids, the IEEE 14-Bus System is selected as a template. The IEEE 14 Bus-System, which is taken from the PowerFactory library, is shown in **Figure 18.**

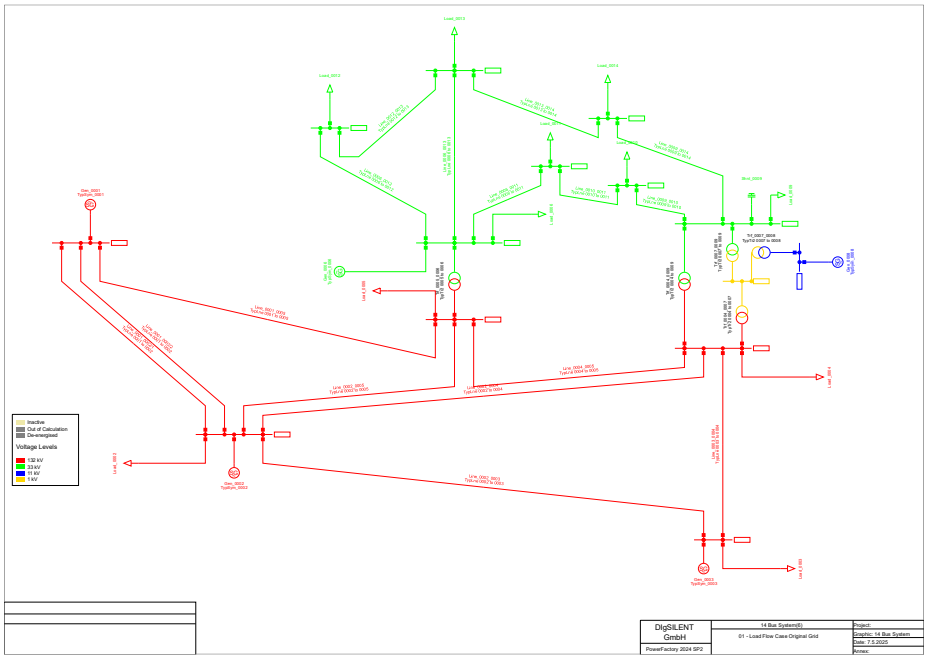

Figure 18. IEEE 14 Bus System (PowerFactory, 2024).

To study the frequency response of the power plant solution with respect to the study cases presented in Subchapter 5.2, the IEEE 14-Bus System from the PowerFactory library is modified according to **Table 7**, without changing its original configuration.

	Original	Modified
Bus number	14	23
Generator	5	10
Load	11	12
Wind Power Plant (with parallel machines)	0	1
PV Power Plant (with parallel machines)	0	6
BESS	0	2
Transformer	5	12

Table 7. The original and modified IEEE 14 Bus System.

Modified IEEE 14-Bus System consists of 23 buses, ten generators (ICE generating sets), twelve loads, one wind power plant (with parallel machines), six PV power plants (with parallel machines), two BESSs (with parallel machines), twelve transformers, and transmission lines.

The number of buses and transformers has increased due to the addition of generation units. Transformers are used to convert the bus voltages of ICE generating sets (11 kV), PV and wind power plants (0.69 kV), and BESSs (0.63 kV) to the grid voltage.

The grid voltage is chosen as 33 kV, which is a common medium voltage among grids. The frequency of the grid is 50 Hz, and the total load is chosen as 100 MW. One thing to note is that the modified 14 Bus-System used for simulation studies is not based on real-life microgrids but was created for analysis purposes.

5.1.1 Generation Units

5.1.1.1 ICE Generating Sets

ICE generating sets are used for synchronous generation. The model provided for ICE generating sets is the Wärtsilä 20V31SG. The rating of each generating set is 14.7 MVA. Ten generating sets were created since the total load is chosen as 100 MW for simulation

studies. Wärtsilä ICE generating sets can be run in three different frequency control modes, namely droop control, isochronous control, and true kW control. For this thesis, droop control was utilized. The droop setting of the ICE generating set was set to 0.04 (4%) for the simulation study cases. The operation principle of droop control is explained in Appendix 2.

The Wärtsilä 20V31SG ICE generating set block diagram, with components and controllers, is shown in **Figure 19.** The details of the generating set block diagram are not discussed, not only because they are beyond the scope of this thesis, but also due to confidentiality reasons.

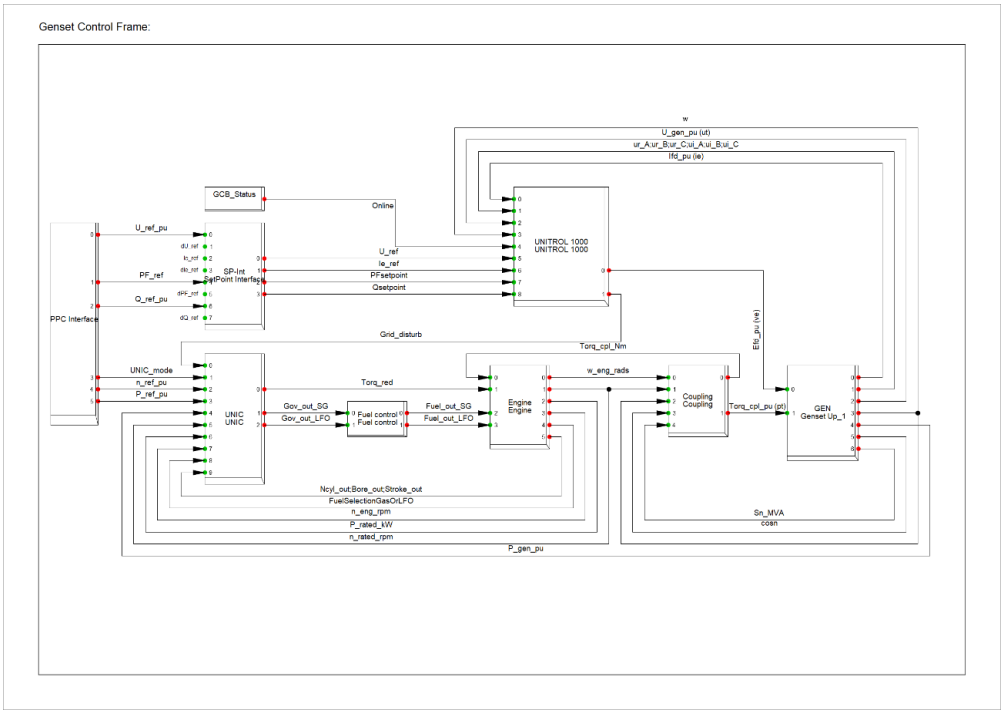

Figure 19. Wärtsilä ICE generating set control frame.

5.1.1.2 Wind Power Plants

For wind power plants, the "WECC WTG Type4A" model is used from the DIgSILENT PowerFactory library **(Figure 20).** The rated apparent power of the model is 2 MVA, and

rated frequency is 50 Hz. 25 parallel machines (totaling 50 MVA) are chosen for simulation studies to generate proper output power for each simulation study case.

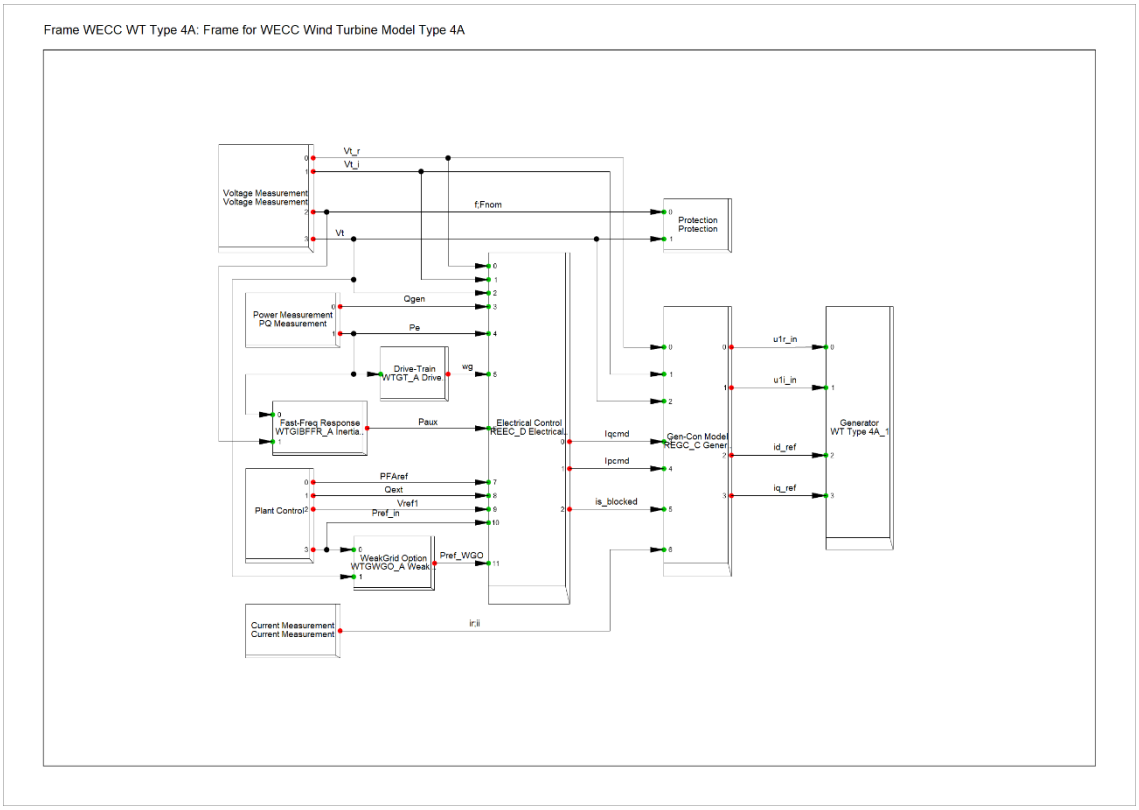

Figure 20. Frame of WECC Type 4A wind turbine generator (PowerFactory, 2024).

In this wind power plant model, the Type 4 wind turbine generator is used. The generator is connected to the grid via an inverter. For the inverter control, Renewable Energy Electrical Control (REEC) is used **(Figure 21),** which is the most recent inverter control model created by WECC (Ashourian & Gras, 2022).

REEC receives active and reactive power demands from Plant Control (**Figure 22),** calculates the required active and reactive currents accordingly, and sends them to the Renewable Energy Generator/Converter (REGC).

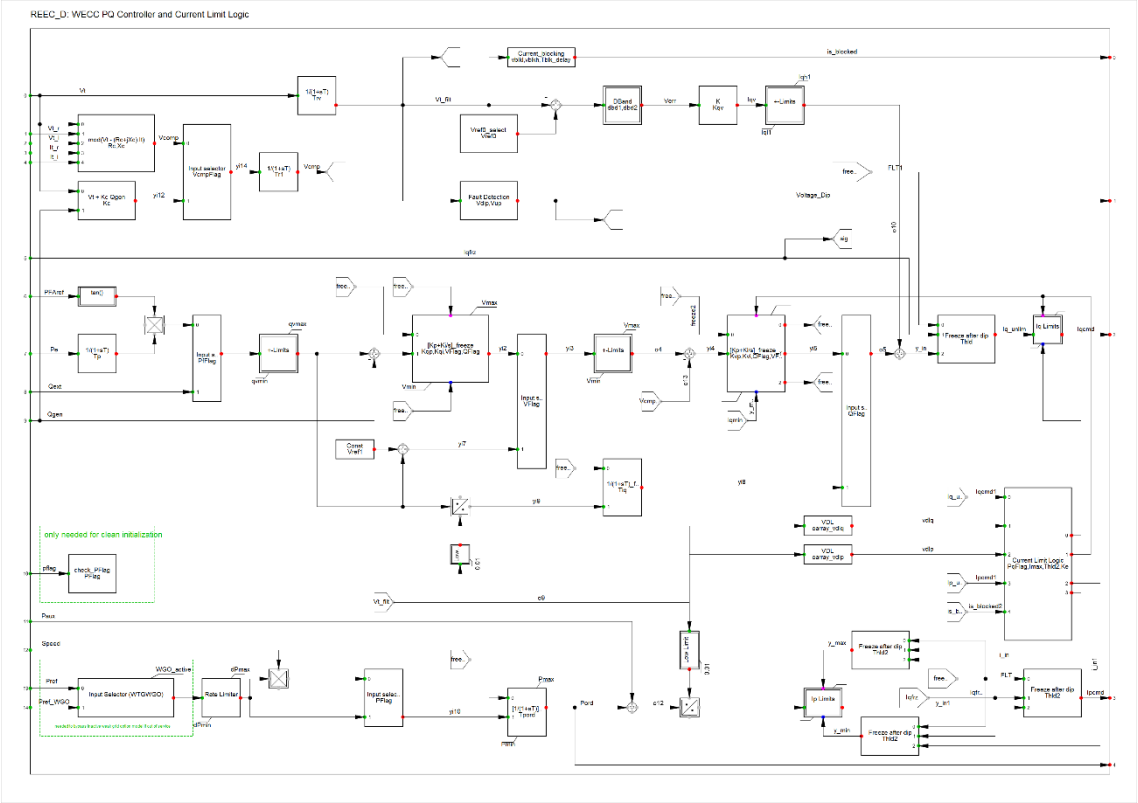

Figure 21. Active and reactive power control by REEC (PowerFactory, 2024).

The REGC (**Figure 22)** receives active and reactive current commands, Ipcmd and Iqcmd respectively, from the REEC (California Independent System Operator, 2021). By employing PID controllers, the REGC controls the active and reactive currents to be injected into the grid. Moreover, the terminal voltage and ensuring that the current injection is within the operational limits of the generator are also considered.

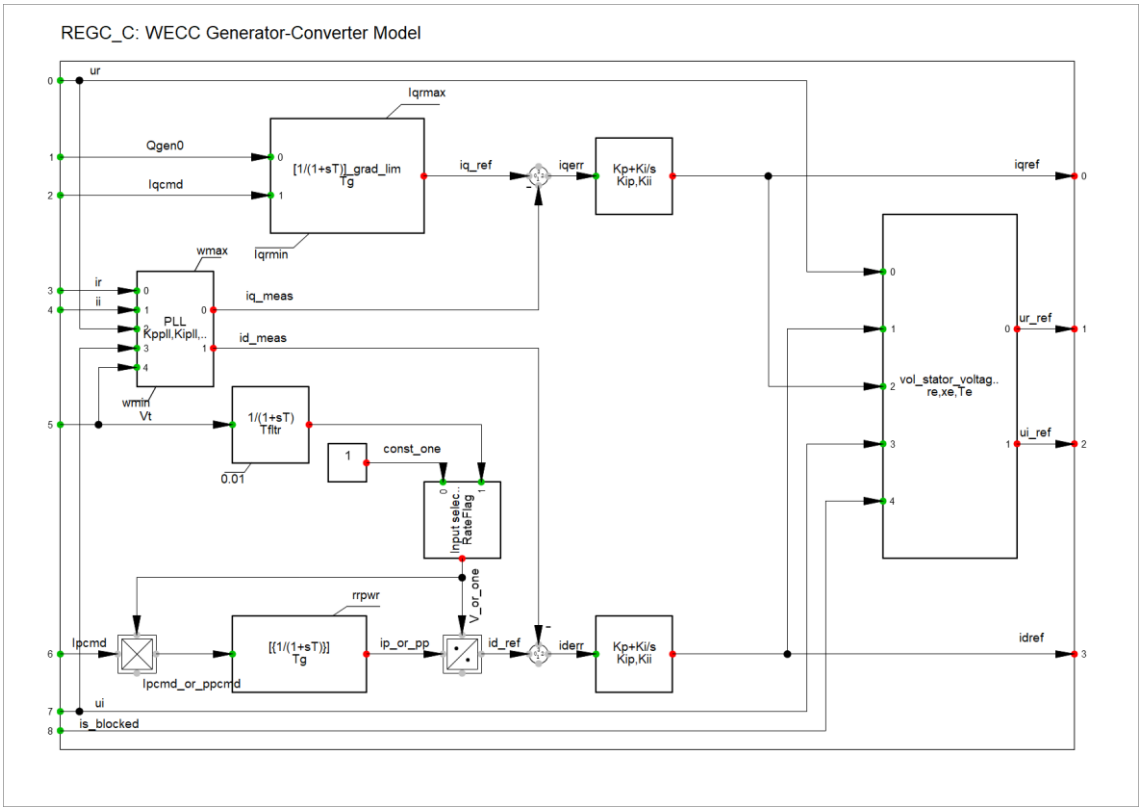

Figure 22. WECC Generator-Converter Model (PowerFactory, 2024).

The WECC Type 4A model is a grid-following inverter model since the model delivers currents id_ref and iq_ref based on the grid conditions it observes. The maximum rate of increase in active power was set to 2 pu/s, while the maximum rate of decrease was set to –2 pu/s for the simulation studies.

5.1.1.3 PV Power Plants

For PV power plants, the “WECC Distributed Small PV Plants” model is used from the DIgSILENT PowerFactory library (**Figure 23).** The rated apparent power of the model is 25 MVA, and the rated frequency is 50 Hz. Six units have been created to generate the proper output power according to the simulation cases.

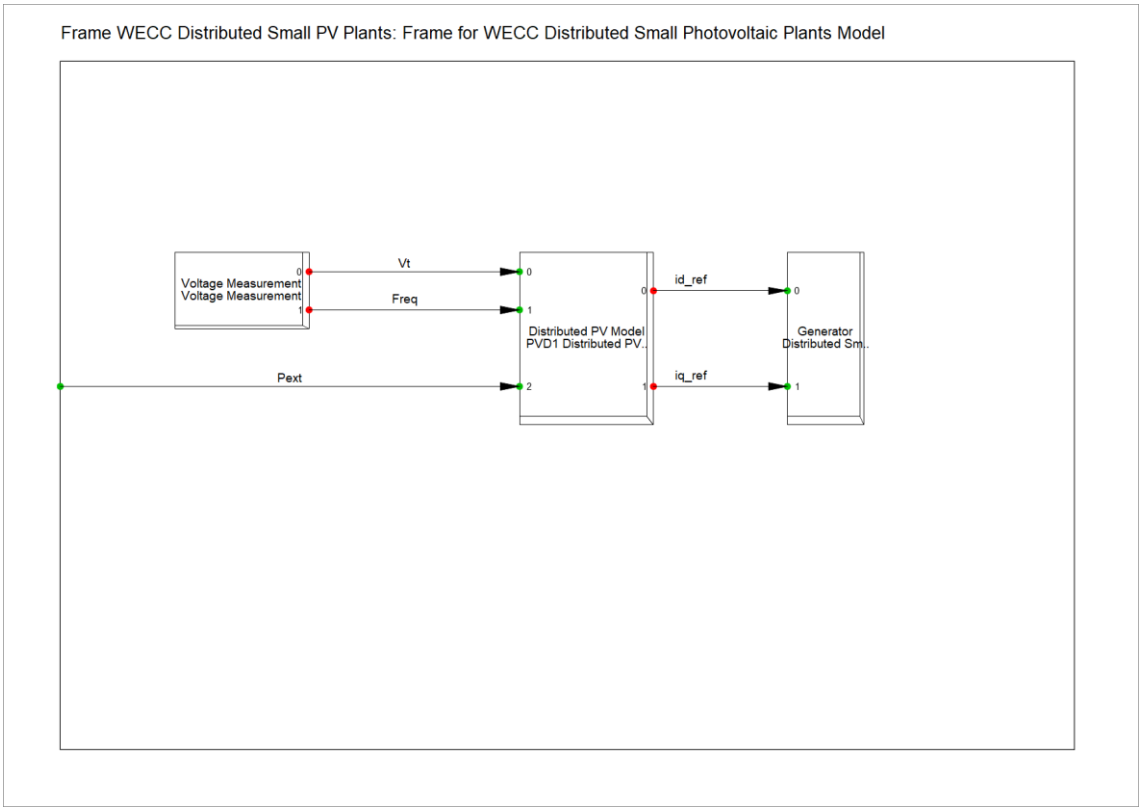

Figure 23. The WECC Distributed Small PV Plants model (PowerFactory, 2024).

The inverters in this PV power plant model are also grid-following. In this model, active power is controlled by frequency-droop (f–P droop) control (**Figure 24**). In this control, the active power output changes based on frequency deviations from the reference frequency (Freq_ref). A deadband (fdbd) is utilized to prevent power changes for small frequency deviations. When frequency drops below the deadband, the droop gain (Ddn) changes the active power output accordingly.

In this model, reactive power is controlled by Volt/Var (V–Q) control (**Figure 24**). In this control, the reactive power output changes based on terminal voltage (Vt) using a Volt/Var droop function: between the low (v0) and high (v1) voltage thresholds, the inverter changes reactive power output. The slope of the droop is defined as dqdv. The Ddn and dqdv parameters were set to zero for the simulation studies.

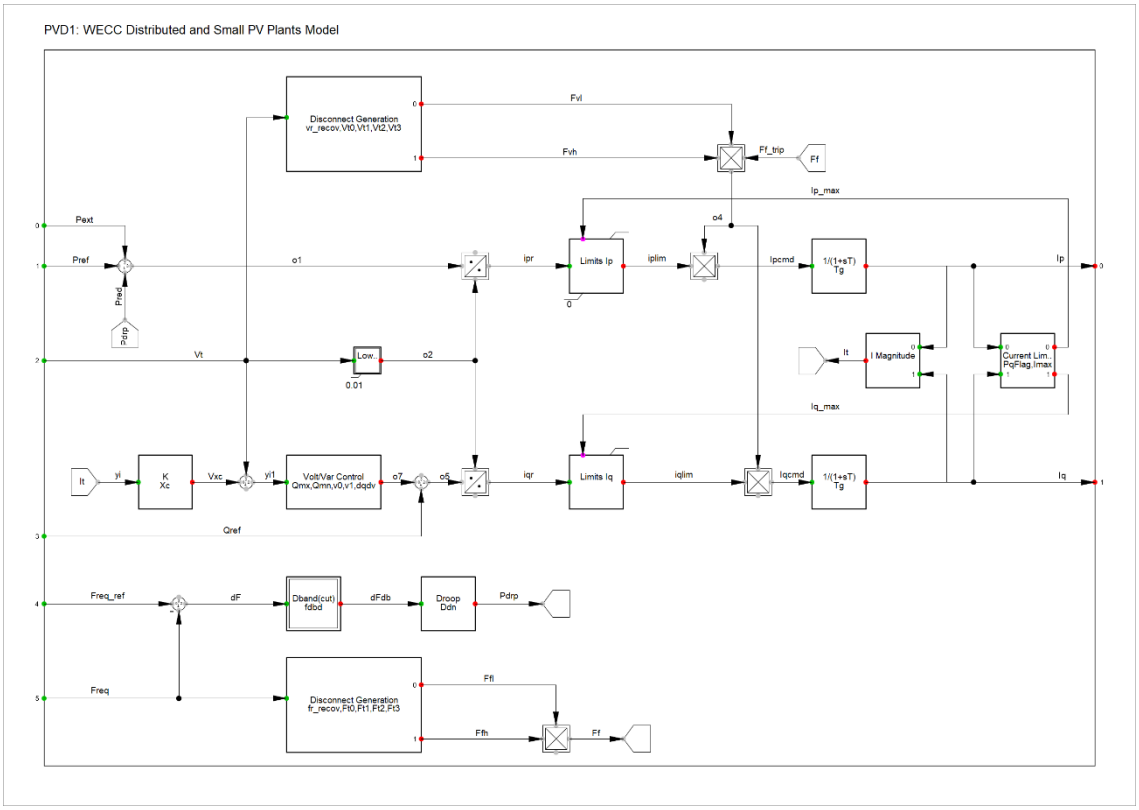

Figure 24. Active and reactive power control of the WECC Distributed Small PV Plants model (PowerFactory, 2024).

5.1.2 BESSs

The rating of the BESS used in the simulation studies is 3.62 MVA. Two units, each with two parallel machines, have been created. The inverters used in the BESSs are grid-forming, and they use active power droop f(P) and reactive power droop V(Q) with settings of –1 Hz/pu and 0.03 %/pu, respectively. In terms of RoCoF, the BESS can handle frequency changes at a rate of up to 6 Hz per second.

The BESS model is provided by one of the leading inverter manufacturers. The block diagram and details of the BESS model will not be discussed, not only because they are beyond the scope of this thesis, but also due to confidentiality reasons.

5.1.3 Synchronous Condensers

As mentioned at the end of Subchapter 4.1.3, ICE generating sets can be converted into SCs with some modifications. In the simulation studies, the SC model was created with some modifications to the existing ICE generating set, while its parameters remained unchanged.

5.1.4 Loads

In the simulation studies, a total of 100 MW of active power and 17.18 MVAR of reactive power are connected to the 12 buses shown in **Table 8**. The load distribution is done in such a way as to maintain a balanced voltage profile during steady-state operations, while also considering the disturbances discussed in Subchapter 5.2.

BUS	P (MW)	Q (MVAR)	S (MVA)	pf
BUS 1	5.79	-0.77	5.84	0.99
BUS 2	8.38	1.04	8.44	0.99
BUS 3	15.44	2.70	15.67	0.99
BUS 4	18.45	-1.51	18.51	1.00
BUS 5	6.79	0.62	6.82	1.00
BUS 6	15.59	0.97	15.62	1.00
BUS 9	11.39	6.41	13.07	0.87
BUS 10	3.47	2.24	4.13	0.84
BUS 11	1.35	0.69	1.52	0.89
BUS 12	2.35	0.62	2.43	0.97
BUS 13	5.21	2.24	5.67	0.92
BUS 14	5.75	1.93	6.07	0.95
Total	99.97	17.18	103.81	0.96

Table 8. Loads for simulation models.

5.2 Study Cases

To evaluate the added benefits of each component of the multi-mode power plant solution on frequency stability, 28 study cases were developed and simulated, as shown

in **Table 9.** The general structure is the same for each study case, and it is based on the modified IEEE 14-Bus Model, as mentioned earlier. However, the study cases differ in terms of renewable generation share (40%, 70%, and 100%), types of disturbances (synchronous generation unit trip, largest renewable generation unit trip, and largest load trip), and the use of various power plant operating modes (Modes 1, 3, 6,7, 9, and 10).

In terms of disturbances, the same synchronous generation unit, the same renewable generation unit, and the same load, with the same parametrization, are tripped for all 28 study cases.

Moreover, while creating the study cases, station controllers are added (**Figure 25**) to the generation units during their configuration in order to manage reactive power distribution (i.e., to ensure that proper voltage levels (between 0.95 pu and 1.05 pu) are maintained during steady-state operation before disturbances).

	Name	In Folder	Grid	Out of Servi...	Machines ElmSym,ElmGenstat,ElmPvsys,El...
▶	Station Control	SMASCS_GFM(1)	Grid	☐	...
	Station Control	Grid	Grid	☐	Genset Down_1 ...
	Station Control(2)	Grid	Grid	☐	Genset Up_2 ...
	Station Control(3)	Grid	Grid	☐	Distributed Small PV Plants_4 ...
	Station Control(4)	Grid	Grid	☐	WT Type 4A_1 ...
	Station Control(5)	Grid	Grid	☐	Distributed Small PV Plants_1 ...

Figure 25. Station controllers in PowerFactory.

Study Case	Generation	Disturbance	Mode
1	40% Ren	Synchronous Generation Unit Trip	Mode 1
2	40% Ren	Largest Load Trip	Mode 1
3	40% Ren	Largest Renewable Generation Unit Trip	Mode 1
4	40% Ren	Synchronous Generation Unit Trip	Mode 7
5	40% Ren	Largest Load Trip	Mode 7
6	40% Ren	Largest Renewable Generation Unit Trip	Mode 7
7	40% Ren	Synchronous Generation Unit Trip	Mode 3
8	40% Ren	Largest Load Trip	Mode 3
9	40% Ren	Largest Renewable Generation Unit Trip	Mode 3
10	40% Ren	Synchronous Generation Unit Trip	Mode 9
11	40% Ren	Largest Load Trip	Mode 9
12	40% Ren	Largest Renewable Generation Unit Trip	Mode 9
13	70% Ren	Synchronous Generation Unit Trip	Mode 1
14	70% Ren	Largest Load Trip	Mode 1
15	70% Ren	Largest Renewable Generation Unit Trip	Mode 1
16	70% Ren	Synchronous Generation Unit Trip	Mode 7
17	70% Ren	Largest Load Trip	Mode 7
18	70% Ren	Largest Renewable Generation Unit Trip	Mode 7
19	70% Ren	Synchronous Generation Unit Trip	Mode 3
20	70% Ren	Largest Load Trip	Mode 3
21	70% Ren	Largest Renewable Generation Unit Trip	Mode 3
22	70% Ren	Synchronous Generation Unit Trip	Mode 9
23	70% Ren	Largest Load Trip	Mode 9
24	70% Ren	Largest Renewable Generation Unit Trip	Mode 9
25	100% Ren	Largest Load Trip	Mode 10
26	100% Ren	Largest Renewable Generation Unit Trip	Mode 10
27	100% Ren	Largest Load Trip	Mode 6
28	100% Ren	Largest Renewable Generation Unit Trip	Mode 6

Table 9. Study cases created in Powerfactory.

Details of the study cases are as follows:

Study Cases 1-3 (Figure 26):

- 100 MW load.
- 40% renewable generation, 60% synchronous generation.
- Power plant operates in Mode 1: Only ICE Generating Sets.
- 7 ICE generating sets are active (out of 10).
- Genset Up_1 (**Figure 26**) is the reference machine, the other six ICE generating sets generate 54 MW (9 MW each).
- Wind and solar power plants generate 40 MW.
- Study Case 1 is the synchronous generation unit trip (9 MW, Genset Up_2 in **Figure 26**).
- Study Case 2 is the largest load trip (18.45 MW, Load_0004 in **Figure 26**).
- Study Case 3 is the largest renewable generation unit trip (10 MW, Distributed Small PV Plants in **Figure 26**).

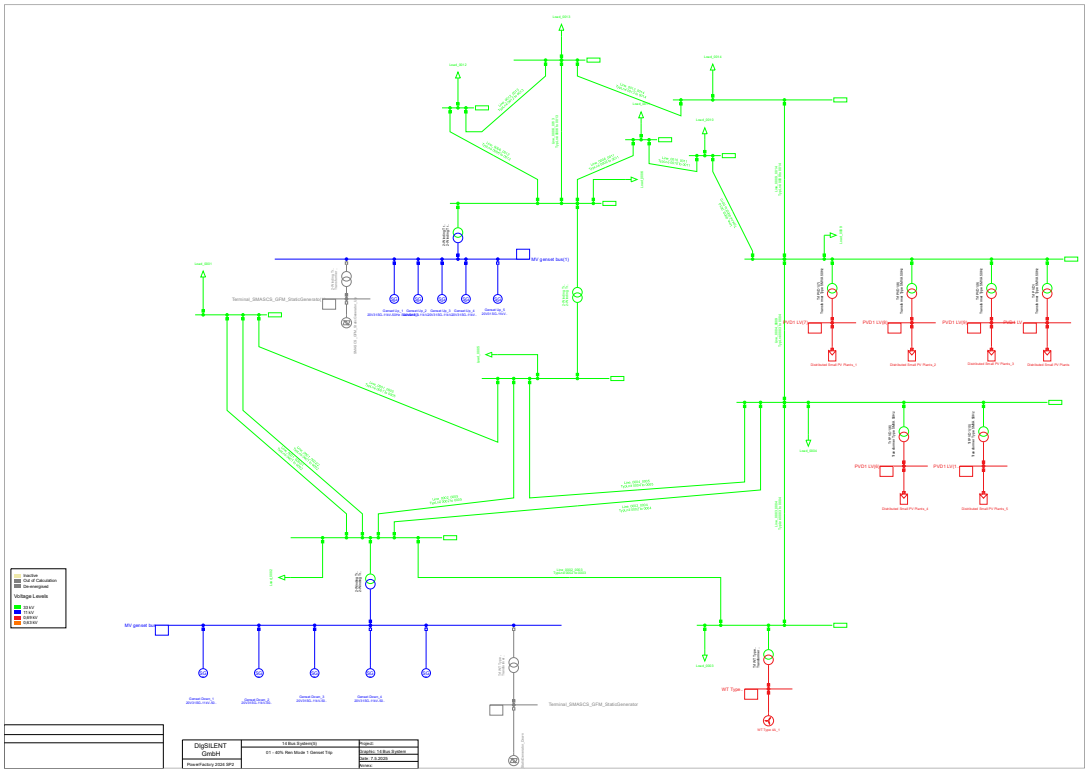

Figure 26. Diagram of Study Cases 1-3.

Study Cases 4-6 (Figure 27):

- 100 MW load.
- 40% renewable generation, 60% synchronous generation.
- Power plant operates in Mode 7: ICE Generating Sets with SC.
- 10 ICE generating sets are active, 3 of them act as SCs.
- Genset Up_1 is the reference machine, the other 6 ICE generating sets generate 54 MW (9 MW each).
- Wind and solar power plants generate 40 MW.
- Study Case 4 is the synchronous generation unit trip (9 MW).
- Study Case 5 is the largest load trip (18.45 MW).
- Study Case 6 is the largest renewable generation unit trip (10 MW).

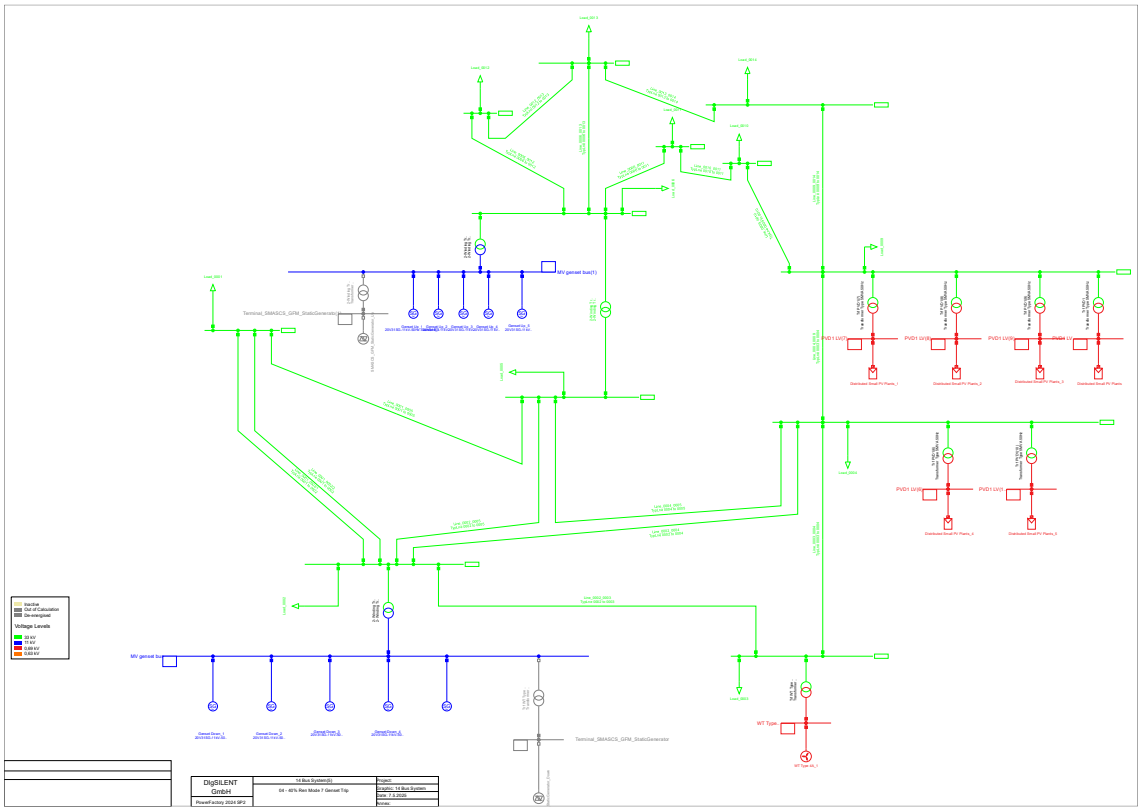

Figure 27. Diagram of Study Cases 4-6.

Study Cases 7-9 (Figure 28):

- 100 MW load.
- 40% renewable generation, 60% synchronous generation.
- Power plant operates in Mode 3: ICE Generating Sets with Power BESS.
- 7 ICE generating sets are active (out of 10).
- Genset Up_1 is the reference machine, the other 6 ICE generating sets generate 54 MW (9 MW each).
- Wind and solar power plants generate 40 MW.
- Two BESS units are active.
- Study Case 7 is the synchronous generation unit trip (9 MW).
- Study Case 8 is the largest load trip (18.45 MW).
- Study Case 9 is the largest renewable generation unit trip (10 MW).

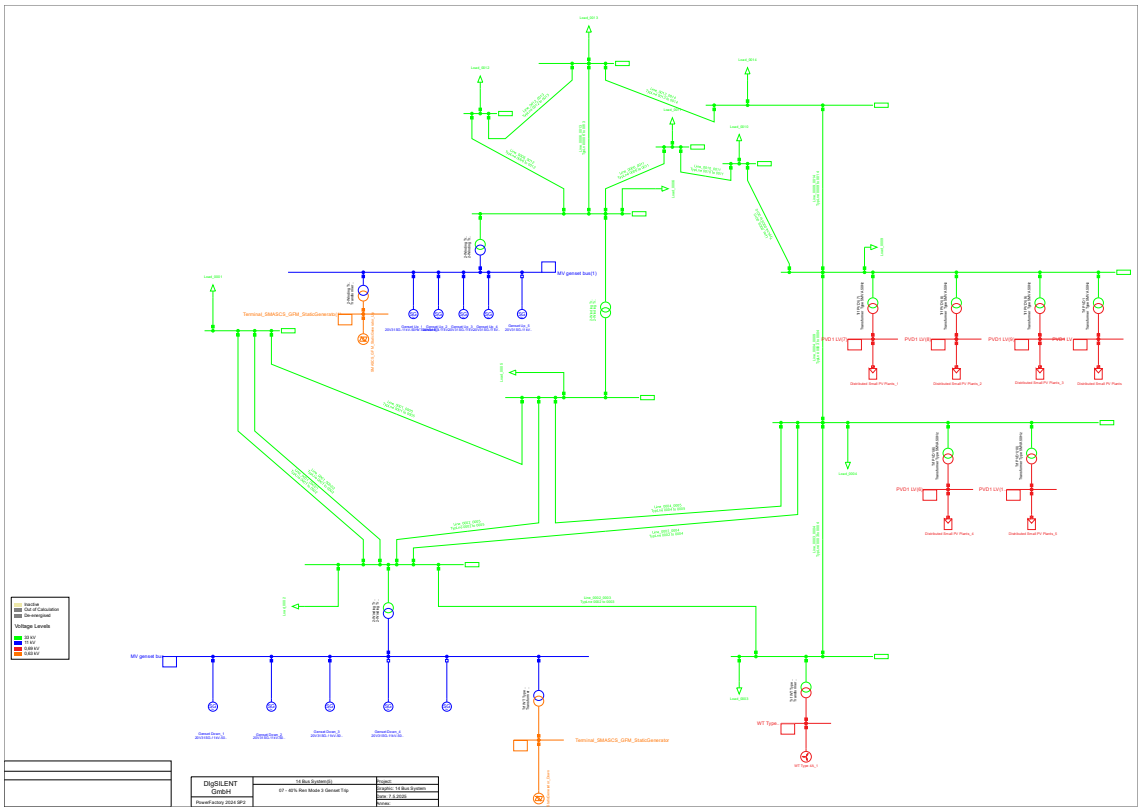

Figure 28. Diagram of Study Cases 7-9.

Study Cases 10-12 (Figure 29):

- 100 MW load.
- 40% renewable generation, 60% synchronous generation.
- Power plant operates in Mode 9: ICE Generating Sets with SC and Power BESS.
- 10 ICE generating sets are active, 3 of them act as SCs.
- Genset Up_1 is the reference machine, the other 6 ICE generating sets generate 54 MW (9 MW each).
- Wind and solar power plants generate 40 MW.
- Two BESS units are active.
- Study Case 10 is the synchronous generation unit trip (9 MW).
- Study Case 11 is the largest load trip (18.45 MW).
- Study Case 12 is the largest renewable generation unit trip (10 MW).

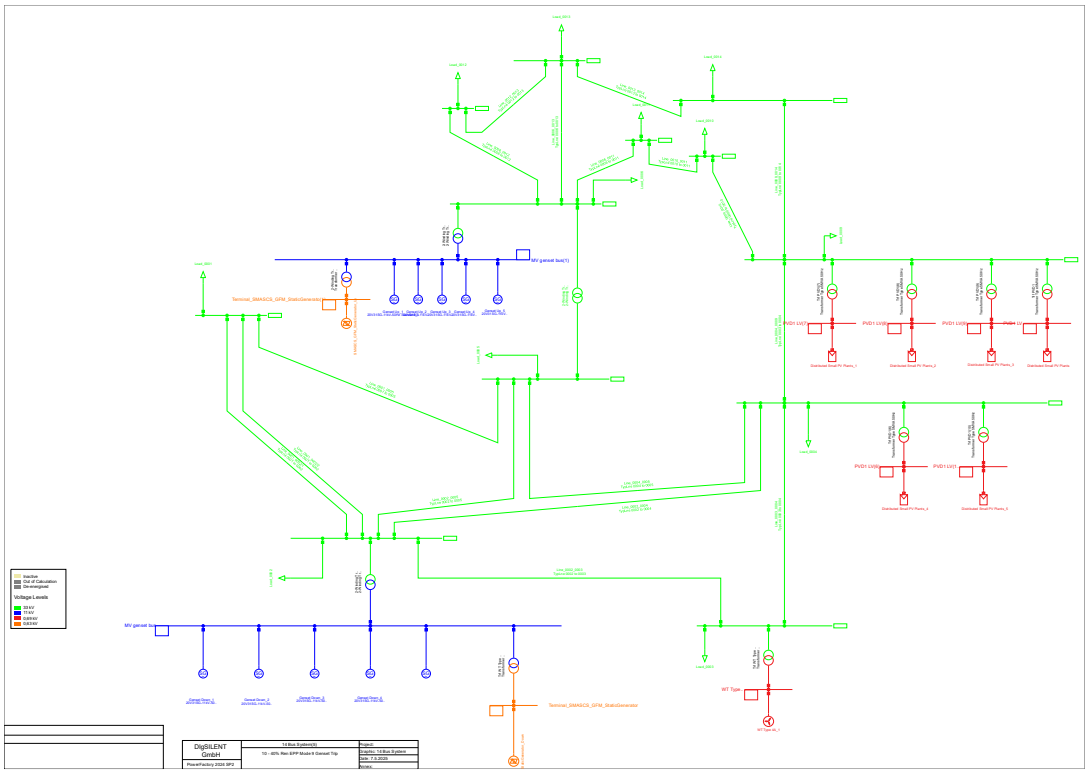

Figure 29. Diagram of Study Cases 10-12.

Study Cases 13-15 (Figure 30):

- 100 MW load.
- 70% renewable generation, 30% synchronous generation.
- Power plant operates in Mode 1: Only ICE Generating Sets.
- 4 ICE generating sets are active (out of 10).
- Genset Up_1 is the reference machine, the other 3 ICE generating sets generate 27 MW (9 MW each).
- Wind and solar power plants generate 70 MW.
- Study Case 13 is the synchronous generation unit trip (9 MW).
- Study Case 14 is the largest load trip (18.45 MW).
- Study Case 15 is the largest renewable generation unit trip (10 MW).

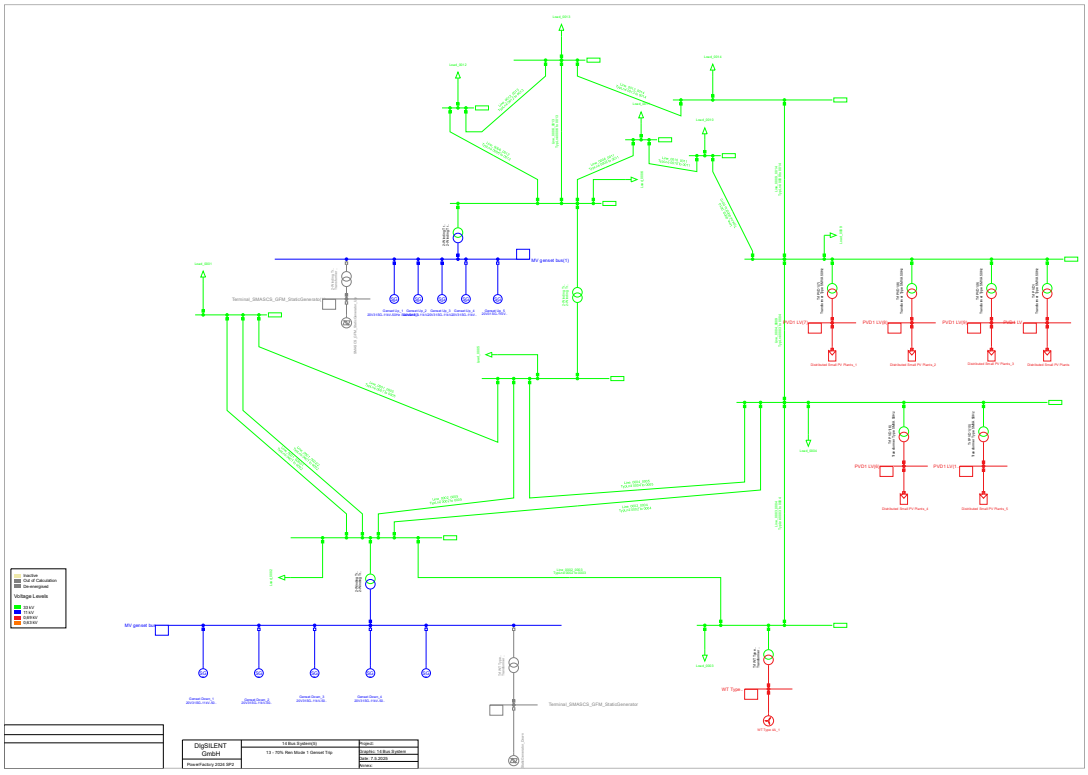

Figure 30. Diagram of Study Cases 13-15.

Study Cases 16-18 (Figure 31):

- 100 MW load.
- 70% renewable generation, 30% synchronous generation.
- Power plant operates in Mode 7: ICE Generating Sets with SC.
- 10 ICE generating sets are active, 6 of them act as SCs.
- Genset Up_1 is the reference machine, the other 3 ICE generating sets generate 27 MW (9 MW each).
- Wind and solar power plants generate 70 MW.
- Study Case 16 is the synchronous generation unit trip (9 MW).
- Study Case 17 is the largest load trip (18.45 MW).
- Study Case 18 is the largest renewable generation unit trip (10 MW).

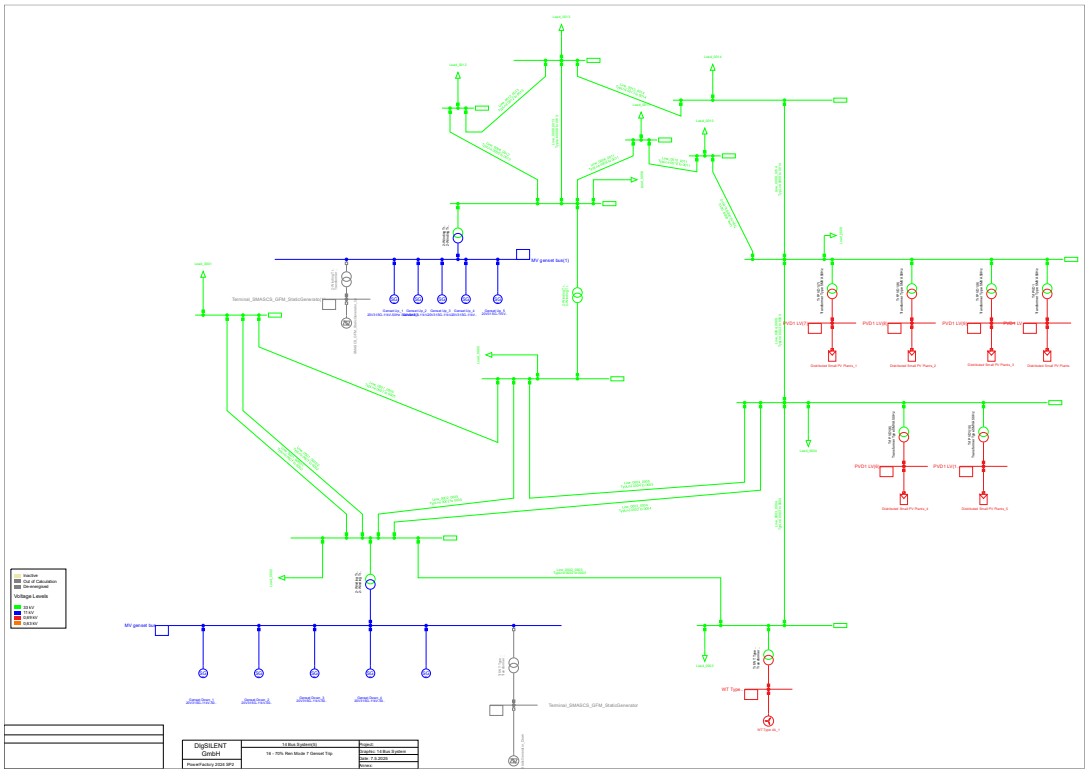

Figure 31. Diagram of Study Cases 16-18.

Study Cases 19-21 (Figure 32):

- 100 MW load.
- 70% renewable generation, 30% synchronous generation.
- Power plant operates in Mode 3: ICE Generating Sets with Power BESS.
- 4 ICE generating sets are active (out of 10).
- Genset Up_1 is the reference machine, the other 3 ICE generating sets generate 27 MW (9 MW each).
- Wind and solar power plants generate 70 MW.
- Two BESS units are active.
- Study Case 19 is the synchronous generation unit trip (9 MW).
- Study Case 20 is the largest load trip (18.45 MW).
- Study Case 21 is the largest renewable generation unit trip (10 MW).

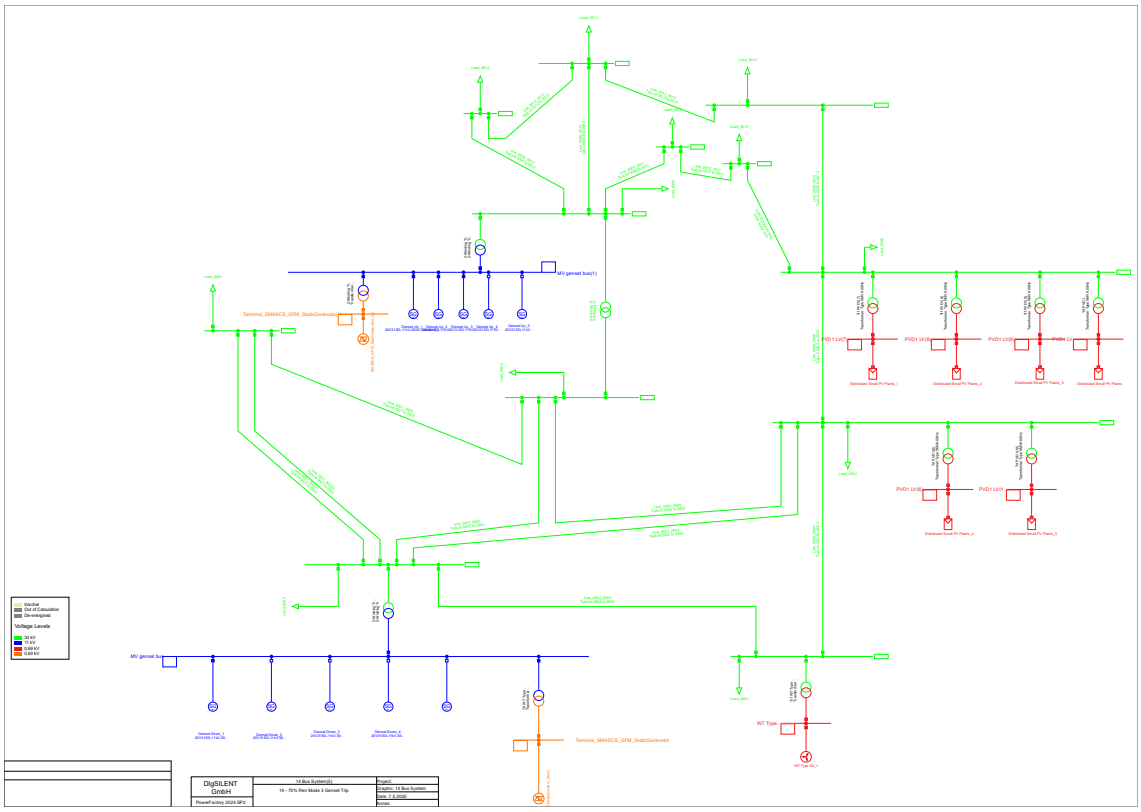

Figure 32. Diagram of Study Cases 19-21.

Study Cases 22-24 (Figure 33):

- 100 MW load.
- 70% renewable generation, 30% synchronous generation.
- Power plant operates in Mode 9: ICE Generating Sets with SC and Power BESS.
- 10 ICE generating sets are active, 6 of them act as SCs.
- Genset Up_1 is the reference machine, the other 3 ICE generating sets generate 27 MW (9 MW each).
- Wind and solar power plants generate 70 MW.
- Two BESS units are active.
- Study Case 22 is the synchronous generation unit trip (9 MW).
- Study Case 23 is the largest load trip (18.45 MW).
- Study Case 24 is the largest renewable generation unit trip (10 MW).

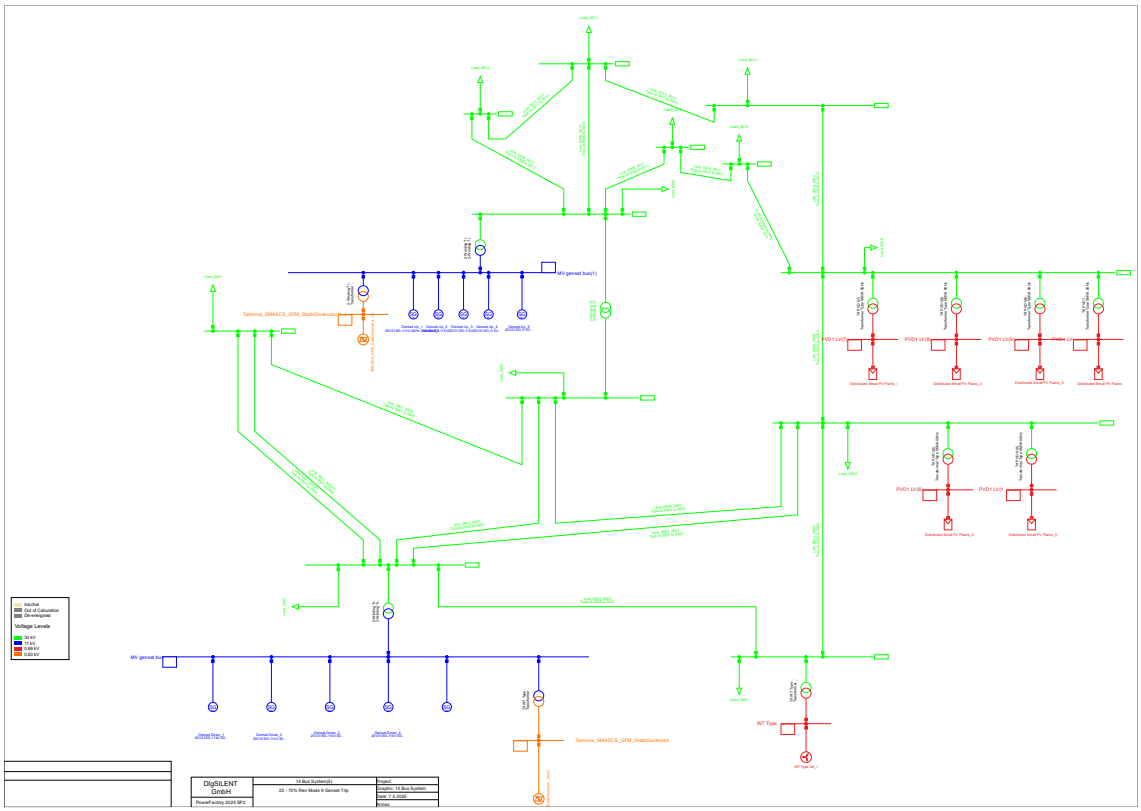

Figure 33. Diagram of Study Cases 22-24.

Study Cases 25-26 (Figure 34):

- 100 MW load.
- 100% renewable generation.
- Power plant operates in Mode 10: Power BESS.
- Wind and solar power plants generate 100 MW.
- Two BESS units are active, with the one connected to the bus “MV genset bus (1)” (**Figure 34)** chosen as the reference machine.
- Study Case 25 is the largest load trip (18.45 MW).
- Study Case 26 is the largest renewable generation unit trip (10 MW).

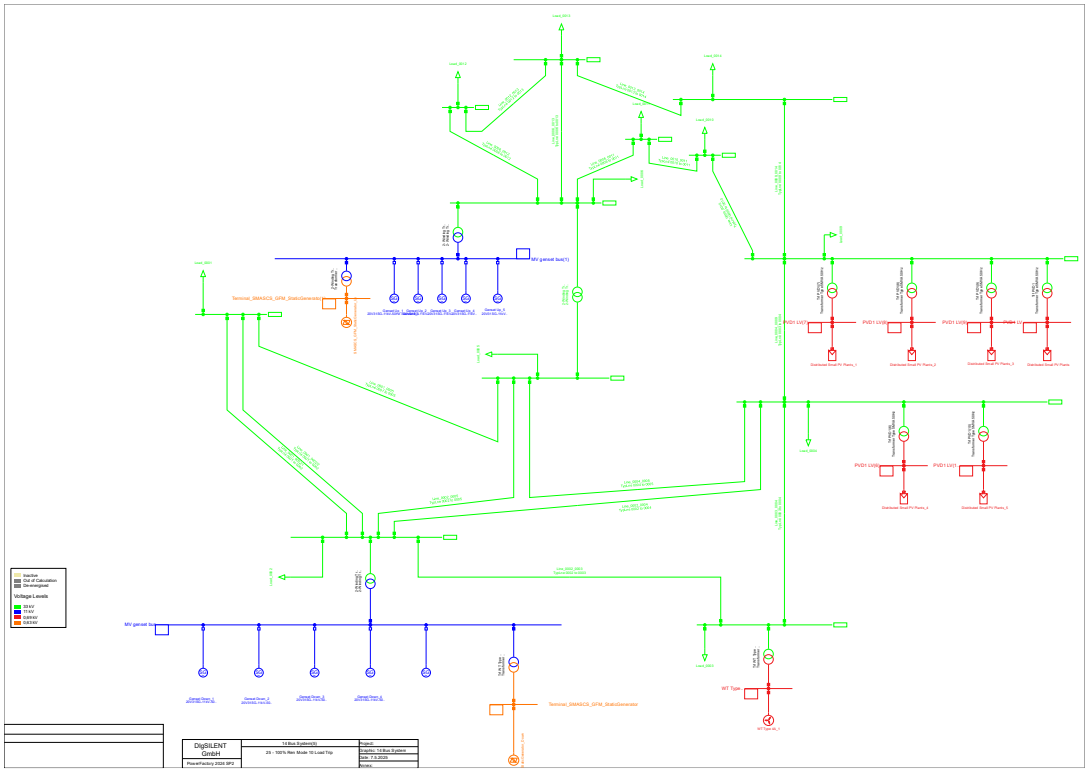

Figure 34. Diagram of Study Cases 25-26.

Study Cases 27-28 (Figure 35):

- 100 MW load.
- 100% renewable generation.
- Power plant operates in Mode 6: SC with Power BESS.
- Wind and solar power plants generate 100 MW.
- 10 ICE generating sets are active, all of them act as SCs.
- Two BESS units are active, with the one connected to the “MV genset bus (1)” chosen as the reference machine.
- Study Case 27 is the largest load trip (18.45 MW).
- Study Case 28 is the largest renewable generation unit trip (10 MW).

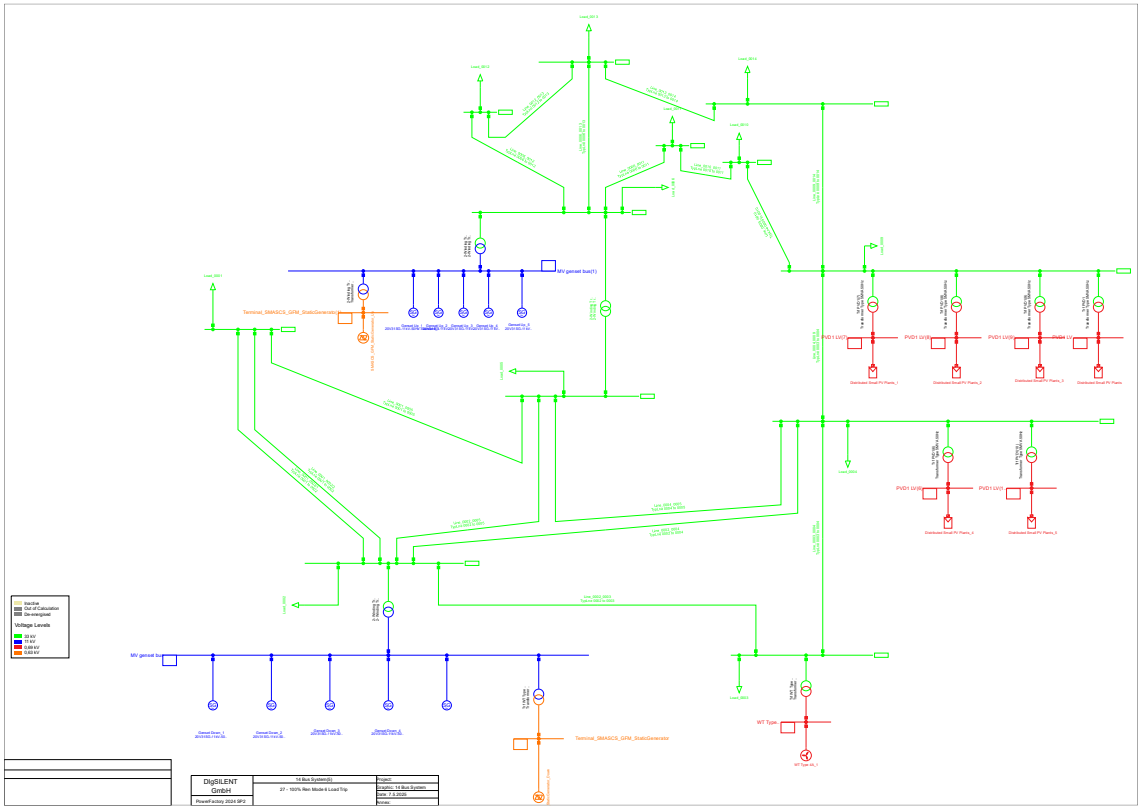

Figure 35. Diagram of Study Cases 27-28.

6 Simulations Results and Analysis

In this thesis, frequency stability simulations were analyzed based on the results of primary frequency control with the droop controller, as no secondary frequency controller was used in simulation models. Detailed information about frequency control levels and the droop controller can be found in Appendix 1 and Appendix 2.

To analyze the simulation results, the terms RoCoF, frequency nadir, and frequency peak are used. RoCoF refers to the rate of change of frequency. The frequency nadir is the smallest value of the frequency, while the frequency peak is the highest value of the frequency after disturbances.

To evaluate the frequency nadir, frequency peak, and RoCoF for each study case, predefined values are needed to determine whether the results are acceptable. For the evaluation of the frequency nadir, values of 47.5 Hz and above are considered acceptable. For the frequency peak, values of 51.5 Hz and below are considered acceptable. These values are chosen as references because power generation units are allowed to disconnect at or beyond these thresholds (ENTSO-E, 2018).

On the other hand, the frequency nadir and peak were generally reached approximately one second after the disturbance began in every study case, as shown in the following subchapters. Therefore, the acceptable RoCoF value is selected as ±1.5 Hz/s (ENTSO-E, 2018).

Since frequency is a global parameter, the system frequency response was taken from Bus_0005 (randomly chosen) in all study cases. The simulation results will be analyzed in the following three subchapters, each corresponding to a different renewable generation share: 40%, 70%, and 100%.

6.1 40% Renewable Generation

6.1.1 Synchronous Generation Unit Trip

The aim of this section is to evaluate the frequency responses of different power plant modes under the disturbance of a synchronous generation unit trip. For this purpose, one ICE generating set unit (9 MW, 9% of the total active power generation) was tripped at the first second.

The frequency responses of different power plant modes, as well as the corresponding frequency nadir and RoCoF values, are presented in **Figure 36** and **Table 10,** respectively.

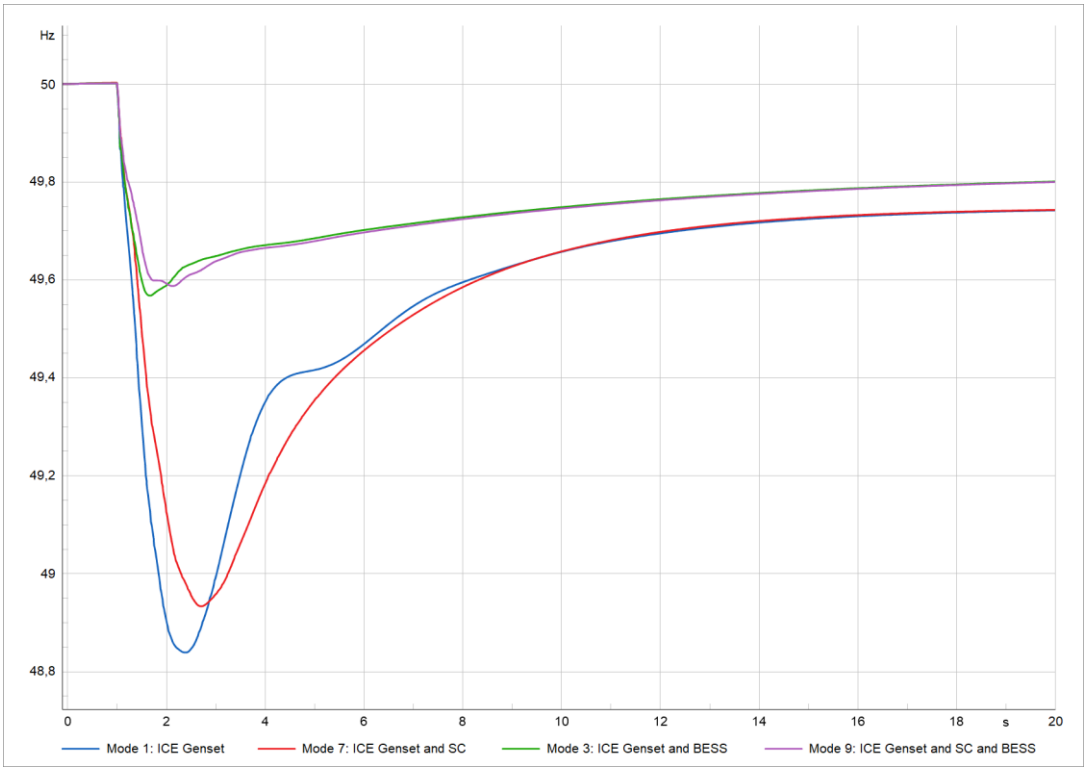

Figure 36. Frequency response of different modes to a synchronous generation unit trip (40% renewable generation).

In this disturbance, frequency decreased because the total generation suddenly dropped below the total load at the beginning of the disturbance.

Power Plant Mode	Frequency nadir (Hz)	Maximum frequency deviation (Hz)	RoCoF(Hz/s)
Mode 1	48.84	–1.16	–0.85
Mode 7	48.93	–1.07	–0.61
Mode 3	49.57	–0.43	–0.65
Mode 9	49.59	–0.41	–0.36

Table 10. Frequency response of different modes to a synchronous generation unit trip (40% renewable generation).

According to **Table 10,** all four modes remained within the acceptable ranges for frequency nadir (47.5 Hz and above) and RoCoF (–1.5 Hz/s and above), indicating a successful response to the disturbance. The comparison of the performance of the power plant modes is as follows:

In Mode 1, seven ICE generating sets (out of ten) were active before the synchronous generation unit trip. The trip was compensated by increasing the output power of the remaining six ICE generating sets and that of the wind power plants (solar power plants did not contribute to the frequency response due to their parameter settings). In this mode, the trip resulted a maximum frequency deviation of –1.16 Hz from the reference frequency (50 Hz), and a RoCoF of –0.85 Hz/s.

In Mode 7, as well as seven ICE generating sets, three SCs were active before the synchronous generation unit trip (SCs were created by the conversion of ICE generating sets to SCs). As a result, the trip was compensated by increasing the output power of the remaining six ICE generating sets, wind power plants, as well as the inertial response from SCs. With the additional contribution of SCs during the disturbance, the maximum frequency deviation was reduced by 7.8% (from –1.16 Hz to –1.07 Hz), and RoCoF was reduced by 28.2% (from –0.85 Hz/s to –0.61 Hz/s) when compared to Mode 1.

In Mode 3, as well as seven ICE generating sets, two BESSs were active before the synchronous generation unit trip. As a result, the trip was compensated by increasing the output power of the remaining six ICE generating sets, wind power plants, as well as

fast response (discharging) of BESSs. With the additional contribution of BESSs during the disturbance, the maximum frequency deviation was reduced by 62.9% (from –1.16 Hz to –0.43 Hz), and the RoCoF was reduced by 23.5% (from –0.85 Hz/s to –0.65 Hz/s) when compared to Mode 1.

In Mode 9, as well as seven ICE generating sets, three SCs and two BESSs were active before the synchronous generation unit trip. As a result, the trip was compensated by increasing the output power of the remaining six ICE generating sets, wind power plants, as well as the inertial response from SCs and the fast response (discharging) of BESSs. With the additional contribution of SCs and BESSs during the disturbance, the maximum frequency deviation was reduced by 64.7% (from –1.16 Hz to –0.41 Hz), and RoCoF was reduced by 57.7% (from –0.85 Hz/s to –0.36 Hz/s) when compared to Mode 1.

Lastly, it is important to note from the results of Mode 7 and Mode 3 that, although SCs improved RoCoF more effectively than BESSs, BESSs performed better in terms of frequency deviation. This is because, while SCs provide instantaneous inertia through their rotating mass, which helps slow down frequency changes, BESSs inject or absorb power quickly, enabling a more precise and rapid response to sudden frequency fluctuations.

In summary, the results clearly show that Mode 9 of the power plant, ICE generating sets, SCs, and BESSs, achieved the best frequency stability performance in terms of both frequency deviation and RoCoF during this disturbance.

6.1.2 The Largest Load Trip

The aim of this section is to evaluate the frequency responses of different power plant modes under the disturbance of the largest load trip. For this purpose, the largest load (18.45 MW, 18.45% of the total load) was tripped at the first second.

The frequency responses of different power plant modes, as well as the corresponding frequency peak and RoCoF values, are presented in **Figure 37** and **Table 11,** respectively.

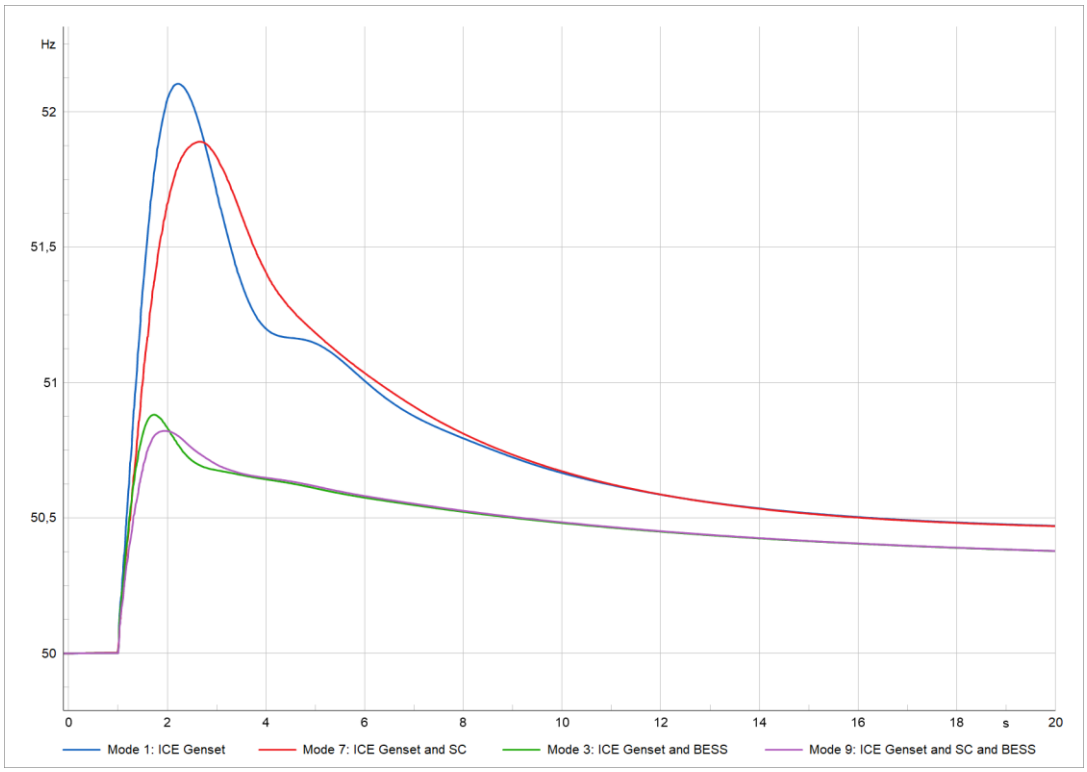

Figure 37. Frequency response of different modes to the largest load trip (40% renewable generation).

In this disturbance, frequency increased because the total load suddenly dropped below the total generation at the beginning of the disturbance.

Power Plant Mode	Frequency peak (Hz)	Maximum frequency deviation (Hz)	RoCoF(Hz/s)
Mode 1	52.10	2.10	1.81
Mode 7	51.89	1.89	1.13
Mode 3	50.88	0.88	1.14
Mode 9	50.82	0.82	0.82

Table 11. Frequency response of different modes to the largest load trip (40% renewable generation).

According to **Table 11,** Mode 1 and Mode 7 failed to respond successfully to the disturbance due to its magnitude. Both modes could not remain within the acceptable frequency range (51.5 Hz and below), and Mode 1 also failed to stay within the acceptable RoCoF range (1.5 Hz/s and below). The comparison of the performance of the power plant modes is as follows:

In Mode 1, seven ICE generating sets were active before the largest load trip. The trip was compensated by decreasing the output power of the seven ICE generating sets and that of the wind power plants. In this mode, the trip caused a maximum frequency deviation of 2.10 Hz from the reference frequency (50 Hz), and a RoCoF of 1.81 Hz/s.

In Mode 7, as well as seven ICE generating sets, three SCs were active before the largest load trip. As a result, the trip was compensated by decreasing the output power of the seven ICE generating sets, wind power plants, as well as the inertial response from SCs. With the additional contribution of SCs during the disturbance, the maximum frequency deviation was reduced by 10.0% (from 2.10 Hz to 1.89 Hz), and RoCoF was reduced by 37.6% (from 1.81 Hz/s to 1.13 Hz/s) when compared to Mode 1.

In Mode 3, as well as seven ICE generating sets, two BESSs were active before the largest load trip. As a result, the trip was compensated by decreasing the output power of the seven ICE generating sets, wind power plants, as well as the fast response (charging) of BESSs. With the additional contribution of BESSs during the disturbance, the maximum frequency deviation was reduced by 58.1% (from 2.10 Hz to 0.88 Hz), and the RoCoF was reduced by 37.0% (from 1.81 Hz/s to 1.14 Hz/s) when compared to Mode 1.

In Mode 9, as well as seven ICE generating sets, three SCs and two BESSs were active before the largest load trip. As a result, the trip was compensated by decreasing the output power of the seven ICE generating sets, wind power plants, as well as the inertial response from SCs and the fast response (charging) of BESSs. With the additional contribution of SCs and BESSs during the disturbance, the maximum frequency deviation

was reduced by 61.0% (from 2.10 Hz to 0.82 Hz), and RoCoF was reduced by 54.7% (from 1.81 Hz/s to 0.82 Hz/s) when compared to Mode 1.

In summary, the results showed that although the acceptable ranges of frequency deviation and RoCoF were marginally achieved with the utilization of Mode 3 of the power plant during this disturbance, Mode 9 ensured the best frequency stability performance in terms of both frequency deviation and RoCoF.

6.1.3 The Largest Renewable Generation Unit Trip

The aim of this section is to evaluate the frequency responses of different power plant modes under the disturbance of the largest renewable generation unit trip. For this purpose, the largest generation unit (10 MW, 10% of the total active power generation) was tripped at the first second.

The frequency responses of different power plant modes, as well as the corresponding frequency nadir and RoCoF values, are presented in **Figure 38** and **Table 12,** respectively.

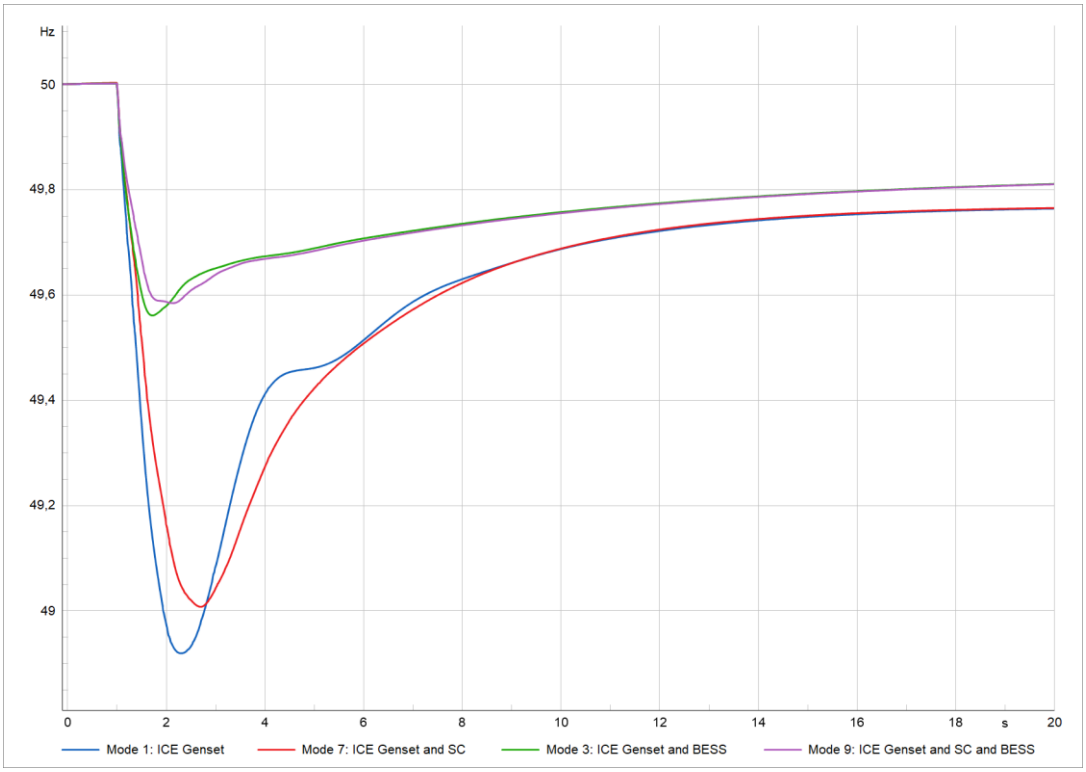

Figure 38. Frequency response of different modes to the largest renewable generation unit trip (40% renewable generation).

In this disturbance, frequency decreased because the total generation suddenly dropped below the total load at the beginning of the disturbance.

Power Plant Mode	Frequency nadir (Hz)	Maximum frequency deviation (Hz)	RoCoF(Hz/s)
Mode 1	48.92	–1.08	–0.81
Mode 7	49.01	–0.99	–0.61
Mode 3	49.56	–0.44	–0.62
Mode 9	49.58	–0.42	–0.37

Table 12. Frequency response of different modes to the largest renewable generation unit trip (40% renewable generation).

According to **Table 12,** all four modes remained within the acceptable ranges for frequency nadir (47.5 Hz and above) and RoCoF (–1.5 Hz/s and above), indicating a successful response to the disturbance. The comparison of the performance of the power plant modes is as follows:

In Mode 1, seven ICE generating sets were active before the largest renewable generation unit trip. The trip was compensated by increasing the output power of the seven ICE generating sets and that of the wind power plants. In this mode, the trip caused a maximum frequency deviation of –1.08 Hz from the reference frequency (50 Hz), and a RoCoF of –0.81 Hz/s.

In Mode 7, as well as seven ICE generating sets, three SCs were active before the largest renewable generation unit trip. As a result, the trip was compensated by increasing the output power of the seven ICE generating sets, wind power plants, as well as the inertial response from SCs. With the additional contribution of SCs during the disturbance, the maximum frequency deviation was reduced by 8.3% (from –1.08 Hz to –0.99 Hz), and RoCoF was reduced by 24.7% (from –0.81 Hz/s to –0.61 Hz/s) when compared to Mode 1.

In Mode 3, as well as seven ICE generating sets, two BESSs were active before the largest renewable generation unit trip. As a result, the trip was compensated by increasing the output power of the seven ICE generating sets, wind power plants, as well as the fast response (discharging) of BESSs. With the additional contribution of BESSs during the disturbance, the maximum frequency deviation was reduced by 59.3% (from –1.08 Hz to –0.44 Hz), and the RoCoF was reduced by 23.5% (from –0.81 Hz/s to –0.62 Hz/s) when compared to Mode 1.

In Mode 9, as well as seven ICE generating sets, three SCs and two BESSs were active before the largest renewable generation unit trip. As a result, the trip was compensated by increasing the output power of the seven ICE generating sets, wind power plants, as well as inertial response from SCs and the fast response (discharging) of BESSs. With the additional contribution of SCs and BESSs during the disturbance, the maximum frequency deviation was reduced by 61.1% (from –1.08 Hz to –0.42 Hz), and RoCoF was reduced by 54.3% (from –0.81 Hz/s to –0.37 Hz/s) when compared to Mode 1.

In summary, the results clearly show that Mode 9 of the power plant, ICE generating sets, SCs, and BESSs, achieved the best frequency stability performance in terms of both frequency deviation and RoCoF during this disturbance.

6.2 70% Renewable Generation

6.2.1 Synchronous Generation Unit Trip

The aim of this section is to evaluate the frequency responses of different power plant modes under the disturbance of a synchronous generation unit trip. For this purpose, one ICE generating set unit (9 MW, 9% of the total active power generation) was tripped at the first second.

The frequency responses of different power plant modes, as well as the corresponding frequency nadir and RoCoF values, are presented in **Figure 39** and **Table 13,** respectively.

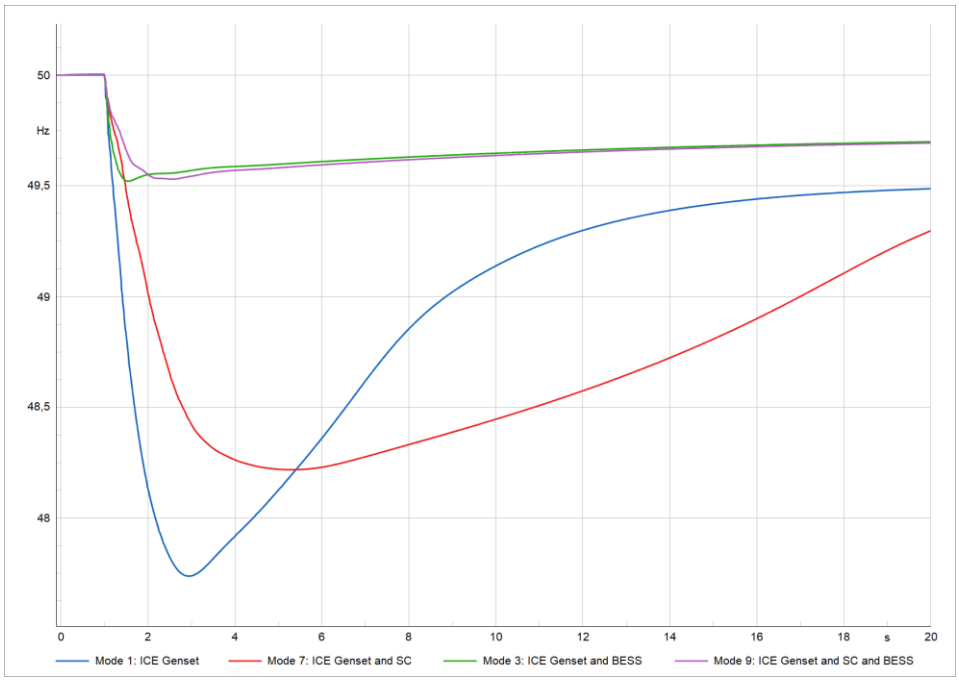

Figure 39. Frequency response of different modes to a synchronous generation unit trip (70% renewable generation).

In this disturbance, frequency decreased because the total generation suddenly dropped below the total load at the beginning of the disturbance.

Power Plant Mode	Frequency nadir (Hz)	Maximum frequency deviation (Hz)	RoCoF(Hz/s)
Mode 1	47.74	–2.26	–1.16
Mode 7	48.22	–1.78	–0.42
Mode 3	49.52	–0.48	–0.87
Mode 9	49.53	–0.47	–0.29

Table 13. Frequency response of different modes to a synchronous generation unit trip (70% renewable generation).

According to **Table 13,** all four modes remained within the acceptable ranges for frequency nadir (47.5 Hz and above) and RoCoF (–1.5 Hz/s and above), indicating a successful response to the disturbance. The comparison of the performance of power plant modes is as follows:

In Mode 1, four ICE generating sets were active before the synchronous generation unit trip. The trip was compensated by increasing the output power of the remaining three ICE generating sets and that of the wind power plants. In this mode, the trip caused a maximum frequency deviation of –2.26 Hz from the reference frequency (50 Hz), and a RoCoF of –1.14 Hz/s.

In Mode 7, as well as four ICE generating sets, six SCs were active before the synchronous generation unit trip. As a result, the trip was compensated by increasing the output power of the remaining three ICE generating sets, wind power plants, as well as the inertial response from SCs. With the additional contribution of SCs during the disturbance, the maximum frequency deviation was reduced by 21.2% (from –2.26 Hz to –1.78 Hz), and RoCoF was reduced by 63.2% (from –1.14 Hz/s to –0.42 Hz/s) when compared to Mode 1.

In Mode 3, as well as four ICE generating sets, two BESSs were active before the synchronous generation unit trip. As a result, the trip was compensated by increasing the output power of the remaining three ICE generating sets, wind power plants, as well as the fast response (discharging) of BESSs. With the additional contribution of BESSs during the disturbance, the maximum frequency deviation was reduced by 78.8% (from –2.26 Hz to –0.48 Hz), and the RoCoF was reduced by 25.0% (from –1.16 Hz/s to –0.87 Hz/s) when compared to Mode 1.

In Mode 9, as well as four ICE generating sets, six SCs and two BESSs were active before the synchronous generation unit trip. As a result, the trip was compensated by increasing the output power of the remaining three ICE generating sets, wind power plants, as well as the inertial response from SCs and the fast response (discharging) of BESSs. With the additional contribution of SCs and BESSs during the disturbance, the maximum frequency deviation was reduced by 79.2% (from –2.26 Hz to –0.47 Hz), and RoCoF was reduced by 74.6% (from –1.14 Hz/s to –0.29 Hz/s) when compared to Mode 1.

In summary, the results clearly show that Mode 9 of the power plant, ICE generating sets, SCs, and BESSs, achieved the best frequency stability performance in terms of both frequency deviation and RoCoF during this disturbance.

6.2.2 The Largest Load Trip

The aim of this section is to evaluate the frequency responses of different power plant modes under the disturbance of the largest load trip. For this purpose, the largest load (18.45 MW, 18.45% of the total load) was tripped at the first second.

The frequency responses of different power plant modes, as well as the corresponding frequency peak and RoCoF values, are presented in **Figure 40** and **Table 14,** respectively.

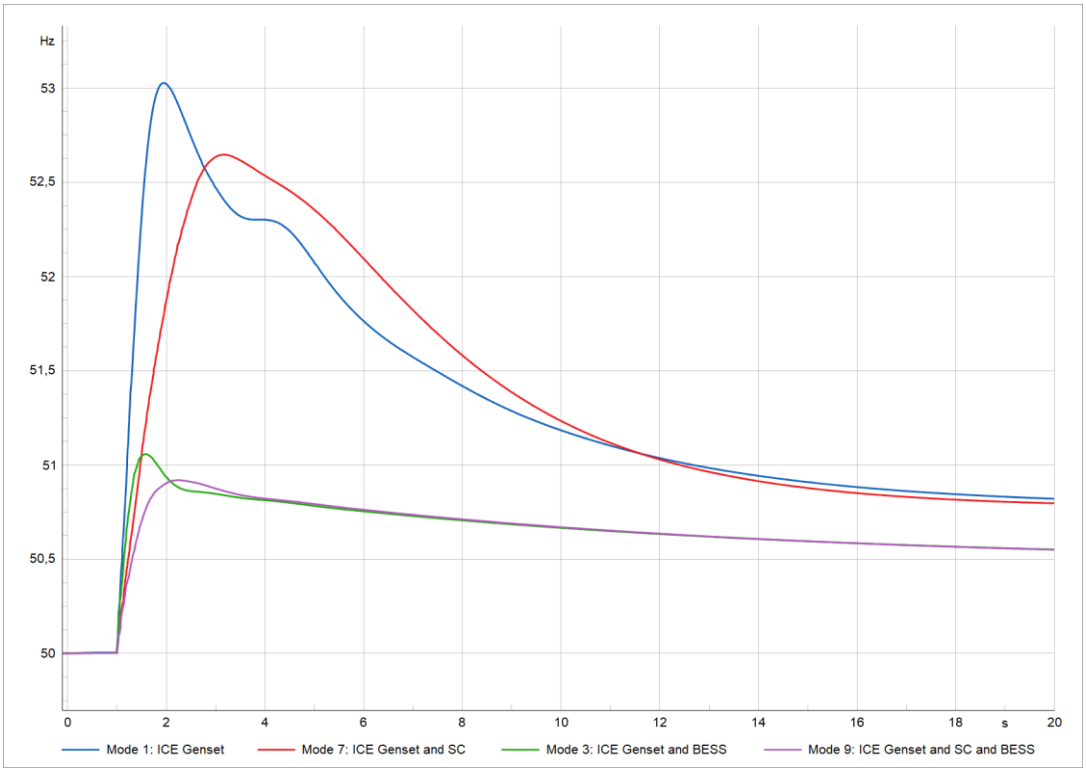

Figure 40. Frequency response of different modes to the largest load trip (70% renewable generation).

In this disturbance, frequency increased because the total load suddenly dropped below the total generation at the beginning of the disturbance.

Power Plant Mode	Frequency peak (Hz)	Maximum frequency deviation (Hz)	RoCoF(Hz/s)
Mode 1	53.03	3.03	3.15
Mode 7	52.65	2.65	1.20
Mode 3	51.06	1.06	1.89
Mode 9	50.92	0.92	0.74

Table 14. Frequency response of different modes to the largest load trip (70% renewable generation).

According to **Table 14,** Mode 1, 7, and 3 failed to respond successfully to the disturbance due to its magnitude. Modes 1 and 7 could not remain within the acceptable frequency range (51.5 Hz and below). Moreover, Modes 1 and 3 failed to stay within the acceptable

RoCoF range (1.5 Hz/s and below). The comparison of the performance of the power plant modes is as follows:

In Mode 1, four ICE generating sets were active before the largest load trip. The trip was compensated by decreasing the output power of the four ICE generating sets and that of the wind power plants. In this mode, the trip caused a maximum frequency deviation of 3.03 Hz from the reference frequency (50 Hz), and a RoCoF of 3.15 Hz/s.

In Mode 7, as well as four ICE generating sets, six SCs were active before the largest load trip. As a result, the trip was compensated by decreasing the output power of the three ICE generating sets, wind power plants, as well as the inertial response from SCs. With the additional contribution of SCs during the disturbance, the maximum frequency deviation was reduced by 12.5% (from 3.03 Hz to 2.65 Hz), and RoCoF was reduced by 61.9% (from 3.15 Hz/s to 1.20 Hz/s) when compared to Mode 1.

In Mode 3, as well as four ICE generating sets, two BESSs were active before the largest load trip. As a result, the trip was compensated by decreasing the output power of the four ICE generating sets, wind power plants, as well as the fast response (charging) of BESSs. With the additional contribution of BESSs during the disturbance, the maximum frequency deviation was reduced by 65.0% (from 3.03 Hz to 1.06 Hz), and the RoCoF was reduced by 40.0% (from 3.15 Hz/s to 1.89 Hz/s) when compared to Mode 1.

In Mode 9, as well as four ICE generating sets, six SCs and two BESSs were active before the largest load trip. As a result, the trip was compensated by decreasing the output power of the four ICE generating sets, wind power plants, as well as the inertial response from SCs and the fast response (charging) of BESSs. With the additional contribution of SCs and BESSs during the disturbance, the maximum frequency deviation was reduced by 69.7% (from 3.03 Hz to 0.92 Hz), and RoCoF was reduced by 76.7% (from 3.15 Hz/s to 0.74 Hz/s) when compared to Mode 1.

In summary, the results showed that the acceptable ranges of frequency deviation and RoCoF were maintained only by Mode 9 of the power plant during this disturbance.

6.2.3 The Largest Renewable Generation Unit Trip

The aim of this section is to evaluate the frequency responses of different power plant modes under the disturbance of the largest renewable generation unit trip. For this purpose, the largest generation unit (10 MW, 10% of the total active power generation) was tripped at the first second.

The frequency responses of different power plant modes, as well as the corresponding frequency nadir and RoCoF values, are presented in **Figure 41** and **Table 15,** respectively.

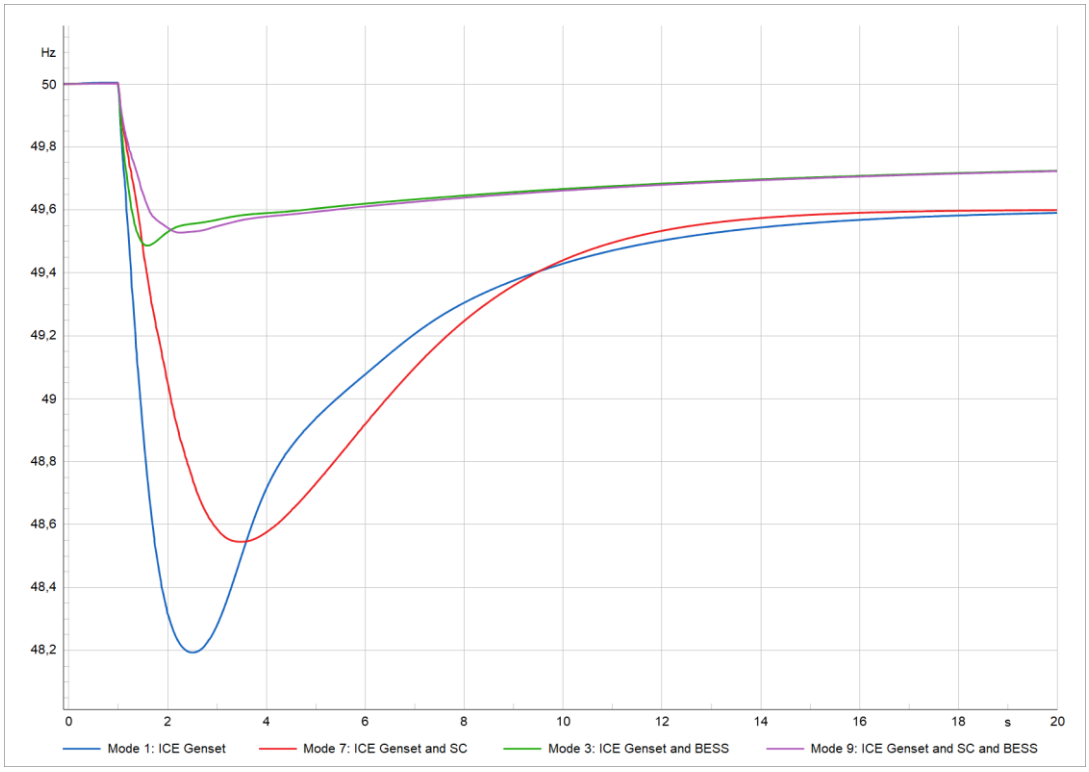

Figure 41. Frequency response of different modes to the largest renewable generation unit trip (70% renewable generation).

In this disturbance, frequency decreased because the total generation suddenly dropped below the total load at the beginning of the disturbance.

Power Plant Mode	Frequency nadir (Hz)	Maximum frequency deviation (Hz)	RoCoF(Hz/s)
Mode 1	48.19	–1.81	–1.22
Mode 7	48.55	–1.45	–0.59
Mode 3	49.49	–0.51	–0.87
Mode 9	49.53	–0.47	–0.37

Table 15. Frequency response of different modes to the largest renewable generation unit trip (70% renewable generation).

According to **Table 15,** all four modes remained within the acceptable ranges for frequency nadir (47.5 Hz and above) and RoCoF (–1.5 Hz/s and above), indicating a successful response to the disturbance. The comparison of the performance of power plant modes is as follows:

In Mode 1, four ICE generating sets were active before the largest renewable generation unit trip. The trip was compensated by increasing the output power of the four ICE generating sets and that of the wind power plants. In this mode, the trip caused a maximum frequency deviation of –1.81 Hz from the reference frequency (50 Hz), and a RoCoF of –1.22 Hz/s.

In Mode 7, as well as four ICE generating sets, six SCs were active before the largest renewable generation unit trip. As a result, the trip was compensated by increasing the output power of the four ICE generating sets, wind power plants, as well as the inertial response from SCs. With the additional contribution of SCs during the disturbance, the maximum frequency deviation was reduced by 19.9% (from –1.81 Hz to –1.45 Hz), and RoCoF was reduced by 51.6% (from –1.22 Hz/s to –0.59 Hz/s) when compared to Mode 1.

In Mode 3, as well as four ICE generating sets, two BESSs were active before the largest renewable generation unit trip. As a result, the trip was compensated by increasing the output power of the four ICE generating sets, wind power plants, as well as the fast response (discharging) of BESSs. With the additional contribution of BESSs during the disturbance, the maximum frequency deviation was reduced by 71.8% (from –1.81 Hz to –0.51 Hz), and the RoCoF was reduced by 28.7% (from –1.22 Hz/s to –0.87 Hz/s) when compared to Mode 1.

In Mode 9, as well as four ICE generating sets, six SCs and two BESSs were active before the largest renewable generation unit trip. As a result, the trip was compensated by increasing the output power of the four ICE generating sets, wind power plants, as well as inertial response from SCs and the fast response (discharging) of BESSs. With the additional contribution of SCs and BESSs during the disturbance, the maximum frequency deviation was reduced by 74.0% (from –1.81 Hz to –0.47 Hz), and RoCoF was reduced by 69.7% (from –1.22 Hz/s to –0.37 Hz/s) when compared to Mode 1.

In summary, the results clearly show that Mode 9 of the power plant, ICE generating sets, SCs, and BESSs, achieved the best frequency stability performance in terms of both frequency deviation and RoCoF during this disturbance.

6.3 100% Renewable Generation

6.3.1 The Largest Load Trip

The aim of this section is to evaluate the frequency responses of different power plant modes under the disturbance of the largest load trip. For this purpose, the largest load (18.45 MW, 18.45% of the total load) was tripped at the first second.

The frequency responses of different power plant modes, as well as the corresponding frequency peak and RoCoF values, are presented in **Figure 42** and **Table 16,** respectively.

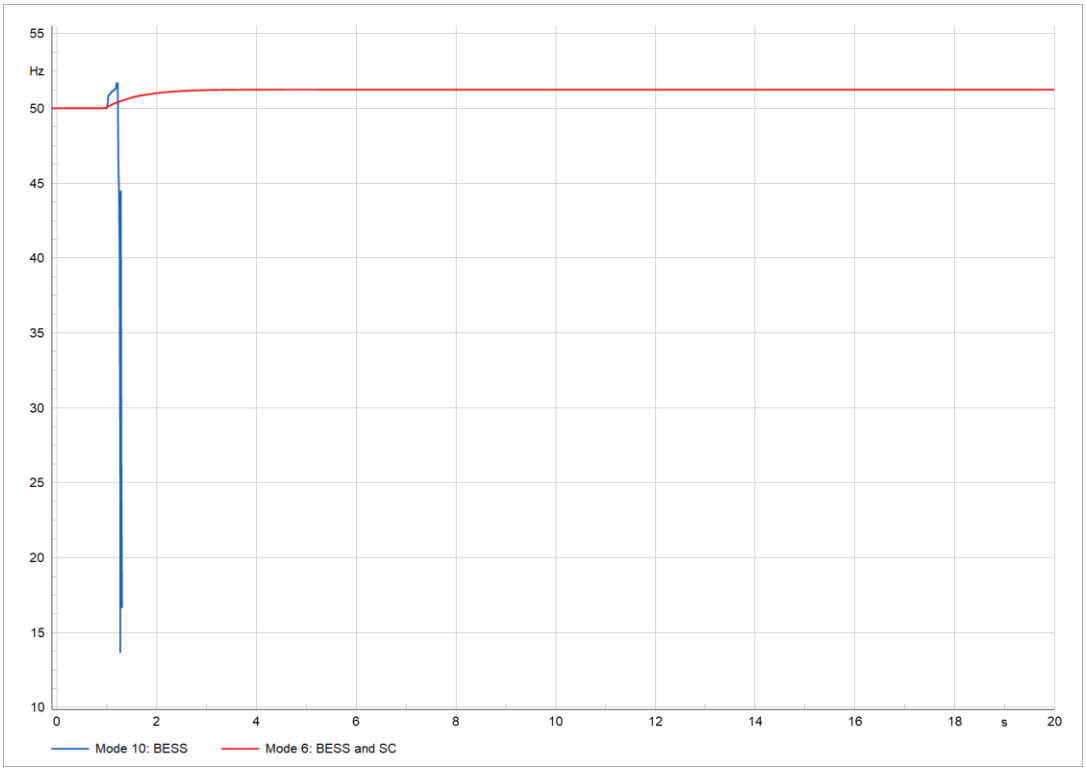

Figure 42. Frequency response of different modes to the largest load trip (100% renewable generation).

In this disturbance, frequency increased because the total load suddenly dropped below the total generation at the beginning of the disturbance.

Power Plant Mode	Frequency peak (Hz)	Maximum frequency deviation (Hz)	RoCoF(Hz/s)
Mode 10	13.66	–36.34	–130.80
Mode 6	51.24	1.24	0.45

Table 16. Frequency response of different modes to the largest load trip (100% renewable generation).

According to **Table 16,** Mode 10 failed to respond successfully to the disturbance due to its magnitude. On the other hand, with Mode 6, the acceptable frequency range (51.5 Hz and below) and RoCoF range (1.5 Hz/s and below) were achieved in response to the disturbance. The comparison of the performance of power plant modes is as follows:

In Mode 10, two BESSs were active before the largest load trip. The trip was attempted to be compensated by decreasing the output power of the wind power plants, as well as the fast response (charging) of BESSs. However, approximately 0.3 seconds after the start of the disturbance, a maximum frequency deviation of –36.34 Hz from the reference frequency (50 Hz) and a RoCoF of –130.80 Hz/s were observed, leading to system instability.

In Mode 6, as well as two BESSs, ten SCs were active before the largest load trip. As a result, the trip was compensated by decreasing the output power of the wind power plants, the fast response (charging) of BESSs, as well as the inertial response from SCs. With the additional contribution of SCs during the disturbance, frequency stability was achieved, as the maximum frequency deviation and RoCoF were reduced to –1.24 Hz (from the reference frequency of 50 Hz) and –0.45 Hz/s, respectively.

In summary, the results demonstrated the significance of SCs and BESS working in conjunction to achieve frequency stability in this case.

6.3.2 The Largest Renewable Generation Unit Trip

The aim of this section is to evaluate the frequency responses of different power plant modes under the disturbance of the largest renewable generation unit trip. For this purpose, the largest generation unit (10 MW, 10% of the total active power generation) was tripped at the first second.

The frequency responses of different power plant modes, as well as the corresponding frequency nadir and RoCoF values, are presented in **Figure 43** and **Table 17,** respectively.

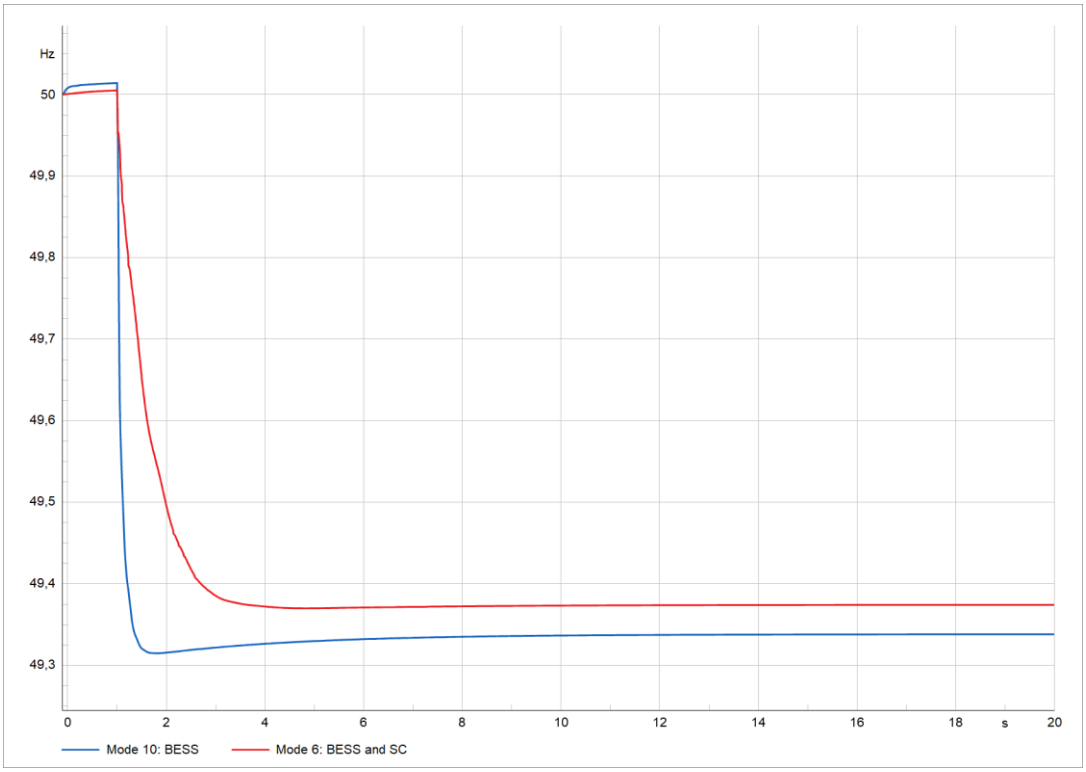

Figure 43. Frequency response of different modes to the largest renewable generation unit trip (100% renewable generation).

In this disturbance, frequency decreased because the total generation suddenly dropped below the total load at the beginning of the disturbance.

Power Plant Mode	Frequency nadir (Hz)	Maximum frequency deviation (Hz)	RoCoF(Hz/s)
Mode 10	49.31	–0.69	–0.95
Mode 6	49.37	–0.63	–0.25

Table 17. Frequency response of different modes to the largest renewable generation unit trip (100% renewable generation).

According to **Table 17,** both modes remained within the acceptable ranges for frequency nadir (47.5 Hz and above) and RoCoF (–1.5 Hz/s and above), indicating a successful response to the disturbance. The comparison of the performance of power plant modes is as follows:

In Mode 10, two BESSs were active before the largest renewable generation unit trip. The trip was compensated by increasing the output power of the wind power plants, as well as the fast response (charging) of BESSs. In this mode, the trip created a maximum frequency deviation of –0.69 Hz from the reference frequency (50 Hz) and a RoCoF of –0.95 Hz/s.

In Mode 6, as well as two BESSs, ten SCs were active before the largest renewable generation unit trip. As a result, the trip was compensated by increasing the output power of the wind power plants, the fast response (charging) of BESSs, and the inertial response from SCs. With the additional contribution of SCs during the disturbance, the maximum frequency deviation was reduced by 8.7% (from –0.69 Hz to –0.63 Hz), and RoCoF was reduced by 73.7% (from –0.95 Hz/s to –0.25 Hz/s) compared to Mode 10.

In summary, the results of this disturbance highlight the importance of BESSs in reducing frequency deviation and the role of SCs in improving RoCoF.

7 Conclusions

The findings from the frequency stability simulations of the flexible multi-mode power plant solution concept indicated that:

- Mode 1 of the power plant (ICE generating sets) successfully maintained frequency stability within the defined limits in response to the synchronous generation trip (9 MW) and the largest renewable energy generation trip (10 MW), but not for the largest load trip (18.45 MW).
- As expected, frequency deviation and RoCoF increase in grids with a higher share of renewables during disturbances.
- The addition of BESSs significantly reduces both frequency deviation and RoCoF in the case of disturbances.
- Comparisons between Mode 1 of the power plant (ICE generating sets) and Mode 3 (ICE generating sets and BESSs) showed that the impact of BESSs on frequency deviation and RoCoF improves in grids with a higher share of renewables (low-inertia grids).
- SCs significantly reduce RoCoF and help to reduce frequency deviations.
- The impact of SCs on RoCoF reduction increases in grids with a higher share of renewables. To evaluate this, Mode 1 of the power plant (ICE generating sets) was compared with Mode 7 (ICE generating sets and SCs), using the same number of SCs (three), under the same disturbances at renewable energy shares of 40% and 70%. One of the comparisons showed that, in the case of a synchronous generation trip, RoCoF was reduced by 28.2% with the 40% renewable generation share and by 34.2% with the 70% renewable generation share. Details of the results can be found in **Table 19** of Appendix 3.
- The results of the largest load trip (the most severe disturbance) at 100% renewable generation (**Table 16**) may serve as an example case demonstrating the importance of the joint operation of BESSs and SCs in maintaining frequency stability in power systems with high renewable energy penetration.

- Mode 9 (ICE generating sets, BESSs, and SCs) of the power plant demonstrated the best frequency stability performance during disturbances, in terms of frequency deviation and RoCoF, in both the 40% and 70% renewable share cases. This was due to the complementary operation of the components, where ICE generating sets and BESSs both quickly respond to power fluctuations and reduce frequency deviation, while SCs improve system inertia and reduce RoCoF.

Overall, the results of the simulation studies demonstrated that frequency stability was maintained by utilizing the appropriate operating modes of the power plant solution concept.

In conclusion, as discussed in detail throughout the thesis, by leveraging ICE generating sets, BESSs, and SCs, “The Flexible Multi-Mode Power Plant Solution” concept offers a promising response to modern grid challenges, including the increasing need for flexibility, stability, controllability of the generation-load balance, reliability, and renewable energy integration. Additionally, the capability of ICE generating sets to operate entirely on hydrogen in the near future will further position this concept as a cleaner and more sustainable solution.

Looking ahead, future studies could explore the performance of the flexible multi-mode power plant solution concept from various perspectives. For example, in terms of frequency stability, a secondary frequency controller can be added to the simulation models for the analysis of frequency stability over longer time frames. Additionally, further simulation cases can be created to evaluate the frequency stability performance of the solution concept not only for islanded operation but also for grid-connected operation.

On the other hand, since the solution concept offers reactive power support, the voltage stability of the grid can also be analyzed, for example, through fault ride-through simulations. Moreover, by employing Modes 2, 5, 8, and 11, steady-state performance

of the solution concept can be assessed through simulation studies such as optimal power flow, economic dispatch, load flow, and quasi-dynamic analysis. Lastly, as advanced work, grid code compliance verification for the solution concept can be performed using hardware-in-the-loop testing, which enables real-time simulation and testing under realistic conditions.

References

Abdulraheem, B. S., & Gan, C. K. (2016). Power system frequency stability and control: Survey. *International Journal of Applied Engineering Research, 11*(8), 5688–5695. https://www.researchgate.net/publication/303811158_Power_System_Frequency_Stability_and_Control_Survey

Agora Energiewende. (2017). *Flexibility in thermal power plants – With a focus on existing coal-fired power plants*. https://www.agora-energiewende.de/fileadmin/Projekte/2017/Flexibility_in_thermal_plants/115_flexibility-report-WEB.pdf

Alatai, S., Salem, M., Ishak, D., Das, H. S., Alhuyi Nazari, M., Bughneda, A., & Kamarol, M. (2021). A review on state-of-the-art power converters: Bidirectional, resonant, multilevel converters and their derivatives. *Applied Sciences, 11*(21), 10172. https://doi.org/10.3390/app112110172

Aruna, S. B., Suchitra, D., Rajarajeswari, R., & Fernandez, S. G. (2021). A comprehensive review on the modern power system reliability assessment. *International Journal of Renewable Energy Research (IJRER), 11*(4), 1750–1760. https://www.ijrer.org/ijrer/index.php/ijrer/article/view/12480

Ashourian, H., & Gras, H. (2022). *WECC PV park model*. EMTPWorks. https://www.emtp.com/documents/EMTP%20Documentation/doc/Renewables/WECC_PV_Park_Models.pdf

Australian Energy Market Commission. (2021). *Final report: National Electricity Amendment (Fast Frequency Response Market Ancillary Service) Rule 2021*. https://www.aemc.gov.au/sites/default/files/2021-07/Fast%20frequency%20response%20market%20ancillary%20service%20-%20Final%20Determination.pdf

Badal, F. R., Das, P., Sarker, S. K., & Das, S. K. (2019). A survey on control issues in renewable energy integration and microgrid. *Protection and Control of Modern Power Systems, 4*, Article 8. https://doi.org/10.1186/s41601-019-0122-8

Billimoria, F., Mancarella, P., & Poudineh, R. (2020). *Market design for system security in low-carbon electricity grids: From the physics to the economics*. Oxford Institute for Energy Studies. https://doi.org/10.26889/9781784671600

Blázquez, J., Fuentes-Bracamontes, R., & Manzano, B. (2019). *A road map to navigate the energy transition* (Insight 59). Oxford Institute for Energy Studies. https://www.oxfordenergy.org/wpcms/wp-content/uploads/2019/10/A-road-map-to-navigate-the-energy-transition-Insight-59.pdf

Bompard, E., Guillaud, X., Monti, A., & Milano, F. (2021). Classical grid control: Frequency and voltage stability. In *Converter-Based Dynamics and Control of Modern Power Systems* (pp. 31–65). Elsevier. https://doi.org/10.1016/B978-0-12-818491-2.00003-1

Byrne, R. H., Nguyen, T. A., Copp, D. A., Chalamala, B. R., & Gyuk, I. (2018). Energy management and optimization methods for grid energy storage systems. *IEEE Access, 6*, 13231–13260. https://doi.org/10.1109/ACCESS.2017.2741578

Caballero-Peña, J., Cadena-Zarate, C., Parrado-Duque, A., & Osma-Pinto, G. (2022). *Distributed energy resources on distribution networks: A systematic review of modelling, simulation, metrics, and impacts*. *International Journal of Electrical Power & Energy Systems, 138*, 107900. https://doi.org/10.1016/j.ijepes.2021.107900

California Independent System Operator. (2021). *Dynamic model review guideline for inverter based interconnection requests*. https://www.caiso.com/Documents/InverterBasedInterconnectionRequestsIBRDynamicModelReviewGuideline.pdf

Chakraborty, S. (2011). Advancements in power electronics and drives in interface with growing renewable energy resources. *Renewable and Sustainable Energy Reviews, 15*(4), 1816–1827. https://doi.org/10.1016/j.rser.2010.12.017

Datta, U., Kalam, A., & Shi, J. (2021). A review of key functionalities of battery energy storage system in renewable energy integrated power systems. *Energy Storage, 3*(5), e224. https://doi.org/10.1002/est2.224

ENTSO-E. (2018). *Rate of Change of Frequency (RoCoF) withstand capability: ENTSO-E guidance document for national implementation for network codes on grid connection*. https://eepublicdownloads.entsoe.eu/clean-documents/Network%20codes%20documents/NC%20RfG/IGD_RoCoF_withstand_capability_final.pdf

European Association for Storage of Energy. (2016). *Hydrogen*. https://ease-storage.eu/wp-content/uploads/2016/03/EASE_TD_Hydrogen.pdf

Gan, G., Junhui, L., Gang, M., & Gangui, Y. (2025). Optimized strategies for peak shaving and BESS efficiency enhancement through cycle-based control and cluster-level power allocation. *arXiv*. https://doi.org/10.48550/arXiv.2502.10268

Hafner, M., & Luciani, G. (Eds.). (2022). *The Palgrave handbook of international energy economics*. Palgrave Macmillan. https://library.oapen.org/handle/20.500.12657/57011

Hassan, Q., Algburi, S., Sameen, A. Z., Al-Musawi, T. J., Al-Jiboory, A. K., Salman, H. M., & Al-Khafaji, A. I. (2024). A comprehensive review of international renewable energy growth. *Energy and Built Environment, 5*(1), 100041. https://doi.org/10.1016/j.enbenv.2023.12.002

Hatziargyriou, N., Milanović, J. V., & Ajjarapu, V. (2021). Definition and classification of power system stability—Revisited & extended. *IEEE Transactions on Power Systems, 36*(4), 3271–3281. https://doi.org/10.1109/TPWRS.2020.3041774

Hidalgo-León, R., Siguenza, D., Sanchez, C., León, J., Jácome-Ruiz, P., Wu, J., & Ortiz, D. (2017). A survey of battery energy storage system (BESS), applications and environmental impacts in power systems. In *2017 IEEE Second Ecuador Technical Chapters Meeting (ETCM)* (pp. 1–6). IEEE. https://doi.org/10.1109/ETCM.2017.8247485

Hillberg, E., Oleinikova, I., & Iliceto, A. (2022). Flexibility benefits for Power System Resilience. *CIGRE Study Committee C6, Technical Brochure No. 26*. https://cse.cigre.org/cse-n026/flexibility-benefits-for-power-system-resilience.html

Hossain, M. A., Pota, H. R., Hossain, M. J., & Blaabjerg, F. (2019). Evolution of microgrids with converter-interfaced generations: Challenges and opportunities. *International Journal of Electrical Power & Energy Systems, 109*, 160–186. https://doi.org/10.1016/j.ijepes.2019.01.038

International Energy Agency. (2022). *Unlocking the potential of DERs: Power system opportunities and best practices*. Retrieved from https://iea.blob.core.windows.net/assets/3520710c-c828-4001-911c-ae78b645ce67/UnlockingthePotentialofDERs_Powersystemopportunitiesandbestpractices.pdf

International Energy Agency. (2024). *Renewables 2024*. https://iea.blob.core.windows.net/assets/17033b62-07a5-4144-8dd0-651cdb6caa24/Renewables2024.pdf

International Renewable Energy Agency (IRENA). (2019). *Flexibility in Conventional Power Plants: Innovation Landscape Brief*. International Renewable Energy Agency. https://www.irena.org/-/media/Files/IRENA/Agency/Publication/2019/Sep/IRENA_Flexibility_in_CPPs_2019.pdf?la=en&hash=AF60106EA083E492638D8FA9ADF7FD099259F5A1

Jaffal, H., Guanetti, L., Rancilio, G., Spiller, M., Bovera, F., & Merlo, M. (2024). Battery energy storage system performance in providing various electricity market services. *Batteries*, 10(3), 69. https://doi.org/10.3390/batteries10030069

Kanojia, S. S., & Suthar, B. N. (2024). Voltage stability index: A review based on analytical method, formulation, and comparison in renewable dominated power system. *International Journal of Applied Power Engineering (IJAPE), 13*(2), 508–520. https://doi.org/10.11591/ijape.v13.i2.pp508-520

Katz, J., Denholm, P., & Cochran, J. (2015). *Balancing area coordination: Efficiently integrating renewable energy into the grid*. National Renewable Energy Laboratory. https://www.nrel.gov/docs/fy15osti/63037.pdf

Khan, M. K., Raza, M., Shahbaz, M., Farooq, U., & Akram, M. U. (2024). Recent advancement in energy storage technologies and their applications. *Journal of Energy Storage, 92*, 112112. https://doi.org/10.1016/j.est.2024.112112

Kılıç, L., & Arsoy, A. B. (2015). Evaluation of frequency control application for distributed generation in Turkey. *International Journal of Electrical Power & Energy Systems*, 67, 501–509. https://doi.org/10.1016/j.ijepes.2014.12.040

Kim, H. T., Jin, Y. G., & Yoon, Y. T. (2019). An economic analysis of load leveling with battery energy storage systems (BESS) in an electricity market environment: The Korean case. *Energies, 12*(9), 1608. https://doi.org/10.3390/en12091608

Kirkerud, J. G., Nagel, N. O., & Bolkesjø, T. F. (2021). The role of demand response in the future renewable northern European energy system. *Energy, 235*, 121336. https://doi.org/10.1016/j.energy.2021.121336

Kundur, P. (1994). *Power system stability and control*. McGraw-Hill.

Kuzemko, C., Mitchell, C., Lockwood, M., & Hoggett, R. (2017). Policies, politics and demand side innovations: The untold story of Germany's energy transition. *Energy Research & Social Science, 28*, 58–67. https://doi.org/10.1016/j.erss.2017.03.013

Landera, Y. G., Zevallos, O. C., Neto, R. C., da Costa Castro, J. F., & Neves, F. A. S. (2023). A review of grid connection requirements for photovoltaic power plants. *Energies, 16*(5), 2093. https://doi.org/10.3390/en16052093

Li, H., Zhang, N., Fan, Y., Dong, L., & Cai, P. (2022). Decomposed modeling of controllable and uncontrollable components in power systems with high penetration of renewable energies. *Journal of Modern Power Systems and Clean Energy, 10*(5), 1164–1173. https://doi.org/10.35833/MPCE.2020.000674

Lopes, J. A. P., Madureira, A. G., Matos, M., Bessa, R. J., Monteiro, V., Afonso, J. L., Santos, S. F., Catalão, J. P. S., Henggeler Antunes, C., & Magalhães, P. (2019). The future of power systems: Challenges, trends, and upcoming paradigms. *Wiley Interdisciplinary Reviews: Energy and Environment, 8*(6), e368. https://doi.org/10.1002/wene.368

Mahdi, S. J., Tan, N. M. L., & Pasupuleti, J. (2021). A review of energy management and power management systems for microgrid and nanogrid applications. *Sustainability, 13*(18), 10331. https://doi.org/10.3390/su131810331

Meegahapola, L. G., Mancarella, P., Flynn, D., & Moreno, R. (2021). Power system stability in the transition to a low carbon grid: A techno-economic perspective on challenges and opportunities. *Wiley Interdisciplinary Reviews: Energy and Environment, 10*(3), e399. https://doi.org/10.1002/wene.399

Meegahapola, L., Sguarezi, A., Bryant, J. S., Gu, M., Conde D., E. R., & Cunha, R. B. A. (2020). *Power system stability with power-electronic converter interfaced renewable power generation: Present issues and future trends*. *Energies*, 13(13), 3441. https://doi.org/10.3390/en13133441

National Renewable Energy Laboratory. (2019). *Grid-scale battery storage: Frequently asked questions* (NREL/TP-6A20-74426). U.S. Department of Energy. https://www.nrel.gov/docs/fy19osti/74426.pdf

PowerFactory. (2024). *IEEE 14 Bus System*.

Rahman, M. M., Oni, A. O., Gemechu, E., & Kumar, A. (2020). Assessment of energy storage technologies: A review. *Energy Conversion and Management, 223*, 113295. https://doi.org/10.1016/j.enconman.2020.113295

Ratnam, K. S., Palanisamy, K., & Yang, G. (2020). Future low-inertia power systems: Requirements, issues, and solutions – A review. *Renewable and Sustainable Energy Reviews, 124*, 109773. https://doi.org/10.1016/j.rser.2020.109773

Rummeny, S., Waffenschmidt, E., Guenther, F., Klenner, F., & Stankat, P. R. (2020). Emergency island operation of a medium-voltage utility grid with a large battery. *CIRED – Open Access Proceedings Journal*, 2020(1), 565–568. https://doi.org/10.1049/oap-cired.2021.0118

S&P Global. (2020, February 24). *What is energy transition?* https://www.spglobal.com/en/research-insights/market-insights/what-is-energy-transition

Samanes, J., Gubía, E., López, J., & Burgos, R. (2020). Sub-synchronous resonance damping control strategy for DFIG wind turbines. *IEEE Access, 8*, 223359–223372. https://doi.org/10.1109/ACCESS.2020.3043818

Shahzad, S., Abbasi, M. A., Ali, H., Iqbal, M., Munir, R., & Kılıç, H. (2023). Possibilities, Challenges, and Future Opportunities of Microgrids: A Review. *Sustainability*, *15*(8), 6366. https://doi.org/10.3390/su15086366

Shrestha, A., & Gonzalez-Longatt, F. (2021). Frequency stability issues and research opportunities in converter dominated power system. *Energies, 14*(14), 4184. https://doi.org/10.3390/en14144184

Soleimani, H., Habibi, D., Ghahramani, M., & Aziz, A. (2024). Strengthening power systems for net zero: A review of the role of synchronous condensers and emerging challenges. *Energies, 17*(13), 3291. https://doi.org/10.3390/en17133291

Sweeney, C., Bessa, R. J., Browell, J., & Pinson, P. (2020). The future of forecasting for renewable energy. *Wiley Interdisciplinary Reviews: Energy and Environment, 9*(2), e365. https://doi.org/10.1002/wene.365

Tang, Z., Yang, Y., & Blaabjerg, F. (2021). Power electronics: The enabling technology for renewable energy integration. *CSEE Journal of Power and Energy Systems, 8*(1), 39–52. https://doi.org/10.17775/CSEEJPES.2021.02850

Tielens, P., & Van Hertem, D. (2016). The relevance of inertia in power systems. *Renewable and Sustainable Energy Reviews, 55*, 999–1009. https://doi.org/10.1016/j.rser.2015.11.016

Wang, Y.-Y., & Mori, A. (2024). A review of dynamic changes in complementarities and transition pathways toward distributed energy resource–based electrical system. *Renewable Energy Focus, 51*, 100626. https://doi.org/10.1016/j.ref.2024.100626

Wärtsilä Energy. (n.d.). *Get ready for sustainable fuels with flexible Wärtsilä power plants*. https://www.wartsila.com/docs/default-source/energy-docs/technology-products/white-papers/wartsila_sustainablefuels_paper.pdf

Wärtsilä. (2020). *New regulatory frameworks for grid flexibility*. Wärtsilä. https://www.wartsila.com/docs/default-source/power-plants-documents/downloads/white-papers/general/new-regulatory-frameworks-for-grid-flexibility.pdf

Wärtsilä. (n.d.). *Wärtsilä Energy – Towards a 100% renewable energy future*. Retrieved May 26, 2025, from https://www.wartsila.com/energy

Xu, Z., Wang, S., Xing, F., & Xiao, H. (2018). *Study on the method for analyzing electric network resonance stability*. *Energies, 11*(3), 646. https://doi.org/10.3390/en11030646

Zhang, Y., Liu, Z.-X., Wang, F., & Chen, Z. (2024). Distributed secondary frequency control and state of charge (SoC) balance for droop-controlled battery energy storage systems (BESSs) with a unified SoC relative variation rate. *Transactions of the Institute of Measurement and Control*. https://doi.org/10.1177/01423312241287248

Zhou, Y., Zhang, R., Kathriarachchi, D., Dennis, J., & Goyal, S. (2023). Grid forming inverter and its applications to support system strength – A case study. *IET Generation, Transmission & Distribution*, 17(3), 391–398. https://doi.org/10.1049/gtd2.12566

Zuo, Y., Yuan, Z., Sossan, F., Zecchino, A., Cherkaoui, R., & Paolone, M. (2021). Performance assessment of grid-forming and grid-following converter-interfaced battery energy storage systems on frequency regulation in low-inertia power grids. *Sustainable Energy, Grids and Networks, 27*, 100496. https://doi.org/10.1016/j.segan.2021.100496

Appendices

Appendix 1. Frequency Control Levels

In power systems, the frequency shows three main characteristics (Bompard et al., 2021):

- Uniformity: At any time, all generators operate in synchronism, which makes the frequency the same at every point in the system. However, with the increasing penetration of renewable (inverter-based) energy generation units, this characteristic changes.
- Coherency: To produce a synchronized voltage waveform, all generation units in the power system must be correlated.
- Stability: Since power system components are designed to operate optimally at nominal frequency, the frequency of the power system must be maintained close to nominal frequency.

To maintain the nominal frequency at any time, the total generated active power and the total consumed active power must be equal (Bompard et al., 2021). In case the former exceeds the latter, the frequency of the power system increases; in case the former falls behind the latter, the frequency of the power system decreases.

As shown in **Figure 44,** there are three frequency control levels in power systems to keep the frequency within acceptable limits.

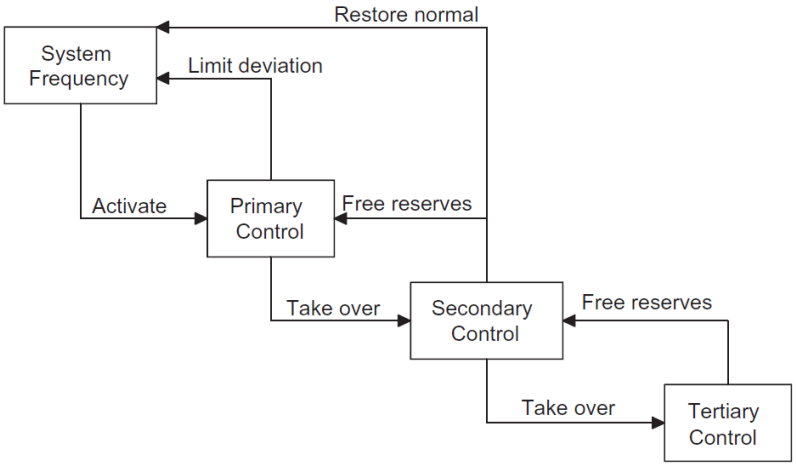

Figure 44. Frequency control levels in power systems (Kılıç & Arsoy, 2015).

Characteristics of the three frequency control levels are shown in **Table 18.**

	Primary control	**Secondary control**	**Tertiary control**
Why is this control used?	To stabilize the frequency any time power unbalance is experienced	To restore the frequency and the interchange flows to their scheduled value	To restore the secondary control reserve, to manage eventual congestions, and to bring back the frequency and the interchange programs to their target if the secondary control reserve is not enough
How is this control achieved?	Automatically		Manually
Where is this control performed?	Locally/ decentralized	Centralized, from the dispatching center	
Who sends the control signal to the source of reserve?	Local sensor	Automatic generation controllers (AGC) located on the TSO premises	Generators, loads or other TSOs
Time activation	2–3 s from the perturbation detection	Continuously, the control order is sent every 1–5 s	Varies from system to system
Full activation	Usually up to 30 s	Usually up to 15 min	Usually between 15 min and 7 h
Resources used	Partially loaded generation units, storage systems, loads, fast/slow starting generation units, changes in exchange programs		

Table 18. Characteristics of the three frequency control levels (Bompard et al., 2021).

Appendix 2. Primary Frequency Control and Droop Controller

As shown in **Figure 45,** a speed governor is employed in synchronous generators for primary frequency control. With the speed governor, the energy flow (steam, water, or gas) to the turbine is adjusted, which changes the active power output of the generator whenever the rotor speed deviation is greater than a predefined value.

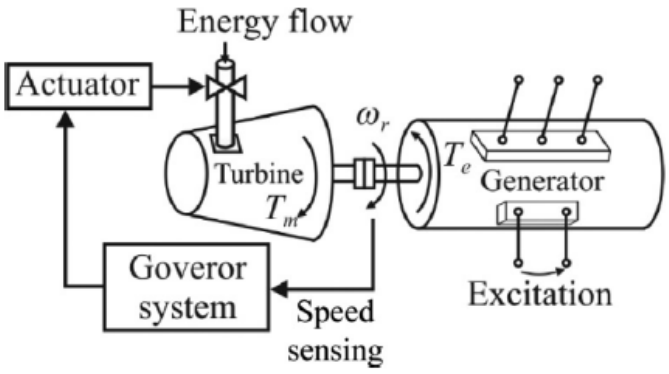

Figure 45. Simplified turbine-generator speed control (Bompard et al., 2021).

Generally, there are three types of governors employed in synchronous machines to regulate frequency, namely, droop (speed-droop), isochronous, and compensated governor (Bompard et al., 2021).

The droop governor is proper to use in interconnected power systems. A droop governor-based frequency control scheme is shown in **Figure 46.**

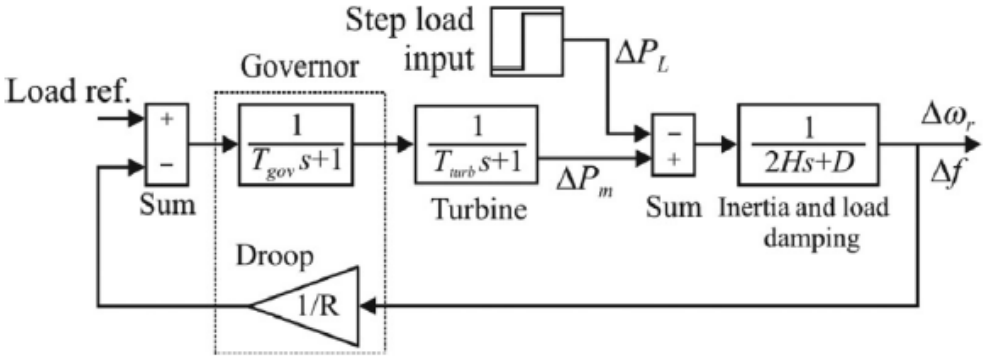

Figure 46. Droop frequency control model of a single synchronous machine (Bompard et al., 2021).

As shown in **Figure 46,** negative feedback exists in droop frequency control. The governor and the turbine are simply expressed by a delay function. Droop, symbolized by R, is the amount of speed (or frequency, in per-unit terms) change required to cause the prime mover mechanism to move from fully closed to fully open.

The droop can be calculated as:

$$R = \frac{\Delta\omega}{\Delta P} \quad (19)$$

The droop can also be calculated as the ratio between the change in frequency from no-load to full-load to reference frequency in per-unit:

$$R = \frac{\omega_{NL}-\omega_{FL}}{\omega_0} = \frac{f_{NL}-f_{FL}}{f_0} \quad (20)$$

Figure 47 shows frequency and active power variation for speed-droop governor.

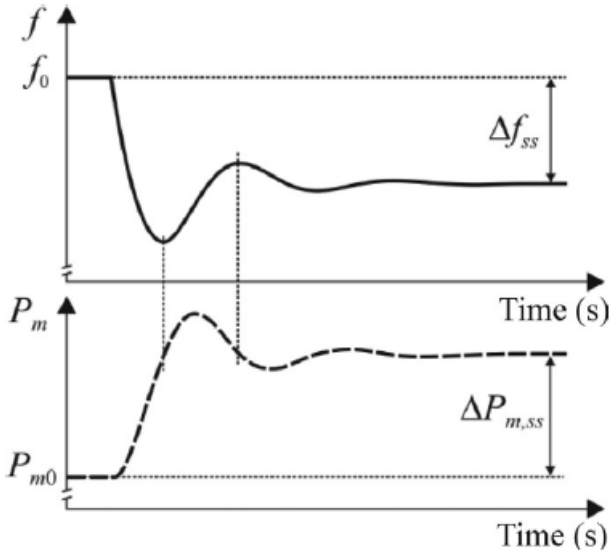

Figure 47. Frequency and active power variation for speed-droop governor (Bompard et al., 2021).

Depending on the power system characteristics, the droop is generally set between 3% and 5%. A 3% droop value means that the generated power changes 100%, in case of 3% frequency variation (Bompard et al., 2021).

On the other hand, if the droop value is zero, this type of governor is called isochronous. In this governor, the valve is kept in the open position until the frequency is reached to the reference value. This type of governor is used on small and isolated power systems (Bompard et al., 2021).

Appendix 3. RoCoF Reduction by SCs

Renewable Share	Disturbance	Mode	RoCoF (Hz/s)	Number of SC	RoCoF reduction by SCs (%)
40 %	Synchronous generation trip	Mode 1	-0.85	0	28.2
40 %	Synchronous generation trip	Mode 7	-0.61	3	
70 %	Synchronous generation trip	Mode 1	-1.14	0	34.2
70 %	Synchronous generation trip	Mode 7	-0.75	3	
40 %	The largest load trip	Mode 1	1.81	0	37.6
40 %	The largest load trip	Mode 7	1.13	3	
70 %	The largest load trip	Mode 1	3.15	0	49.5
70 %	The largest load trip	Mode 7	1.59	3	
40 %	The largest renewable generation trip	Mode 1	-0.81	0	24.7
40 %	The largest renewable generation trip	Mode 7	-0.61	3	
70 %	The largest renewable generation trip	Mode 1	-1.22	0	30.3
70 %	The largest renewable generation trip	Mode 7	-0.85	3	

Table 19. RoCoF reduction by SCs.